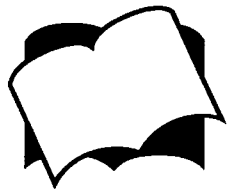

1090

Name	
E-Mail-Adresse	**daniel.marty@palaeojura.ch**
Bestelldatum	**2005-01-19 09:14:37**

Signatur

Zeitschrift	**Colorado School of Mines**
ISSN	
Band/Heft	**81**
Jahr	
Autor des Artikels	**Hardie, L.A., Shinn, E.A.**
Titel des Artikels	**Carbonate depositional environments, modern and ancient**
Seiten	**1-74**

Vermerk der Bibliothek

COLORADO SCHOOL OF MINES QUARTERLY
Volume 81 January 1986 Number 1

CARBONATE DEPOSITIONAL ENVIRONMENTS
Modern and Ancient

PART 3: TIDAL FLATS

by

Lawrence A. Hardie
Department of Earth and Planetary Sciences
The Johns Hopkins University
Baltimore, Maryland 21218

Eugene A. Shinn
U.S. Department of the Interior
Geological Survey
Fisher Island Station
Miami Beach, Florida 33139

Series Edited by

John E. Warme
Geology Department
Colorado School of Mines

and

Keith W. Shanley
Tenneco Oil Company
6162 S. Willow Drive
Englewood, Colorado 80155

$20.00

Colorado School of Mines Press
Golden, Colorado 80401

Colorado School of Mines Press
Managing Editor and Director of Publications
Jon W. Raese

The editor of *Colorado School of Mines Quarterly* welcomes original contributions on mineral resources engineering, the earth sciences, and the environment. Manuscripts, subscriptions to the *Quarterly* ($50.00 per year) and orders for back issues should be sent to the Publications Department, Colorado School of Mines, Golden, Colorado 80401. Toll-free numbers: 1-800/245-1060 (within Colorado), 1-800/446-9488 (outside Colorado). Ask for extension 3607.

Library of Congress Cataloging-in-Publication Data
(Revised for part 3)
ISBN 0-918062-66-7
Carbonate depositional environments, modern and ancient.

(Colorado School of Mines quarterly, 0163-9153 ; v. 80, no. 3, v. 81, no. 1)
Includes bibliographies.
Contents: pt. 1. Reefs, zonation, depositional facies, and diagenesis / by Noel P. James and Ian G. MacIntyre— —pt. 3. Tidal Flats / by Eugene A. Shinn, Lawrence A. Hardie.
1. Rocks, Carbonate. 2. Sedimentation and deposition. 3. Reefs. 4. Tidal flats. I. James, Noel P. II. MacIntyre, Ian G. III. Series.

TN210.C68 vol. 80, no. 3 622 s [552'.1] 85-22384
[QE471.15.C3)

Quarterly
USPS 452-240
Published quarterly by Colorado School of Mines Press
at Golden, Colorado 80401
Second-class postage paid at Golden, Colorado
Printed in the United States of America
Postmaster please send form 3579 to:
Colorado School of Mines Press
Golden, Colorado 80401

6-02-0538

CONTENTS

FIGURES

TABLES

FOREWORD

"*Carbonate Depositional Environments: Modern and Ancient*," is a series of *Colorado School of Mines Quarterlies*, beginning with volume 80, number 3, 1985. This published series arose from material presented in lectures and in short courses given at the Colorado School of Mines during the spring semester of 1985. Fourteen well-known authorities lectured on their specialties within the realm of carbonate rocks. The public lectures were sponsored by the SOHIO Petroleum Company, and the short courses were offered through the CSM Office of Special Programs and Continuing Education.

Speakers and topics, in order of appearance, spring semester 1985:

James Lee Wilson Lloyd C. Pray	Carbonate Platforms: eustasy, porosity, erosion, preservation
Eugene A. Shinn Lawrence A. Hardie	Tidal Flats: cycles, diagenesis
Ian G. Macintyre Noel P. James	Reefs: cements, geologic history, evolution
Paul M. Harris Clyde H. Moore	Shelf Carbonates: facies, diagenesis, and petroleum potential
Henry T. Mullins Michael A. Arthur	Slopes and Basins: evolution, diagenesis, source rocks
Lynton S. Land Robin G.C. Bathurst	Diagenesis: dolomitization, pressure solution, isotopes
Robley K. Matthews Robert B. Halley	Diagenesis: eustasy, porosity, depth relationships

In their presentations, the authors covered both modern and ancient examples, diagenesis, applied aspects, overviews of past work and recent progress, as well as major unanswered problems within their specialties.

The lectures and short courses were so well attended and accepted that we believe this state-of-the-art material should be made available to interested scientists everywhere and arranged for publication in the *Quarterly*.

We thank all of the people who expedited publishing this series, including the authors, SOHIO Petroleum Company, CSM Office of Special Programs and Continuing Education (Janice Hepworth, Director), and CSM Press. Special thanks go to Jon Raese who accepted and methodically edited the manuscripts.

We trust that the readers will benefit from the material in these *Quarterlies* as much as we have.

Part 3 of this series, "Tidal Flats," contains material presented by Eugene A. Shinn and Lawrence A. Hardie. We thank them for their outstanding efforts in preparing this material for publication.

John E. Warme, Director
Exploration Geosciences Institute
Colorado School of Mines

Keith W. Shanley
Tenneco Oil Company

Colorado School of Mines Exploration Geosciences Institute
Publication Number 3

ACKNOWLEDGMENTS

We wish to salute Robert N. Ginsburg of the University of Miami, who inoculated us with his carbonate tidal-flat fever from which, happily, neither of us has recovered.

L.A. Hardie would like to thank former students Tom Tourek, Peter Garrett, Juergen Reinhardt, Hal Wanless, Joe Smoot, Bob Demicco, Ray Mitchell and present students Chau Nguyen, Mary Barrett, Bob Goldhammer, Edith Newton, Mark Harris and Paul Dunn for teaching him how to look at carbonate rocks. Some of the work reported here by Hardie was supported by NSF grants EA8217130, EAR7809156, GA31076 and GA1345.

E.A. Shinn's review is based on a "half-life" of personal tidal-flat studies under the auspices of Shell Development Company and Royal Dutch Shell. Numerous people provided Shinn with valuable input over the years. They include Robert N. Ginsburg, R. Michael Lloyd, S. Duff Kerr, Peter R. Rose, Ken Hsu, Bruce Purser, Paul Enos, Ronald D. Perkins, Robert B. Halley, Fred Meisner, Robert J. Dunham, Jerry Koch, Kees DeGroot, Lawrence Hardie, Perry Roehl and others too numerous to mention here. Shinn also thanks John Warme, Keith Shanley, and especially Jon Raese who did the final editing and arranged for publication. Finally, Shinn thanks Barbara Lidz, without whose critical editing and preparation of illustrations this publication would not have been possible.

INTRODUCTION: TIDAL-FLAT CARBONATES AND COMPARATIVE SEDIMENTOLOGY

Lawrence A. Hardie

Spectacular advances in our understanding of carbonate deposition have resulted from studies of modern carbonate tidal flats that began in the 1960s. These studies were triggered by the work of Illing (1954) and Newell and Rigby (1957) on the modern carbonate sediments of the Bahamas, and by Ginsburg's (1955, 1960) rediscovery of Black's (1933) pioneer work on modern algal laminated carbonates of Andros Island, Bahamas. The new studies led to the discoveries of Holocene supratidal "dolomite" (for example, Alderman and Skinner 1957; Wells 1962; Curtis and others 1963; Deffeyes and others 1965; Illing and others 1965; Shinn and others 1965), which inspired more intensive examination of the environments of modern shallow-water carbonates. At the same time, application of the preliminary results to ancient carbonates (for example, Fischer 1964; Bosellini 1965; Aitken 1966; Bosellini 1967; Laporte 1967; Matter 1967; Roehl 1967; Schenk 1967) demonstrated that carbonate rocks preserved a wide variety of primary depositional and diagenetic features found in modern tidal-flat carbonates. Precise interpretations of the sedimentary record of carbonates were now possible using modern sediments as a key to ancient rocks. Johannes Walther's "ontological method" expounded in 1894 (see Middleton 1973) had finally found its way into carbonate sedimentology. Ginsburg (1974) formalized this approach under the name of "comparative sedimentology."

Three modern areas of carbonate tidal flats have emerged as the principal sources of our information on carbonate tidal-flat processes and their sedimentary record. These areas are the Bahamas and Florida (Shinn and others 1965, 1969; Gebelein 1974; Hardie 1977; Enos and Perkins 1979; Monty 1967, 1972; Monty and Hardie 1976), Shark Bay in Western Australia (Logan and others 1970, 1974; Hoffman 1976; Playford and Cockbain 1976), and the Persian (Arabian) Gulf (Shearman 1966; Kinsman 1966; Kendall and Skipwith 1968, 1969; Butler 1969, 1970; Evans and others 1969; Purser 1973; McKenzie and others 1980; Patterson and Kinsman 1977, 1981, 1982). The information available in these and other modern carbonate tidal flats is by no means exhausted. We have much to learn about how to read the record of environmental parameters (Hardie 1977, pages 188-189), about early diagenetic processes (the origin of supratidal "dolomite" is yet to be fully resolved), and about the important stratigraphic question of the geometries of tidal-flat deposits and how they are generated. Nonetheless, the power of comparative sedimentology in the study of ancient carbonate tidal-flat deposits and their vertical sequences is now well documented (Lucia 1972; Ginsburg 1975; Shinn 1983; James 1984). This approach will be the framework of this treatise on carbonate tidal-flat deposition.

REFERENCES

Alderman, A.R., and Skinner, H.C.W., 1957, Dolomite sedimentation in the southeast of South Australia: American Journal of Science, volume 255, pages 561-567.

Aitken, J.D., 1966, Middle Cambrian to Middle Ordovician cyclic sedimentation, southern Rocky Mountains of Alberta: Bulletin of Canadian Petroleum Geology, volume 14, pages 405-411.

Black, M.M., 1933, The algal sediments of Andros Island, Bahamas: Philosophical Transactions of the Royal Society, London, series B, volume 222, pages 165-192.

Bosellini, A., 1965, Analisi petrografica della "Dolomia Principale" nel Gruppo di Sella (regione Dolomitica): Memorie Geopaleontologiche dell' Università di Ferrara, volume 1, pages 49-109.

Bosellini, A., 1967, La tematica deposizionale della Dolomia Principale (Dolomiti e Prealpi Venete): Bollettino della Società Geologica Italiana, volume 86, pages 133-169.

Butler, G.P., 1969, Modern evaporite deposition and geochemistry of coexisting brines, the sabkha, Trucial Coast, Arabian Gulf: Journal of Sedimentary Petrology, volume 39, pages 70-89.

Butler, G.P., 1970, Holocene gypsum and anhydrite of the Abu Dhabi sabkha, Trucial Coast: an alternative explanation of origin: Third Symposium on Salt, Northern Ohio Geological Society, Cleveland, Ohio, pages 120-152.

0163-9153/86/8101-0001 $00.20/0

Curtis, R., Evans, G., Kinsman, D.J.J., and Shearman, D.J., 1963, Association of dolomite and anhydrite in the Recent sediments of the Persian Gulf: Nature, volume 197, pages 679-680.

Deffeyes, K.S., Lucia, F.J., and Weyl, P.K., 1965, Dolomitization of Recent and Plio-Pleistocene sediments by marine evaporite waters on Bonaire, Netherlands Antilles: Society of Economic Paleontologists and Mineralogists, Special Publication 13, pages 71-88.

Enos, P., and Perkins, R.D., 1979, Evolution of Florida Bay from island stratigraphy: Bulletin of the Geological Society of America, volume 90, pages 59-83.

Evans, G., Schmidt, V., Bush, P., and Nelson, H., 1969, Stratigraphy and geologic history of the sabkha, Abu Dhabi, Persian Gulf: Sedimentology, volume 12, pages 145-159.

Fischer, A.G., 1964, The Lofer cyclothems of the Alpine Triassic: Bulletin of the Geological Survey of Kansas, volume 169, pages 107-149.

Gebelein, C.D., 1974, Modern Bahamian platform environments: Field trip guidebook, Geological Society of America Annual Meetings, Miami Beach, 106 pages.

Ginsburg, R.N., 1955, Recent stromatolitic sediments from south Florida (abstract): Journal of Paleontology, volume 19, page 723.

Ginsburg, R.N., 1960, Ancient analogues of Recent stromatolites: International Geological Congress Report XXI, Part XXII, pages 26-35.

Ginsburg, R.N., 1974, Introduction to comparative sedimentology of carbonates: American Association of Petroleum Geologists Bulletin, volume 58, pages 781-786.

Ginsburg, R.N., 1975, editor, Tidal deposits: Springer-Verlag, New York, 428 pages.

Hardie, L.A. 1977, editor, Sedimentation on the modern carbonate tidal flats of northwest Andros Island, Bahamas: Johns Hopkins Press, Baltimore, 202 pages.

Hoffman, P., 1976, Stromatolite morphogenesis in Shark Bay, Western Australia, *in* Walter, M.R., editor, Stromatolites: Elsevier, New York, pages 261-273.

Illing, L.V., 1954, Bahamian calcareous sands: American Association of Petroleum Geologists Bulletin, volume 38, pages 1-95.

Illing, L.V., Wells, A.J., and Taylor, J.C.M., 1965, Penecontemporary dolomite in the Persian Gulf: Society of Economic Paleontologists and Mineralogists, Special Publication 13, pages 89-111.

James, N.P., 1984, Shallowing-upward sequences in carbonates, *in* Walker, R.G., editor, Facies models, Second Edition: Geoscience Canada, Reprint Series 1, pages 213-228.

Kendall, C.G.St.C., and Skipwith, P.A.D'E., 1968, Recent algal mats of a Persian Gulf lagoon: American Association of Petroleum Geologists Bulletin, volume 38, pages 1040-1058.

Kendall, C.G.St.C., and Skipwith, P.A.D'E., 1969, Geomorphology of a Recent shallow-water carbonate province: Khor al Bazam, Trucial Coast, southwest Persian Gulf: Bulletin of the Geological Society of America, volume 80, pages 865-892.

Kinsman, D.J.J., 1966, Gypsum and anhydrite of Recent age Trucial Coast, Persian Gulf: Second Symposium on Salt, volume 1, pages 302-326, Northern Ohio Geological Society, Cleveland, Ohio.

Laporte, L.F., 1967, Carbonate deposition near mean sea level and resulting facies mosaic: Manlius formation (Lower Devonian) of New York State: American Association of Petroleum Geologists Bulletin, volume 51, pages 73-101.

Logan, B.W., Davies, G.R., Read, J.F., and Cebulski, D.E., 1970, Carbonate sedimentation and environments, Shark Bay, Western Australia: American Association of Petroleum Geologists Memoir 13, 223 pages.

Logan, B.W., Read, J.F., Hagan, G.M., Hoffman, P., Brown, R.G., Woods, P.T., and Gebelein, C.D., 1974, Evolution and diagenesis of Quarternary carbonate sequences, Shark Bay, Western Australia: American Association of Petroleum Geologist Memoir 22, 358 pages.

Lucia, F.J., 1972, Recognition of evaporite-carbonate shoreline sedimentation: Society of Economic Paleontologists and Mineralogists Special Publication 16, pages 160-191.

McKenzie, J.A., Hsü, K.J., and Schneider, J.F., 1980, Movement of subsurface waters under the sabkha, Abu Dhabi, UAE, and its relation to evaporative dolomite genesis: Society of Economic Paleontologists and Mineralogists Special Publication 28, pages 11-30.

Matter, A., 1967, Tidal flat deposits in the Ordovician of western Maryland: Journal of Sedimentary Petrology, volume 37, pages 601-609.

Middleton, G.V., 1973, Johannes Walther's law of the correlation of facies: Bulletin of the Geological Society of America, volume 84, pages 979-988.

Monty, C.L.V., 1967, Distribution and structure of recent stromatolitic algal mats, eastern Andros Island, Bahamas: Annales de la Societé Geologique de Belgique, volume 90, pages 55-100.

Monty, C.L.V., 1972, Recent algal stromatolite deposits, Andros Island, Bahamas, Preliminary report: Geologische Rundschau, volume 62, pages 742-783.

Monty, C.L.V., and Hardie, L.A., 1976, The geological significance of the freshwater blue-green algal calcareous marsh, *in* Walter, M.R., editor, Stromatolites: Elsevier, New York, pages 447-478.

Newell, N.D., and Rigby, J.K., 1957, Geological studies on the Great Bahama Bank: Society of Economic Paleontologists and Mineralogists Special Publication 5, pages 15-72.

Patterson, R.J., and Kinsman, D.J.J., 1977, Marine and continental groundwater sources in a Persian Gulf coastal sabkha: American Association of Petroleum Geologists, Studies in Geology, volume 4, pages 381-397.

Patterson, R.J. and Kinsman, D.J.J., 1981, Hydrologic framework of 2 sabkhas along the Arabian Gulf: American Association of Petroleum Geologists Bulletin, volume 65, pages 1457-1475.

Patterson, R.J., and Kinsman, D.J.J., 1982, Formation of diagenetic dolomite in coastal sabkha along Arabian (Persian) Gulf: American Association of Petroleum Geologists Bulletin, volume 66, pages 28-43.

Playford, P.E., and Cockbain, A.E., 1976, Modern algal stromatolites at Hamelin Pool, a hypersaline barred basin in Shark Bay, Western Australia, *in* Walter, M.R., editor, Stromatolites: Elsevier, New York, pages 389-413.

Purser, B.H., 1973, editor, The Persian Gulf: Springer-Verlag, New York, 471 pages.

Roehl, P.O., 1967, Stony Mountain (Ordovician) and Interlake (Silurian) facies analogs of Recent low-energy marine and subaerial carbonates, Bahamas: American Association of Petroleum Geologists Bulletin, volume 51, pages 1979-2032.

Schenk, P.D., 1967, The Macumber Formation of the Maritime Province, Canada—a Mississippian analogue to Recent strand-line carbonates of the Persian Gulf: Journal of Sedimentary Petrology, volume 37, pages 365-376.

Shearman, D.J., 1966, Origin of marine evaporites by diagenesis: Transactions of the American Institute of Mining, Metallurgical, and Petroleum Engineers (B), volume 75, pages 208-215.

Shinn, E.A., 1983, Tidal flat environment: American Association of Petroleum Geologists Memoir 33, pages 173-210.

Shinn, E.A., Ginsburg, R.N., and Lloyd, R.M., 1965, Recent supratidal dolomite from Andros Island, Bahamas: Society of Economic Paleontologists and Mineralogists Special Publication 13, pages 112-123.

Shinn, E.A., Lloyd, R.M., and Ginsburg, R.N., 1969, Anatomy of a modern carbonate tidal flat, Andros Island, Bahamas: Journal of Sedimentary Petrology, volume 39, pages 1202-1228.

Wells, A., 1962, Primary dolomitization in Persian Gulf: Nature, volume 194, pages 274-275.

CARBONATE TIDAL-FLAT DEPOSITION: TEN BASIC ELEMENTS

Lawrence A. Hardie

1. Tidal flats differ from beaches in that they are protected from open ocean waves. Tidal flats occur, therefore, in settings:

(a) Separated from the open ocean by a wide, shallow shelf lagoon that dampens the incoming waves, as for example, Andros Island tidal flats on the Great Bahama Banks (figure 1A);

(b) Behind barrier islands that separate back barrier lagoons from open ocean waves, as for example, Abu Dhabi in the Persian Gulf (figure 1B); and

(c) In restricted embayments, as in Shark Bay in Western Australia.

2. Tidal range determines the basic physiography of a tidal-flat system (Davies 1964; Hayes 1976). A microtidal range (< 2 m) promotes the development of barrier bars behind which the tidal flats accrete. A mesotidal range (2 – 4 m) produces a patchy barrier system breached by numerous inlets. A macrotidal range (> 4 m) leads to open tidal flats without barriers.

3. The daily oscillations of the tides (typically less than a meter to a few meters) subdivide tidal flats into three basic depositional-ecological zones (figure 2):

(a) The supratidal zone, which is above mean high water and is flooded by seawater only during spring high tides and storm surges;

(b) The intertidal zone, which is between mean high water and mean low water, and is flooded and exposed daily by the tides; and

(c) The subtidal zone, which is below mean low water. The upper part of this zone may be exposed on rare occasions during strong offshore winds.

Because of the normal variations in tidal range and height, and the effects of storms, the boundaries between these tidal zones are transitional rather than sharp, as is demonstrated by a plot of surface elevation versus frequency of exposure for the Andros Island tidal flats (figure 3; see Ginsburg and others 1977).

4. Tidal flats are partly land and partly sea and so experience a range of conditions unmatched by any other sedimentary environment. The steep gradient of environmental conditions from subtidal to supratidal produces the richest variety of sedimentary and early diagenetic features present in carbonate rocks, features such as flat laminae, wavy and crinkled laminae, thin beds, stromatolites, thrombolites, mud cracks, prism cracks, sheet cracks, flat pebble and round pebble gravels, rippled and cross-bedded intraclast-, skeletal- and peloidal-sands, pelleted lime mud, fenestral pores, burrows, evaporite minerals, evaporite casts and molds, caliche crusts, pisoids, tepee structures, root casts and molds, etc., are common. These features, highly sensitive to frequency of exposure, are systematically zoned over a short (cm to meter-scale) vertical thickness of sediment (figure 4). It is this sensitivity that makes tidal-flat deposits so important in the geological record. Not only are they precise sea-level gauges, but they preserve a wealth of information about tidal regime and range, water circulation, water chemistry, and climate. Subtidal deposits record, in their primary textures, structures and biota, information about salinity and circulation intensity. Intertidal deposits, in their sedimentary structures and thickness, record information on tidal regime and range. Supratidal deposits accumulate in an essentially subaerial realm and so they record, in primary and diagenetic features such as algal tufa, caliche or evaporites, information on the climate of the region.

5. The large number of possible combinations and permutations of circulation, salinity, tides and climate, together with physiography, allows for many varieties of tidal-flat deposit.

0613-9153/86/8101-0003 $00.20/0

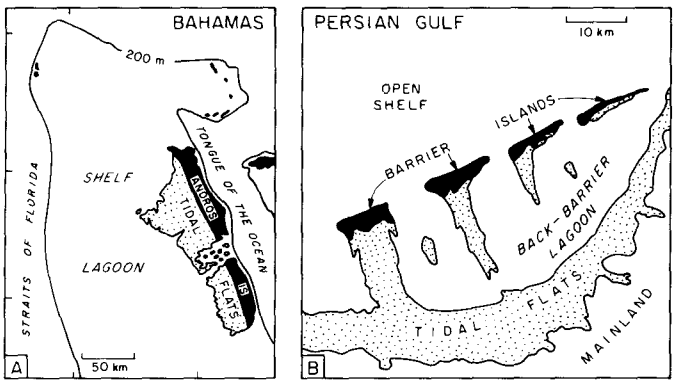

Figure 1.—Typical nucleation sites of carbonate tidal flats: (A) Platform margin island, for example, Andros Island, Bahamas. (B) Continental margin, for example, Persian Gulf.

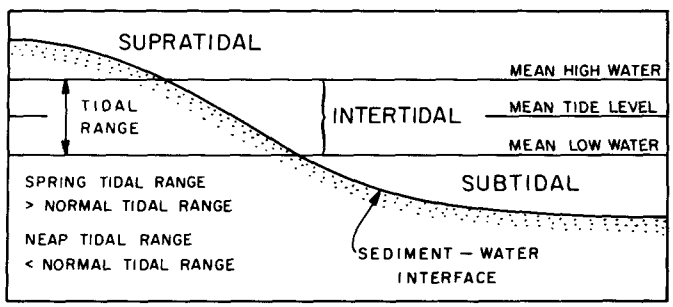

Figure 2.—Terminology for tidal zones.

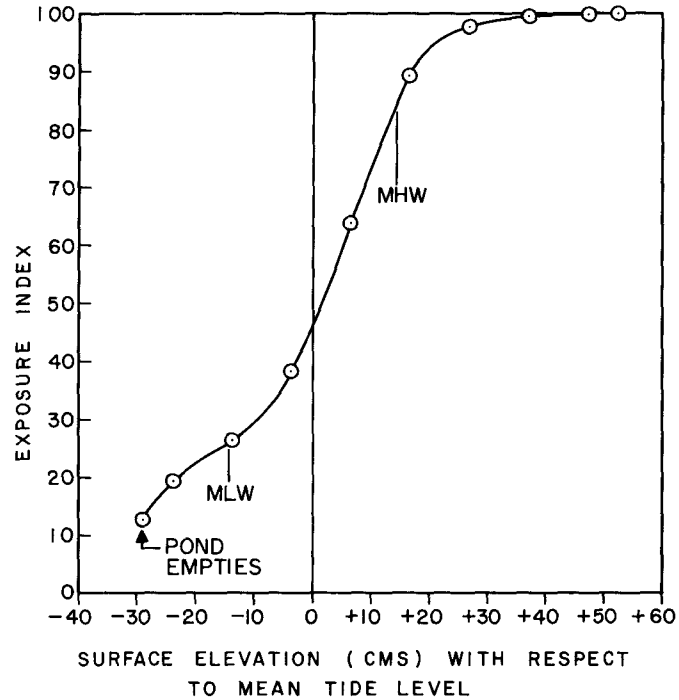

Figure 3.—The transitional nature of tidal zones as exemplified by the Andros Island tidal flats. Plotted here is mean exposure index as a function of relative surface elevation for a tidal pond-levee system on Andros Island (see Hardie 1977, figure 3). MHW = mean high water, MLW = mean low water.

No two modern tidal flats are quite the same today and even different areas of the same tidal flat are different. This also seems to be true for ancient tidal-flat deposits (compare, for example, Fischer 1964; Laporte 1967; Matter 1967; Roehl 1967; Schenk 1967; Bosellini and Hardie 1973; Ginsburg 1975; Reinhardt and Hardie 1976; Demicco 1983; among many others). Therefore, in using the comparative sedimentology approach, care must be taken not to try to force an ancient deposit to fit one of our few modern models. It is better to use a "building block" approach (Hardie 1977, pages 188-189), in which an ancient deposit is matched by piecing together appropriate parts taken from different modern tidal-flat systems.

6. Because tidal flats are in wave-protected settings, they are preferential sites for mud accumulation. Carbonate mud is generated mainly in the shallow offshore by calcareous organisms (Stockman and others 1967) and direct chemical precipitation (Shinn and others 1985), although it can be produced in quantity on the supratidal flats, for example, as algal tufa (Hardie 1977). The offshore mud is transported shoreward and onto the tidal flats by tidal currents and severe onshore storms. In microtidal systems such as the Bahamas, storms are the only important agents of sediment delivery to the tidal flats (Hardie and Ginsburg 1977), and so play a central role in the growth of the tidal-flat sediment wedge (see later).

7. Carbonate tidal flats may nucleate on:

(a) A continental mainland, as in the Persian Gulf (figure 1B);

(b) Isolated islands within a lagoon, as in Florida Bay (Enos and Perkins 1979); or

(c) Platform-margin islands, as on the Great Bahama Banks (figure 1A).

In the stratigraphic record, then, tidal-flat deposits may occur as landward wedges that pinch out toward the platform margin, as a patchwork of lenses within shelf-lagoon deposits, and as seaward wedges that pinch out toward the craton or the platform center.

8. Marine carbonate sedimentation is most profuse in shallow tropical waters that are warm and clear. Such conditions are also conducive to prolific growth of blue-green algal mats that can influence deposition by binding, trapping and precipitation of sediment (Walter 1976). In modern marine carbonate environments, browsing and burrowing by organisms have restricted these algal mats to the supratidal zone (Garrett 1970), hypersaline lagoons (Logan and others 1974), and hard substrates in a few agitated subtidal localities (Dravis 1983). By analogy, Phanerozoic browsers and burrowers were likely important factors restricting algal lamination mainly to tidal-flat deposits (Garrett 1970).

9. Early cementation is a characteristic feature of modern

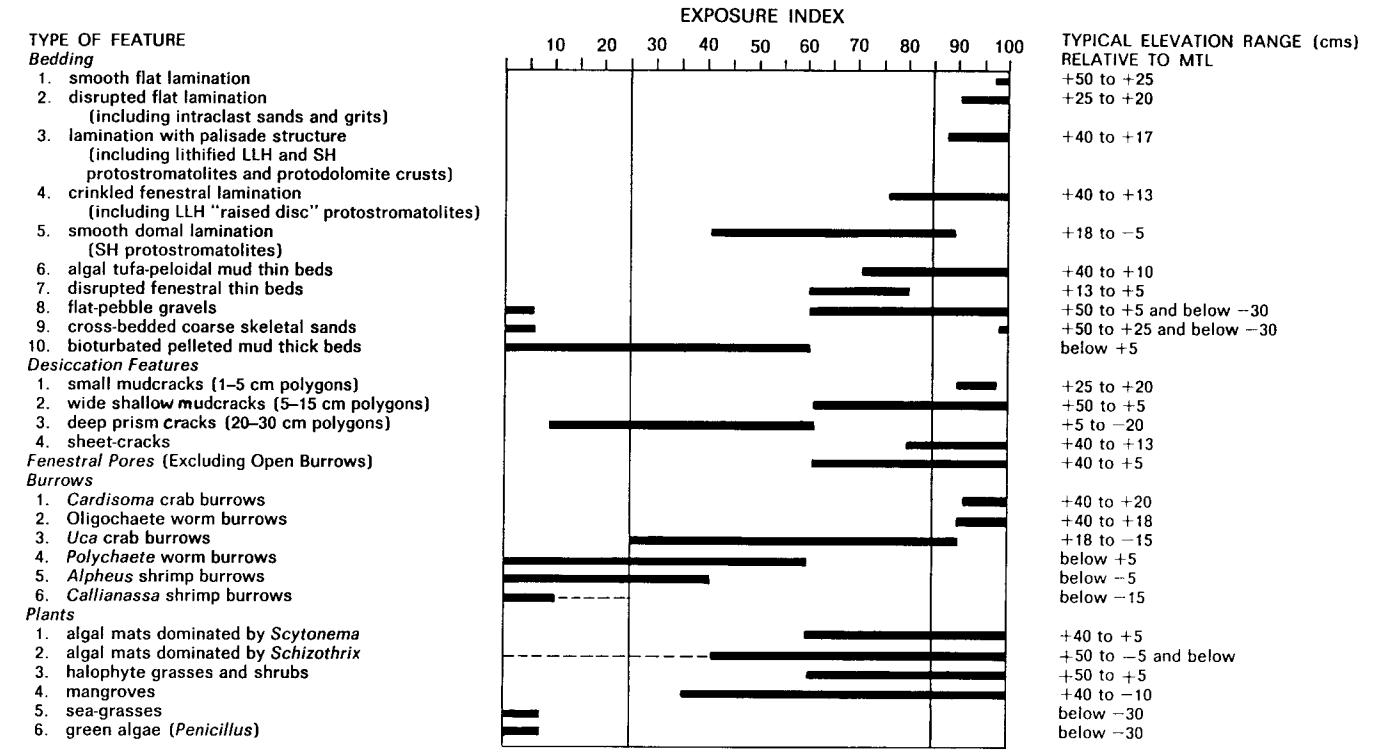

Figure 4.—Zonation of features across the northwest Andros Island tidal flats. Sedimentary and biogenic features are plotted as a function of the Exposure Index of the surface environment in which the features occur. Solid lines represent measured ranges, dashed lines represent estimated ranges. From Hardie (1977, figure 4).

marine carbonate environments (James and Choquette 1984) and plays a crucial role in the preservation of primary textures and structures in the muddy sediments of tidal flats. Without early cementation, features such as peloids, intraclasts, fenestral pores, burrows and rootholes would be lost by compaction on shallow burial (Shinn and Robbin 1983).

10. Carbonate tidal-flat facies typically occur as layer-cake sequences of stacked "cycles," 1-10 m thick, each composed internally of an upward succession of subtidal ➧ intertidal ➧ supratidal subfacies. The origin of this cyclicity is a question that has yet to be resolved (see following discussion).

REFERENCES

Bosellini, A., and Hardie, L.A., 1973, Depositional theme of a marginal marine evaporite: Sedimentology, volume 20, pages 5-27.

Davies, J.L., 1964, A morphogenetic approach to world shorelines: Zeitschrift für Geomorphologie, volume 8, pages 127-142.

Demicco, R.V., 1983, Wavy and lenticular-bedded carbonate ribbon rocks of the Upper Cambrian Conococheague Limestone, Central Appalachians: Journal of Sedimentary Petrology, volume 53, pages 1121-1132.

Dravis, J.J., 1983, Hardened subtidal stromatolites, Bahamas: Science, volume 219, pages 385-386.

Enos, P., and Perkins, R.D., 1979, Evolution of Florida Bay from island stratigraphy: Bulletin of the Geological Society of America, volume 90, pages 59-83.

Fischer, A.G., 1964, The Lofer cyclothems of the Alpine Triassic: Bulletin of the Geological Survey of Kansas, volume 169, pages 107-149.

Garrett, P., 1970, Phanerozoic stromatolites: noncompetitive ecological restriction by grazing and burrowing animals: Science, volume 169, pages 171-173.

Ginsburg, R.N., 1975, editor, Tidal deposits: Springer-Verlag, New York, 428 pages.

Ginsburg, R.N., Hardie, L.A., Bricker, O.P., Garrett, P., and Wanless, H.R., 1977, Exposure index: a quantitative approach to defining position within the tidal zone, *in* Hardie, L.A., editor, Sedimentation on the modern carbonate tidal flats of northwest Andros Island, Bahamas: Johns Hopkins Press, Baltimore, pages 7-11.

Hardie, L.A., 1977, Sedimentation on the modern carbonate tidal flats of northwest Andros Island, Bahamas: Baltimore, The Johns Hopkins University Press, The Johns Hopkins University Studies in Geology, number 22, 202 pages.

Hardie, L.A., and Ginsburg, R.N., 1977, Layering: the origin and environmental significance of lamination and thin bedding, *in* Hardie, L.A., editor, Sedimentation on the modern carbonate tidal flats of northwest Andros Island, Bahamas: Johns Hopkins Press, Baltimore, pages 50-123.

Hayes, M.O., 1976, Morphology of sand accumulation in estuaries: an introduction to the symposium, *in* Gronin, L.E., editor, Estuarine research, volume II: Academic Press, London, pages 3-22.

James, N.P., and Choquette, P.W., 1984, Diagenesis 6: Limestone—the sea floor diagenetic environment: Geoscience Canada, volume 10, pages 162-179.

Laporte, L.F., 1967, Carbonate deposition near mean sea level and resulting facies mosaic: Manlius Formation (Lower Devonian) of New York State: American Association of Petroleum Geologists Bulletin, volume 51, pages 73-101.

Logan, B.W., Hoffman, P., and Gebelein, C.D., 1974, Algal mats, cryptalgal fabrics and structures, Hamelin Pool, Western Australia: American Association of Petroleum Geologists Memoir, volume 22, pages 140-194.

Matter, A., 1967, Tidal flat deposits in the Ordovician of Western Maryland: Journal of Sedimentary Petrology, volume 37, pages 601-609.

Reinhardt, J., and Hardie, L.A. 1976, Selected examples of carbonate sedimentation, Lower Paleozoic of Maryland: Maryland Geological Survey Guidebook 5, 53 pages.

Roehl, P.O., 1967, Stony Mountain (Ordovician) and Interlake (Silurian) facies analogs of Recent low-energy marine and subaerial carbonates, Bahamas: American Association of Petroleum Geologists Bulletin, volume 51, pages 1979-2032.

Schenk, P.E., 1967, The Macumber Formation of the Maritime Province, Canada—a Mississippian analogue to Recent strand-line carbonates of the Persian Gulf: Journal of Sedimentary Petrology, volume 37, pages 365-376.

Shinn, E.A. and Robbin, D.M., 1983, Mechanical and chemical compaction in fine-grained shallow-water limestones: Journal of Sedimentary Petrology, volume 53, pages 595-618.

Shinn, E.A., Steinen, R.P., Lidz, B.H., and Halley, R.B., 1985, Bahamian whitings—no fish story: American Association of Petroleum Geologists Bulletin, volume 69, page 307.

Stockman, K.W., Ginsburg, R.N., and Shinn, E.A., 1967, The production of lime mud by algae in south Florida: Journal of Sedimentry Petrology, volume 37, pages 633-648.

Walter, M.R., 1976, editor, Stromatolites: Elsevier, New York, 790 pages.

MODERN CARBONATE TIDAL FLATS: THEIR DIAGNOSTIC FEATURES

Eugene A. Shinn

Sources of Data

With most sedimentary deposits, we gain our knowledge of processes and diagnostic features using the uniformitarianism approach, that is, we study modern examples for keys to the past. Unlike the deep ocean basins where more than 70 percent of the world's carbonates are being deposited, the study of shallow-water carbonates, and, in particular, tidal flats, is geographically limited; while carbonates are currently being deposited over millions of square kilometers of seafloor, there are relatively few areas of extensive tidal-flat deposition available for examination. A look at the geologic record, however, shows that tidal flats have at times rivaled the deep oceans in areal extent. This disparity reflects the well documented postglacial worldwide rise in sea level. The shallows, where tidal flats are forming today, have only been flooded during the past 5,000-6,000 years, and those flats that have accreted seaward have done so in spite of an overall rise in sea level. Because of this rapid sea-level rise, somewhat more special geological settings may be required for the development of tidal flats than in the past.

The areas available for study include the humid flats of northwest and southwest Andros Island in the Bahamas (figure 5), to a lesser extent the area west of Abaco Island in the Bahamas, and a sizable accumulation in a relatively more arid climate of the Caicos Islands south of the Bahamas archipelago. By far the largest tidal flats are found along the southern shore of the Persian Gulf, and, together with the tidal flats of Western Australia, represent the only extensive and truly arid examples available for study.

The challenge, then, is to extract the salient principles from modern examples and project that information into the distant past. For example, whether a flat is hundreds of kilometers wide or just a few, it seems unlikely that the mechanics and sedimentary processes would have been significantly different in the past than today. Likewise, regardless of whether the ocean's chemistry was different in the past, it is unlikely that the overall processes of surficial dolomitization and diagenesis were different. The rates of dolomitization and other diagenetic processes, however, may have been different than they are on today's tidal flats.

One way to project present information into the past is to mentally project today's processes into the future. The resulting model can then be used as a model for the ancient sequences. For example, because many areas have been flooded for only a few thousand years, there has been little sediment accumulation. Study of sedimentary processes in these areas, however, can lead to a prediction of how sedimentation will proceed during the next 10,000 years. A model established in this way often looks surprisingly similar in size and makeup to ancient tidal flats where the geologic setting may have been similar. With this principle in mind, the salient features of both humid and arid tidal flats are described and an attempt is made to predict what will happen in the future.

Humid Tidal Flats—Andros Island

The tidal flats of Andros Island are among the most studied in the world (figure 5). Significant contributions to our knowledge of these areas have been made by Black (1933), Shinn and others (1965, 1969), Hardie (1977), Ginsburg and Hardie

0163-9153/86/8101-0007 $00.20/0

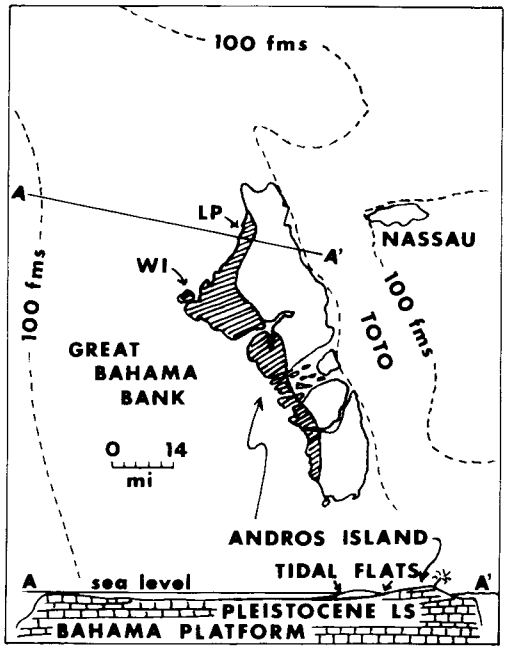

Figure 5.—Geologic setting showing leeward location of tidal flats on western Andros Island (hatched). LP = Loggerhead Point, informally called Three Creeks area. WI = Williams Island, and isolated area of tidal-flat sedimentation (hatched). TOTO = Tongue of the Ocean. Modified from Shinn (1968).

(1975), and Shinn (1983). Two widely distributed films* show additional details impossible to appreciate from the written work.

Three main environments are evident—supratidal marsh, intertidal channeled belt, and subtidal—each of which can be broken down into several subenvironments.

Supratidal Zone

By far the most diagnostic and important zone in all tidal flats, regardless whether the climate is humid or arid, is that zone of sedimentation a few centimeters above normal high-tide level, the supratidal zone. This zone is flooded only a few times each month either when the sun and moon align to provide maximum gravitational pull (that is, so-called spring tides that occur during full moon and new moon), or when storms cause flooding due to wind or low barometric pressure, such as during a tropical storm or hurricane. Most sedimentation throughout tidal flats occurs during storm flooding, which is especially important in the supratidal environment. Once deposited well above normal high tide by storms, such sediments are exposed for prolonged periods, and may not be flooded even during spring tides. It is this exposure that causes development of the many diagnostic features of supratidal sedimentation. Because this exposure is so important, Ginsburg and others (1977) made careful measurements of exposure duration in different zones to establish what they called the "exposure index." Exposure index is essentially the percent of time during which any particular environment is exposed above tide level.

Exposure is important not only because it creates certain sedimentary structures, but also because it preserves them by preventing bioturbation. Even in humid areas, the supratidal zone is generally too saline for many terrestrial burrowers and plants and at the same time too dry for marine burrowers and plants. At times, the waters are almost fresh; thus, the zone is one of widely fluctuating conditions unsuitable for most organisms. This area is conducive, however, to the growth of blue-green algae which form distinctive mats.

Desiccation cracks, that is, mud cracks, are the most diagnostic indicator of exposure. Mud cracks are easily recognized, requiring no more special equipment than the naked eye. They form when high tides, generally storm-driven, flood the tidal flat and deposit a layer of sediment. During subsequent exposure, these layers dewater and shrink to form the familiar V-shaped cracks that separate the resulting "mud polygons." Deep cracks and large polygons form in thick layers and conversely shallow cracks and smaller polygons form in thin layers. Layers may contain thinner laminations, approximately 1 mm thick, usually formed as graded laminae of pelleted sediment.

Mud cracks in carbonates are generally different from those in clays. Both begin as V-shaped cracks, but cracks in carbonates become rounded, and resulting polygons appear as sausages in cross section (figure 6). See Shinn (1968, 1983) and Hardie (1977) for more graphic examples. Syneresis cracks that form under standing water in clay sediments are not known in carbonates at the present time.

Algal mats, or stromatolites, are well known on all tidal flats and are generally restricted to the supratidal zone, though they can extend their range down into the upper intertidal zone, especially in arid areas. Their distribution appears to be controlled by browsing organisms (Garrett 1970); however, substrate change and competition may have caused algae to retreat from subtidal zones (Pratt 1982). Regradless of the cause, it is generally agreed that stromatolites moved from subtidal to supratidal environments after the Precambrian.

Algal mats, like storm-deposited layers, can be thick (cms) or thin (mms) (figure 7A). In some parts of the supratidal zone where the exposure index is high, algal mat growth is rarely interrupted by sediment influx; thus, they form thick, tufted

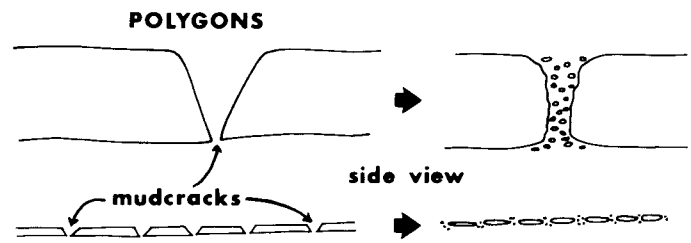

Figure 6.—Evolution of desiccation or mud cracks in thick and thin storm layers. Note that V-shaped cracks evolve into vertical, rounded, sediment-filled cracks.

*"Bahama Tidal Flats," 1961 (16 mm, 30 min.), prepared by E.A. Shinn and R.N. Ginsburg, and available from Shell Development Company, Houston, Texas. "Stratigraphic Traps: The Tidal Flat Model," 1981 (16 mm or video, 17 min.), American Association of Petroleum Geologists, Tulsa, Oklahoma.

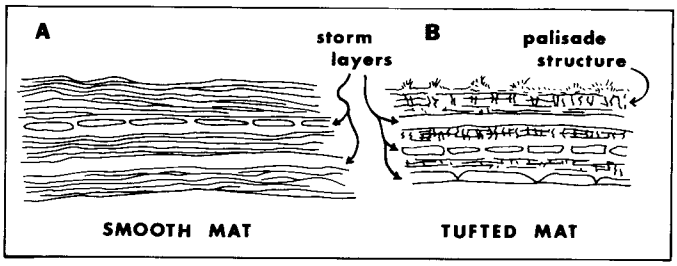

Figure 7.—(A) Thin algal laminations with enclosed storm layers deposited in area of frequent sedimentation and high exposure index. (B) Algal mats from area of infrequent sediment deposition, such as on the supratidal marsh at Andros. Long period of time between sedimentation events allows algae to grow vertically and produce palisade structures and moss-like tufts. Individual storm layers are usually thicker than those associated with smooth thin algal laminations.

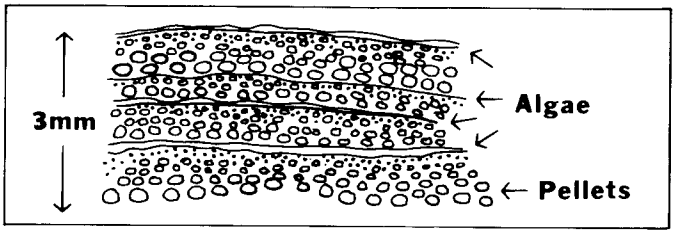

Figure 8.—Thin algal mats, commonly just a skin of algae, form in areas of frequent sedimentation such as beach ridges and levees. Grains consist of soft sand-size pellets which are often graded and capped by an algal skin. In such settings individual sediment layers are actually lenses and cannot be traced laterally for more than a few centimeters. Thick storm layers, such as those in the supratidal marsh, can be traced laterally for tens of meters.

mats (figure 7B). Such mats generally contain vertical, palisade-like features. These thick mats are most abundant in the extensive supratidal marsh which is discussed later.

Thin algal mats (figure 8) form in areas more frequently flooded by sediment-laden water than do thick mats. This kind of sedimentation is generally restricted to supratidal subenvironments, such as levees and beach ridges. In these settings algal laminations simply punctuate laminations produced by physical sedimentation. Lamination generally is caused by thin layers of graded pellets deposited during spring-tide flooding. During the week or weeks of exposure between sedimentation events, thin mats grow over the surface. This green "skin" of algae is readily visible in the field but almost impossible to detect a few centimeters below the surface or in thin section.

Between the extremes described above, there exists every imaginable variation in thickness and character, yet regardless of the variations, these features are easy to recognize.

The third diagnostic supratidal feature consists of voids called "bird's-eye" voids or fenestrae. In ancient rocks these voids are often filled with calcite cement which sparkles in the sun, giving rise to the term "bird's-eyes." Fenestrae, named by Tebbutt and others (1965), or fenestral fabric for the rock containing them, is considered a better term. These features have been formed experimentally (Shinn 1968) and recently reevaluated (Shinn 1983) and described in numerous examples of modern supratidal sediments (Ginsburg and Hardie 1975; Hardie 1977; Shinn 1983, to name a few). Their origin is in part the same as keystone vugs (Dunham 1970).

Fenestrae are considered reliable indicators of supratidal conditions when they occur in fine-grained carbonates or in coarse-grained sediment, but only when they are associated with mud cracks and stromatolites or other features more indicative of tidal-flat deposition and exposure. Fenestrae have recently been found to be unreliable indicators of supratidal conditions when occurring in sand-size pelleted sediment not directly associated with other supratidal features (Shinn 1983). In areas of submarine cementation, Shinn (1983) found fenestral-like voids that formed in water between 1 and 6 m deep. Their origin is the result of redeposition of grapestone lumps, considered to be incipient stages of submarine cementation. Due to their irregular shape, grapestone lumps resist packing during deposition, and irregular voids between the lumps are the result. The margins of such lumps are generally bored or eroded and may allow distinction from "true" fenestrae, but careful observation is required. The sequence of events is sketched in figure 9.

Three main types of fenestrae occur both in the modern and ancient sequences: spherical or bubble-like, planar, and irregular voids (figure 10). The first two occur mainly in fine-grained sediment or rocks and the latter in more grainy sediment or rocks. The bubble-like voids are considered to be formed by bubbles of air trapped in sediment. They form either as bubbles trapped in algal slime, which subsequently is covered by sediment, or by air coalescing as the tide rises (Shinn 1968). Keystone vugs in carbonate beach sands form when the tide rises and air coalesces with enough force to push grains away, often resulting in a keystone arrangement at the top of the void. The "keystone" prevents collapse (figure 10). Rapid cementation in such environments eventually preserves the voids. In muddy tidal-flat sediments the same is probably the case, except that the sediment is so sticky that a true "keystone" at the top of the void is not necessary for preservation.

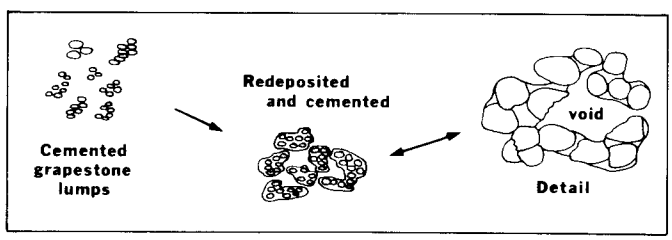

Figure 9.—Sequence of events leading to formation of fenestrae or bird's-eye-like voids in submarine grainstones. First, grains are cemented by aragonite to form grapestone lumps. Lumps get bored and eroded, then redeposited and cemented. Voids result from incomplete packing of irregularly shaped lumps. In detail this kind of void is best identified by truncated grains and cement surrounding portions of the voids. True supratidal bird's-eye or fenestrae may lack truncation of grains and cement around voids.

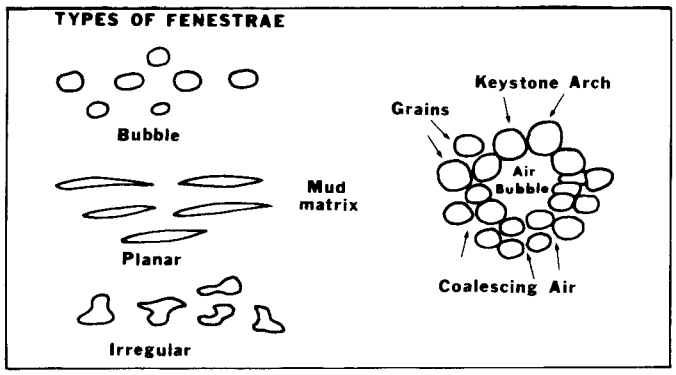

Figure 10.—Three kinds of fenestrae or bird's-eye voids. Bubble-shaped ones are usually in poorly laminated muds, planar-shaped ones are usually in laminated or stromatolitic deposits, and irregular fenestrae are usually restricted to pelleted sand-size grains. Detail at right shows a keystone vug as formed in a beach. An air bubble creates a void and grains at the top form a keystone arch that prevents collapse. Rapid cementation preserves the void.

Planar-shaped voids probably result from continual shrinkage and swelling caused by alternate wetting and drying. Some may result from partial collapse of spherical or bubble-formed voids, and many are controlled by parallel algal laminations. Surface algal mats are commonly leathery, and during the heat of the day, trapped gas causes them to blister, forming hollow hemispheres several centimeters across. At night the hemispheres flatten, but the stretched algal mat resists flattening and small recumbent folds are produced. The sequence of events is shown in figure 11.

Supratidal zones generally occur in three subenvironments: the marsh, levees, and beach ridges.

Supratidal Marsh. By far the most extensive and important is the supratidal marsh (the equivalent of the sabkha in arid regions). The marsh is the landwardmost part of the tidal-flat belt and separates the channeled intertidal zone from the land (figure 12). The marsh generally lacks well-developed channels, but a few narrow creeks extend into it. The surface of the marsh is brown to black in color due to extensive thick algal cover. A few stunted black mangroves occur, and sawgrass increases

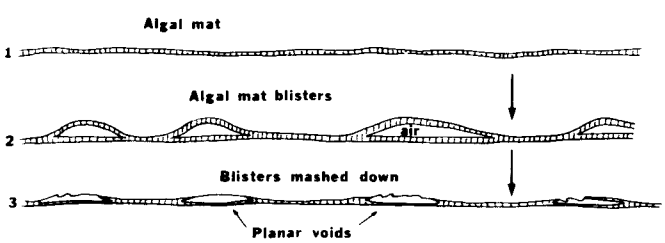

Figure 11.—One explanation for formation of planar fenestrae. Gas raises thin leathery algal mat to form hollow domes. When stretched, domes are mashed down and voids form like rumples in a carpet.

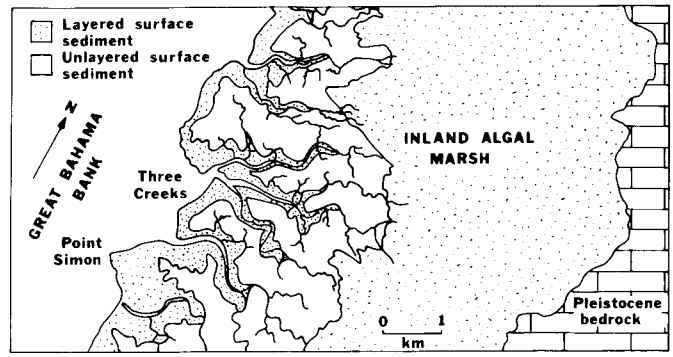

Figure 12.—Map of Three Creeks and Point Simon (also known as Loggerhead Point, figure 3.1) area on Andros Island showing location of supratidal (layered) environments and subtidal and intertidal (unlayered) environments of deposition.

in abundance toward land. On Andros, the "land" consists of karsted Pleistocene limestone. Sawgrass is present most of the year, reflecting fresh interstitial water and ponded rain water. As one would expect, salinity decreases in a landward direction.

There are minor topographic changes on the marsh and an elevation change of only a centimeter or two causes distinct changes in the sedimentary structures. For example, where the surface is slightly higher than the surrounding areas, thin, lightly cemented crusts form and algal mats are measurably thinner.

In places the marsh sediment is slightly more than a meter thick and extends in a seaward direction beneath the intertidal channel belt and offshore subtidal environment. In a landward direction the accumulation gradually thins until Pleistocene bedrock is exposed. In places the exposed portion of the marsh is as much as 2 km wide and tens of kilometers long. In addition to being the most extensive environment of deposition, sedimentary structures produced in the marsh are the easiest to recognize.

Diagnostic features of marsh sediment include thickness and lateral continuity of both storm laminations and algal mats. Shinn and others (1969) concluded that the storm layers are thickest in the marsh because only the most severe storms, that is, hurricanes, are capable of flooding the area, and floodwater caused by a hurricane will be more sediment-laden than floodwater caused by smaller storms. These storm floodwaters must pass over the more seaward supratidal environments to reach the marsh, but they apparently flood at velocities too great to allow significant deposition. Once the marsh is flooded as high as is possible, current velocities are greatly reduced and most of the sediment load is deposited.

Because hurricanes are less frequent (5 to 10 years apart) than lesser storms, there are longer periods during which algal mats develop; consequently, the mats tend to be thicker than in the other supratidal subenvironments. The marsh is frequently wetted by rainfall, especially during the summer. Without rainfall, the mats would dry out and die.

Levees. Smaller transitory supratidal environments exist at the outer bends of tidal channels and gullies within the intertidal

channeled belt. Levee accumulations are similar to those in river deltas; however, levees on river deltas are best developed in the downstream portion of channel meanders, those on tidal flats are developed on the landward part of meanders (figure 13). This distribution is the result of landward transport of sediment during storm flooding, as opposed to river deltas where sediment transport is downstream toward the ocean during flood stages. Some straight but broad tidal channels have well-developed levees along both banks. The main channel at Three Creeks on Andros is a good example.

Levee sediments are laminated but individual laminae are thin (on a mm scale), and each individual lamina is generally composed of graded pellets (figure 14). The most diagnostic feature of laminations is their lack of lateral continuity. An individual lamina, especially the thinner ones, cannot be traced laterally more than a few centimeters (Shinn and others 1969; Hardie 1977).

As in river deltas, the levees reach their highest elevation at the water's edge. Beginning at the edge of the channel, the levees gradually slope downward away from the channel. At some point, usually 20 to 30 m away from main channels and only 5 to 10 m away from smaller channels and gullies, the levee merges with the intertidal zone (figure 15). Supratidal laminations gradually become more disrupted by bioturbation as the levee approaches the intertidal zone. Only minor vestiges of levee lamination remain near the intertidal zone.

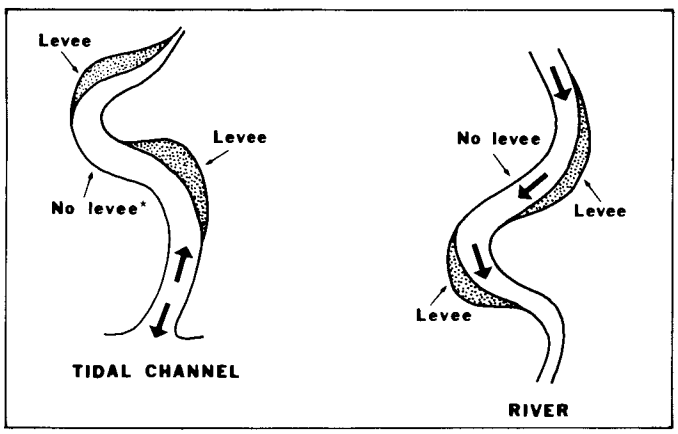

Figure 13.—Comparison between tidal and fluvial channel. In a tidal channel levees are built by flooding tide and therefore are located at upstream outer bends. The ebbing tide carries little sediment, so downstream outer bends do not develop levees. In a river the water flows only one way, thus levees build at downstream outer bends.

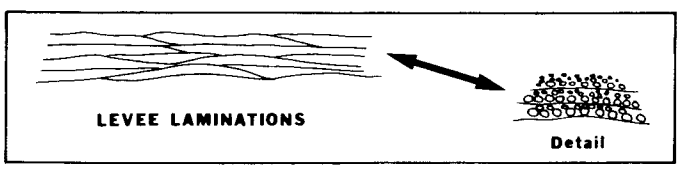

Figure 14.—Graded pellets that form millimeter-thick levee laminations are lenses that extend laterally only a few centimeters at most.

Lateral migration of channels results in continual destruction as well as construction of levees, making levees temporary features. Important implications of levee migration are discussed below.

The construction of levees influences the rest of the system because they act as dams, retarding or preventing drainage of the intertidal zone so that permanent ponds develop. The intertidal and subtidal environments to be discussed later are profoundly influenced by levee development. Levees are also important locations for diagenetic features to form, including dolomite (see below).

Beach ridges. The beach ridge parallels and separates the channeled intertidal belt from the subtidal zone offshore. On a windward-facing tidal flat, the beach ridge is usually better developed and would appear as an offshore barrier island. On the leeward, relatively low-energy side of Andros, however, the beach ridge is only an exaggerated levee (figure 16). The ocean acts essentially as a tidal channel. In many places the beach ridge bends around to parallel major tidal channels and transitionally becomes a levee.

The major differences between levees and the Andros beach ridge is scale and grain size. The beach ridge is at least 30 cm higher than the typical levee, and the distance between the shoreline and the point where it slopes landward toward the intertidal zone is several times greater. As on the levees, the sediment consists of sand-size soft pellets, but the grain size is slightly larger.

Like levees, the beach ridge along the northwest side of Andros Island is slowly but constantly migrating. The seaward side erodes, creating small 30-cm-high cliffs, while active

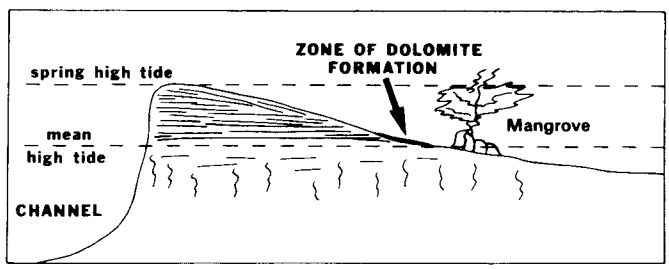

Figure 15.—Cross section of channel levee. Note laminated part of levee is above mean high tide but within the range of spring and storm high tides. Sediment below mean high tide is burrowed. Dolomitic crusts form on the flanks of levee at approximately mean high tide or slightly higher.

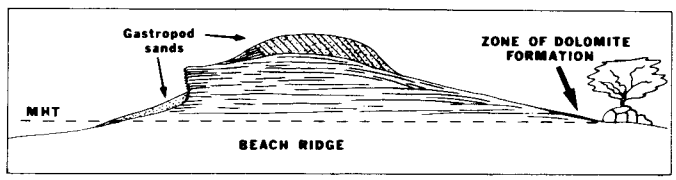

Figure 16.—Cross section of beach ridge which is basically same as levee. Dolomite forms in same elevation as levee on back side and the seaward side is eroded. Major difference is gastropod sands deposited during storms, which are often crossbedded with major dip direction toward land. Mean high tide (MHT).

sedimentation occurs on the back or landward side of the ridge. This combination of sedimentation on the lee side and erosion of the seaward side results in laminated sediment exposed along the seaward cliffs that was originally deposited on the landward side.

In places along the beach ridge, coarse gastropod sand accumulates both on top of the ridge and in small "pocket" beaches where the relatively coherent laminated sediment forms small headlands (figures 16 and 17). At the toe of the beach, the sediment is muddy and continues as such for many kilometers in a seaward direction. The coarse, porous, shelly accumulations form a narrow, discontinuous band parallel to land, seldom more than 30 cm thick. This orientation contrasts with the porous gastropod sands in channels which are oriented more or less perpendicular to the shore.

Dolomitic crusts are diagenetic features that form on both the back side of levees and on the back side of beach ridges. Where the beach ridge has been extensively eroded and migrated landward, dolomitic crusts become exposed near the base of the eroded cliff. Storm waves have in many places

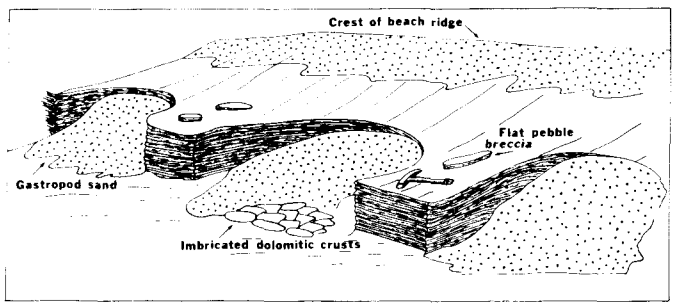

Figure 17.—Sketch showing typical Andros Island beach ridge with eroded "spurs" and pocket beaches lined with gastropod sand, imbricated dolomitic crusts and slabs of laminated redeposited beach ridge sediment.

fragmented and concentrated slabs of the crust, in places forming imbricated flat-pebble breccias. Such accumulations are generally associated and admixed with the gastropod sands discussed above. Flat-pebble breccias of eroded but uncemented, laminated beach-ridge sediment are also common.

Intertidal Zone

The intertidal zone is flooded and exposed twice daily, and forms a relatively minor part of the tidal-flat system. Intertidal flats occur in minor areas seaward of the beach ridge, but they are more abundant landward of the beach ridge and adjacent to supratidal levees. Even though small in areal extent, they are widely scattered within the intertidal channeled belt. Basically, the intertidal zone consists of numerous sinuous belts paralleling the meandering levees. They form a transition zone approximately 10 to 30 meters wide between the levees and subtidal ponds which, in turn, are created by the damming effect of levees. One reason the individual belts of intertidal sediment are so narrow is that the total tidal fluctuation is much reduced because the levees prevent complete tidal exchange.

Although some laminations occur in intertidal sediments, most have been destroyed by bioturbation (figure 18); some fenestral voids also exist in the intertidal sediments. The most noticeable features on intertidal flats include mangrove roots, halophyte grass roots, fiddler crab burrows, and the burrows of various worms. Browsing gastropods eat the stromatolites and their browsing destroys surficial laminations. Gastropods thrive here because of periodic wetting and near normal marine salinities.

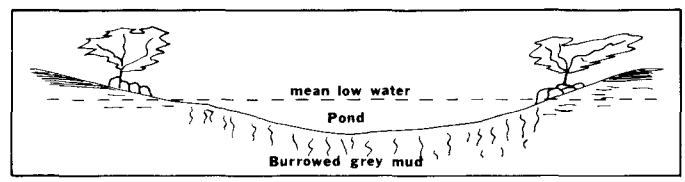

Figure 18.—Cross section of pond formed by channel levees. Sediment in pond is reduced gray burrowed lime-mud lacking laminations. Intertidal sediment flanking pond (shown by the red mangrove) is also burrowed but is oxidized to light tan or cream color.

A major feature of intertidal sediments is color and their cream to light tan color stands out vividly in comparison to the gray, reduced subtidal sediments.

Although minor overall, the most extensive intertidal zone occurs at the inner banks of channel bends where the accreting inner banks are not influenced by the damming effect of levees and are exposed to the same tidal fluctuation as the channels. For this reason the intertidal zone adjacent to meanders supports the most well-developed mangroves. Where the mangroves surround ponds, they are stunted and seldom more than 1.5 m high, but those at inner bends of channels may be 5-10 m high. Their extensive root systems almost completely destroy primary sedimentary structure.

Subtidal Zone

Subtidal sediments vary greatly but occur in three main areas: in ponds, in channels, and offshore. The characteristic features of subtidal sediments are their gray color due to sulfate-reducing bacteria (in fine-grained sediments) and an almost complete lack of sedimentary structures; in addition, reduced sediment has the characteristic rotten egg odor of H_2S.

Coarse-grained sediments, which are restricted to tidal channels, also may have an odor of H_2S but generally lack the gray color. Mixed with almost all the nonreduced coarse-grained sediment, however, are black to gray grains which give the sediment a salt-and-pepper appearance. The presence of "salt-and-pepper" sands in tidal channels, especially at the base of the sequence, appears to be universal. The exact origin of the darkened grains is not clear (probably reduced iron), but they have been buried within reduced fine-grained sediment before being winnowed and concentrated wtih other nondarkened grains in the channel-lag deposit.

Tidal channels. The most important subtidal zone within the tidal flat consists of tidal channels. They are important

because (1) they are the main supply route for offshore sediment entering the tidal-flat system; (2) they allow daily exchange of more normal marine water and promote drainage of rainwater from the flats; (3) they are the sites of the most porous and permeable sediments within the tidal flat; and (4) through the building of levees, they control the locations of ponds, the other major subtidal zone within the tidal-flat system.

Like their siliciclastic counterparts, tidal channels in carbonate tidal flats meander and migrate (figure 19). All the major or main channels on the Andros flats cut down to the underlying bedrock; thus, the record deposited by laterally migrating channels begins at the Pleistocene unconformity. The record of channel migration is that of a modified point bar (Shinn and others 1969; Hardie 1977; Shinn 1983).

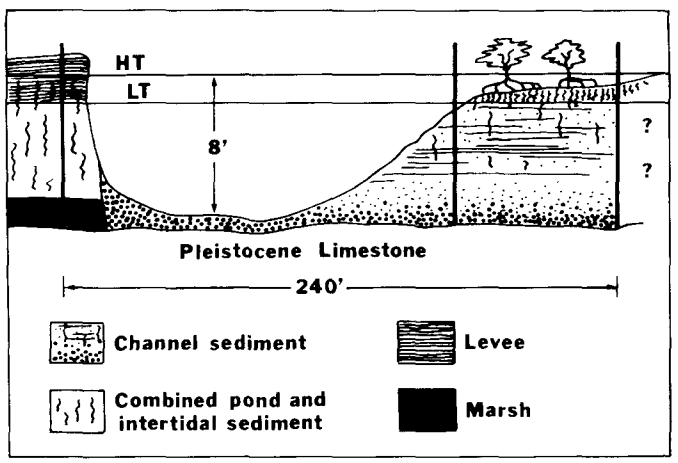

Figure 19.—Cross section of a migrating tidal channel. Vertical lines represent core locations. Note migration is to left, and channel erodes and removes levee, intertidal and subtidal sediment, as well as old marsh deposit at base. Pleistocene bedrock prevents further deepening. The record produced consists of graded gastropod sand, commonly containing fragments of dolomitic or laminated levee sediment, grading upward into burrowed gray subtidal muds overlain by burrowed oxidized intertidal sediment. High tide (HT). Low tide (LT). (After Shinn 1983, reproduced with permission from AAPG.)

The base of this modified point-bar sequence begins with a graded bed consisting principally of gastropod and foraminiferal gravel with an admixture of slabs and chips of dolomite crust, fragments of laminated levee sediment, and rarer fragments of the underlying Pleistocene bedrock. Generally, rock fragments and chips of levee sediment and dolomitic crusts are present only in the bottom 5-10 cm of the sequence. Gastropod and foraminiferal sand up to 1 meter thick overlies the basal portion, and this, in turn, grades upward into pelleted, gray, reduced and burrowed sediment. The gray, fine-grained sediment generally grades upward into oxidized, highly bioturbated, fine-grained sediment within the intertidal zone. The mangroves that proliferate on intertidal point-bars are responsible for much of the bioturbation.

The gastropod-sand portion of the point-bar sequence is composed mainly of whole centimeter-long gastropods and soritid foraminifera having a diameter of 2-3 mm; these sands may be crossbedded. Ideally, the entire point-bar sequence should be bedded and should contain crossbedding, and commonly the basal coarse-grained portion is crossbedded. Due to the abundance of burrowing organisms and plant roots, however, a channel deposit containing the classic point-bar sequences of lamination is rarely present. The point-bar sequence which is restricted to channel meanders represents the most porous and permeable sediments within the tidal flat (figure 20). The straight portions of tidal channels contain less coarse material, but gastropods and foraminifera are still present in greater numbers than in the sediments adjacent to channels.

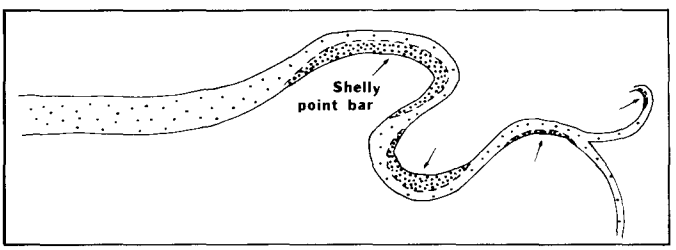

Figure 20.—Sketch showing location of gastropod sands of flood tide point bars. Location is same for large main channels and smaller gullies into which channels grade.

Much of what is known about the Andros tidal channel sequences comes from coring abandoned channels. Channels become abandoned when one channel migrates to a position where it can capture the water flow of another tidal channel. Once tidal flow is reduced, fine-grained sediment rapidly chokes the channel and the porous point bars, and channel lags are buried beneath less permeable, fine-grained sediment. When infilling sediment reaches the intertidal zone, the nearly filled channel is invaded by stunted red mangroves. Eventually the mangroves die when sedimentation is sufficient to reach the supratidal zone. Levees on either side of channels are also preserved when a channel becomes abandoned.

Lateral channel migration of more than 30-50 m has not been documented by coring. It appears that migration has not proceeded farther because of insufficient time. First, the flats have only existed 3,000-5,000 years because of rising sea level, and second, the zone of active channels has been migrating landward as the tidal flat complex retreats and onlaps the land. Given stable sea-level conditions and more time, tidal channels would repeatedly migrate and remigrate over the same area many times, resulting in a sheet-like deposit of porous and permeable sediment. The sheet of channel sands would directly overlie the Pleistocene bedrock. Continual migration also implies that supratidal levees and the dolomite that forms there would be continually reworked and recreated, resulting in a gradual increase in dolomite concentration within channel deposits. This aspect of channels will be discussed later when we attempt to project into the future.

Smaller channels and gullies seldom cut down to Pleistocene bedrock and are generally underlain by the older supratidal marsh. These small channels and gullies, however, do migrate laterally and deposit porous and permeable gastropod-rich channel lag deposits.

Ponds. The ponded areas trapped between levees and the intertidal flats are seldom exposed to air; thus, the sediments are burrowed, lack sedimentary laminations, and are reduced. These gray, reduced, fine-grained sediments contain some whole gastropods and a considerable amount of soritid foraminifera. Foraminifera live in the ponds, generally attached to mangrove leaves that litter the bottom, and are preserved there when they die. Pond sediment is usually no more than a meter thick. Subtidal pond sediments usually rest on underlying supratidal marsh sediment, but because their location is controlled by the location of shifting tidal channels, they may eventually come to rest on sediments deposited in other subenvironments. In general, pond sediments are fine-grained and highly bioturbated. These sediments contain some mottling of oxidized intertidal sediment, especially near pond margins, but otherwise they are almost identical to the adjacent offshore subtidal sediments.

Offshore adjacent marine subenvironment. The offshore environment is the largest subenvironment, although not actually a part of the tidal-flat sedimentary record at northwest Andros because there the flats have been retreating and building a net onlap or transgressive sequence. On southwest Andros, however, the flats have built seaward (offlap) so that offshore marine sediments have become incorporated into the tidal-flat sequence.

The offshore sediments west of Andros are highly burrowed, gray, reduced pelletal muds containing miliolid and soritid foraminifera and scattered darkened grains. The major burrower is the ghost shrimp *Callianassa*, which makes characteristic lined tubular burrows (figure 21). Sparse *Penicillus* sp. and *Rhipocephalus* sp., two related blue-green algae, turtle grass and eel grass are in this zone. Some scattered *Halimeda* plants are present and their abundance increases farther offshore.

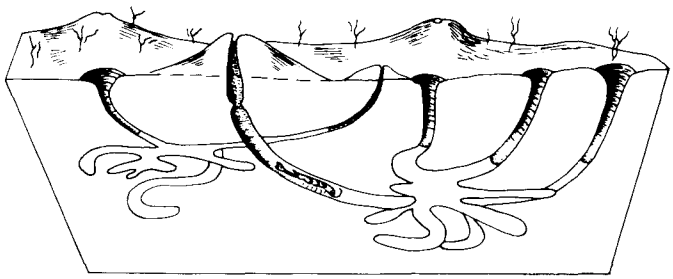

Figure 21.—Cutaway view of offshore marine sediment showing *Callianassa* shrimp burrows which convert the sediment into a Swiss cheese of galleries. Mounds are located at excurrent tunnels. Water enters funnel-shaped openings.

The offshore sediments extend seaward (westward) at least 100 km to the west edge of the Great Bahama Bank. Beginning between 10 and 20 km offshore, the soft pellets that compose the mud transitionally become harder and an abundance of faunal components such as foraminifera, mollusks, and algae (mainly *Halimeda*) increases slightly. In general, grain size of the sediment becomes slightly coarser than are the muddier sediments within 10 km of the tidal flats. Even farther seaward, the pelletal components become thoroughly cemented to form a sediment packstone/grainstone. Although the individual pellets are hard, they are not cemented together to form rock as in the Persian Gulf. Directly west and southwest of the tidal flats, at a transitional point approximately 10 km from the west edge of the bank, the sediment becomes more skeletal and becomes a coralgal grainstone. To the northwest of the Andros tidal flats, where the bedrock is shallower, the sediments comprising the westernmost 10 km of the bank are oolitic. The ooid sands form extensive banks that are awash at low tide. All the marine facies except the ooids are extensively burrowed by the shrimp *Callianassa*. Conceivably, in time, given sufficient accretion, all the various facies on the Bahama Bank will be capped by tidal-flat facies.

The offshore marine environment is important because its fine-grained equivalents in ancient sequences could contain organic matter and form a source for hydrocarbons. Oil and other fluids migrating updip could become trapped within porous subenvironments of a tidal-flat sequence.

Results from coring have shown that the supratidal marsh sediments extend seaward under the intertidal channeled belt, the beach ridge, and at least 1 km offshore beneath subtidal sediment (figure 22). Offshore, the supratidal marsh sediments are 2-4 m below sea level and thus document the effect of rising sea level. Clearly, the entire tidal-flat complex existed farther seaward from its present location in the past, when sea level was a meter or more below present level.

SOUTHWEST ANDROS

Evidence for Accretion

The flats take on a different character south of the western tip of Andros Island. There the trend of the tidal flat changes from northeast-southwest to a northwest-southeast orientation (figure 23). Gebelein (1974) and associates documented seaward accretion along the southwest shore. Cores and excavations show offshore subtidal sediments beneath the flats, and there are several preserved beach ridges landward of the most recent beach ridge. The preserved ridges are somewhat analogous to the well-known cheniers of the Mississippi Delta. Seaward of the shoreline, the water is so shallow that one has to travel several kilometers offshore to reach water deeper than 1 m.

A feature not present in the northwest tidal flats is the so-called "cabbage palm hammocks." Palm hammocks are sediment highs populated mainly by cabbage palms, but they also contain grasses, tropical hardwoods, and exotics such as orchids (figure 23). The highs on which the palms and associated plants grow were created in two ways—as abandoned beach ridges formed as the flats accreted seaward, and as levees along former tidal channels. The former lie parallel to the shore and the latter are oriented mainly perpendicular to the shore. The supratidal flanks of palm hammocks are generally coated with a dark dolomitic crust which has the appearance of an old asphalt road. Dolomite content of these crusts is greater than any present in the active channel area of northwest Andros, probably because the flanks of palm hammocks are more stable and there has been more time available for dolomitization to take place.

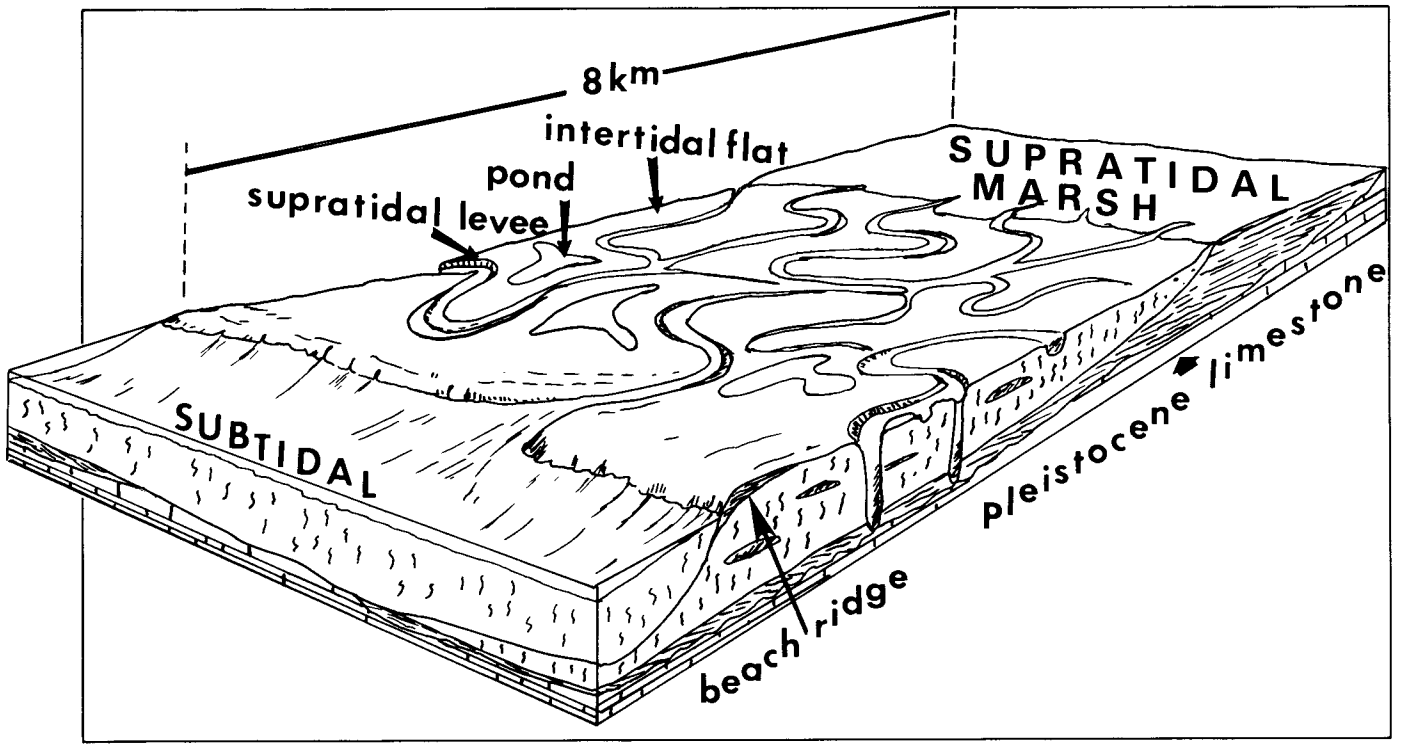

Figure 22.—Diagram showing major depositional environments and onlap of supratidal marsh deposits. Note that marsh sediment extends offshore beneath marine sediment, producing a transgressive or onlap of sedimentation sequence. (After Shinn 1983, reproduced with permission from AAPG.)

Channels along the southwest Andros tidal-flat belt are fewer in number than on the northwest coast, and the ones that exist there are broad and very shallow. Most are only a few centimeters deep, 1 m at most. Whether there are significant porous channel lags in this area is not known. Clearly, there has been a major change in the past few thousand years at southwest Andros. Channels were active in the past, as evidenced by extensive levees (now palm hammocks), and Williams Island (the large mud island at the western tip of Andros, figure 24) is clearly an erosional remnant. The existence of linear palm hammocks (old channel levees), whose trend is the same as those on the southeast coast, show that this island, now 3-4 km offshore, was once part of the southwest Andros tidal-flat complex. The present trend of channels and levees on the northwest Andros flats is approximately 90° to that of the southwest flats.

It seems clear that the northwest Andros tidal flats were once more extensive and extended several kilometers farther offshore than today (figure 24), whereas the southwest flats were less extensive but have been growing seaward. The northwest flats are more exposed to the effects of winter storm winds from the northwest, whereas the southwest coast is in the lee both during prevailing southeast winds and during northwest cold front winds. When sea level was lower, the offshore marine environment was shallower and wave action was retarded so that the northwest flats could accrete seaward. With rising sea level, waves reaching the shore became larger, erosion set in, and the entire package retreated and onlap sedimentation began. The isolation of a portion of the flats to form Williams Island and Billy Island to the west was also a result of rising sea level. The sediment removed from the northwest coast during erosion probably moved southward by longshore drift in response to northwest winds during winter storms. Once sediment-laden water rounds the bend at the western tip of Andros, it encounters quieter, low-energy conditions, allowing sedimentation to occur. The southwest coast probably began accreting seaward at about the same time erosion set in on the northwest coast. A broad bedrock high, where the water depth is as shallow as 1-2 m just west of and extending under Billy Island, probably marks the former western extent of tidal-flat accretion at Andros. Whether the sediment which builds the southwest flats was derived entirely from the eroded northwest flats or came from directly offshore cannot be answered at this time. Regardless of source, the greater abundance of sediment combined with the more sheltered position of the southwest flats led to the choking and filling of tidal channels.

ABACO ISLAND

Tidal flats with many of the same characteristics as those at Andros Island exist on the west side of Abaco Island on the Little Bahama Bank (figure 25). At Abaco, there are fewer tidal channels and sediment thickness is at most 2 m. Although there

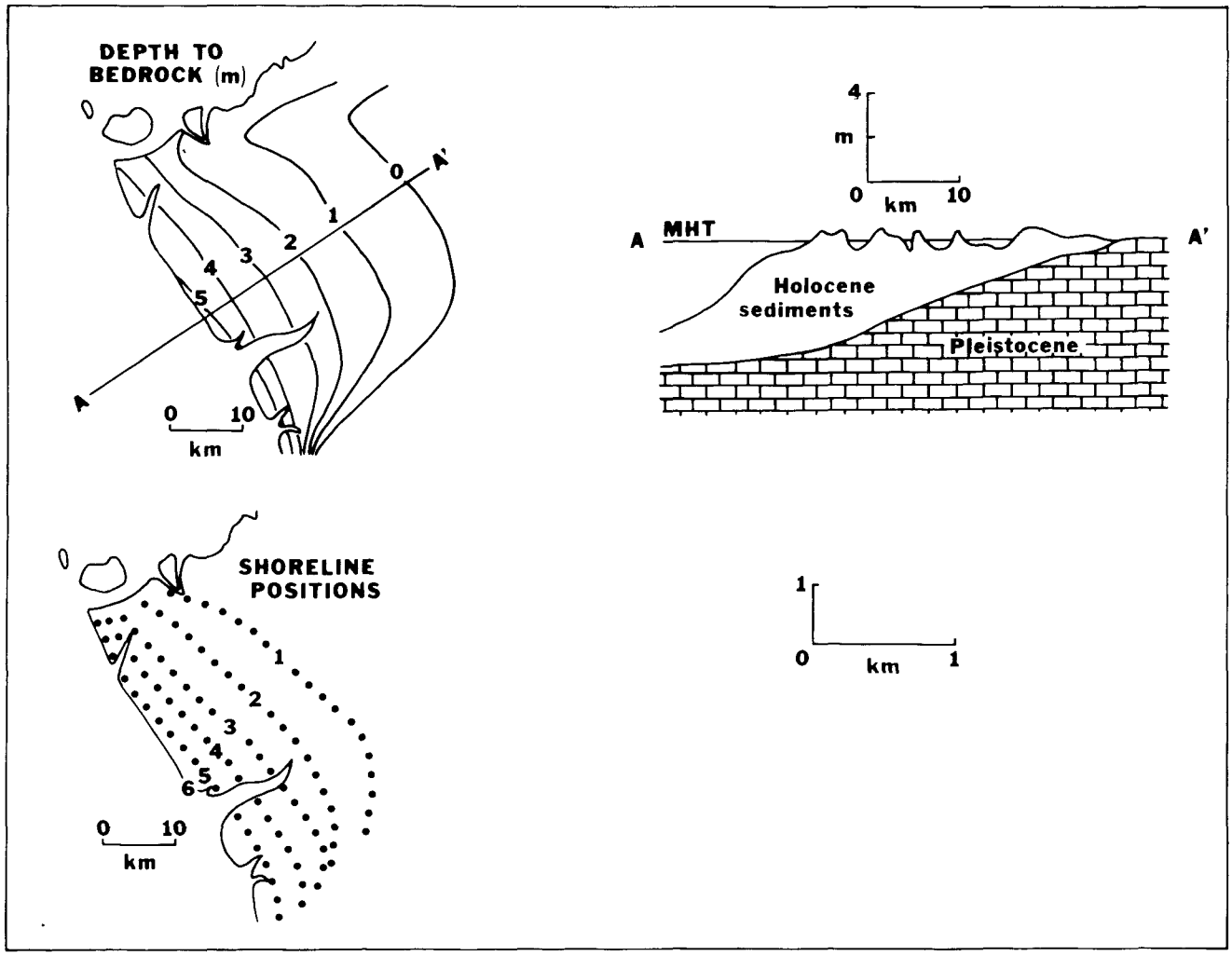

Figure 23.—Details of regressive or offlap sedimentation on southwest coast of Andros Island (modified after the work of Gebelein 1974). Old shorelines, which are beach ridges now populated by palms and called "cabbage palm hammocks," demonstrate seaward accretion. Other palm hammocks (not shown) lie perpendicular to old shorelines along banks of large inactive tidal channels. MHT = mean high tide.

are no published works on the area, observation during several visits by the author suggests that the flats are relatively inactive by comparison with those of Andros.

At Abaco, there are numerous cabbage palm hammocks, and dolomitic crusts surround them just as they do around the hammocks of southwest Andros. Many palm hammocks are surrounded by water seaward of the flats, suggesting extensive transgression and erosion. Though the intertidal channel belt and beach ridge are poorly developed by comparison with those at Andros, it is clear that the conditions which allowed development of the Andros flats, namely low energy in the lee of a Pleistocene island, are the same. Climatically, the two areas are similar, although good rainfall data are lacking for both areas.

CAICOS ISLAND

Caicos Island is on Caicos Bank near Turks Island east of Inagua, which lies at the southern end of the Bahamas archipelago. Caicos Bank can best be described as a miniature Bahama Bank having similar facies changes around the margins and a broad subtidal central area consisting mainly of gray, reduced pelleted mud. The tidal flats are situated in the lee of Caicos Island which occupies the eastern windward side of the platform (figures 26 and 27).

Examinination and coring of a portion of the Caicos tidal flats by the author and ongoing unpublished work by Michael Lloyd, Duff Kerr and Ronald Perkins indicate a sedimentary

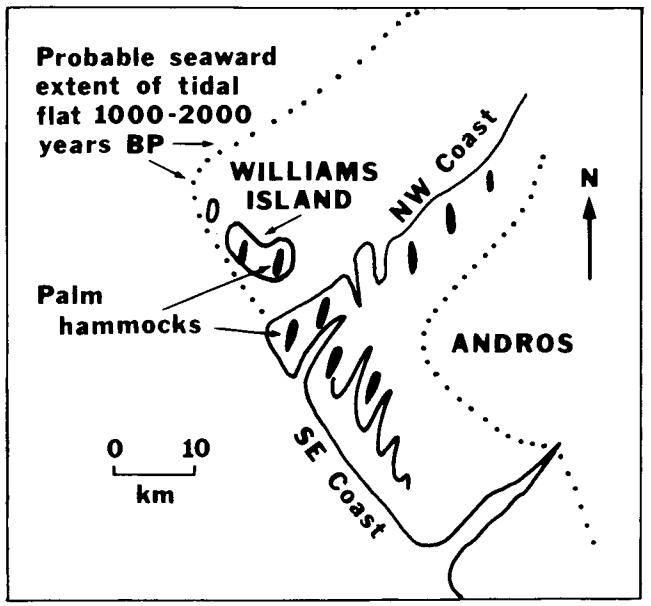

Figure 24.—Western tip of Andros Island. Williams Island is erosional remnant of tidal flat that extended farther to the northwest 1000-2000 years BP. Palm hammocks on Williams Island have same alignment as palm hammocks on tidal flat to southeast. These are not the same palm hammocks that indicate old shorelines as shown in figure 23.

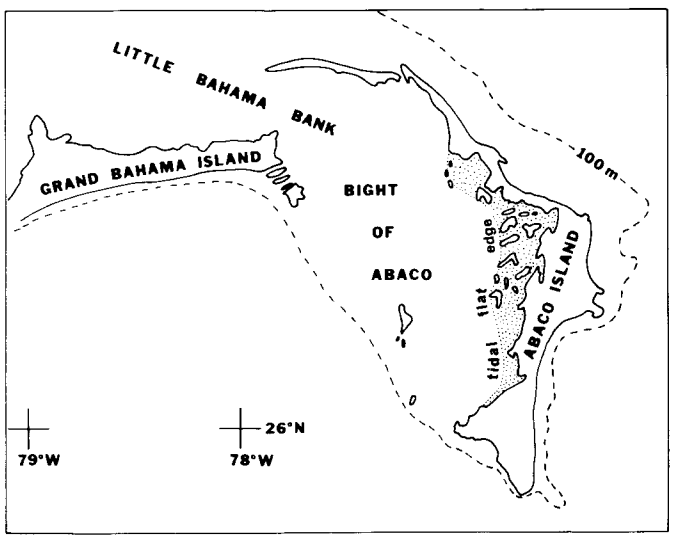

Figure 25.—Portion of Little Bahama Bank showing area of tidal flats in lee of Abaco Island.

facies and geometry almost identical to that of Andros Island. Wanless and Dravis (1984) have also noted similarities with Andros.

Although beach ridges are slightly reduced in size when compared to those of Andros, the intertidal channeled belt and supratidal marsh are almost identical. The supratidal levee, in-

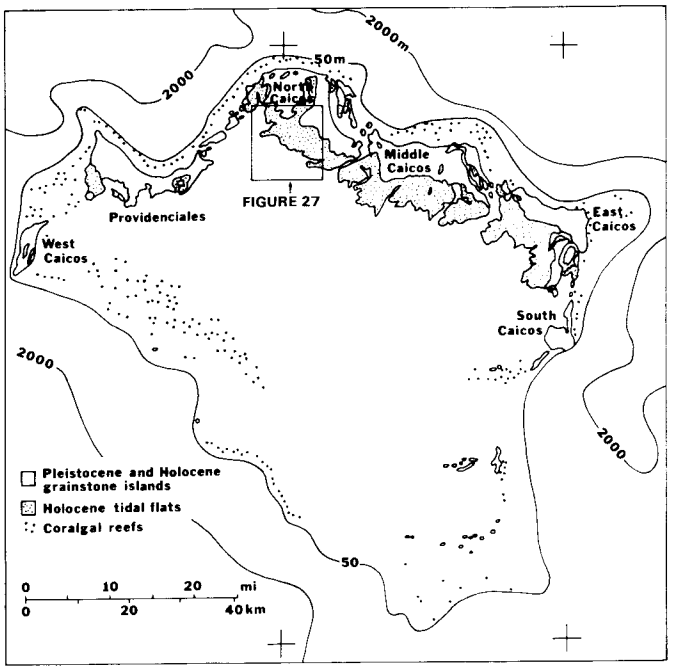

Figure 26.—Generalized facies map of Caicos Bank showing location of tidal-flat deposits in lee of North, Middle and East Caicos Islands.

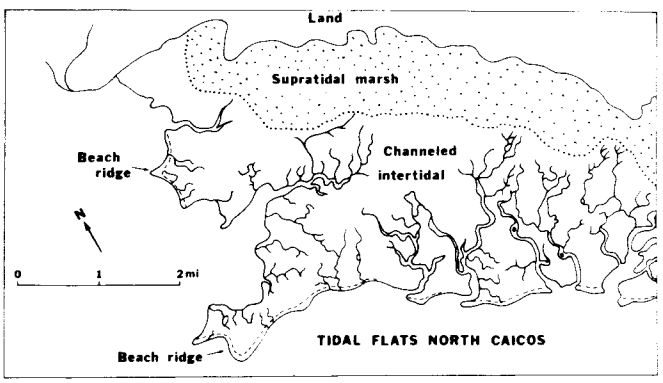

Figure 27.—Detail of area outlined in figure 26. Tidal flats are similar to those of northwest Andros. Note land (Pleistocene eolianite), supratidal marsh and channeled intertidal area which contains tidal channels with levees and point-bar deposits. Beach ridge is present along south shore. Ratio of onlap to offlap sedimentation styles is not known.

tertidal zones bordering the back sides of levees, and subtidal ponds are arranged exactly as they are on Andros. The supratidal marsh is similar and has the same dark algal mats and scattered mangroves and sawgrasses, but the water on Caicos is seldom fresh. Due to a much drier climate and strong trade winds, evaporation at Caicos greatly exceeds Andros. Although the subtidal ponds do not contain evaporites, even though salinites are above normal, there are localized ponds between Pleistocene eolian ridges that contain gypsum. On nearby Turks Island,

solar salt was a source of income to natives for many years and the inactive ponds there still form salt and gypsum accumulations. Nevertheless, the climate is not arid enough to allow preservation of evaporites within the tidal flats. Cores taken on levees, in subtidal ponds, and offshore have no evaporites but contain exactly the same sedimentary features as previously described on Andros.

Arid Tidal Flats—Persian Gulf (Arabian Gulf)

By far the largest and most well known tidal flats are those along the south shore of the Arabian Gulf (figure 28). These arid flats have been extensively studied by Kinsman (1964), Butler (1965), Illing and others (1965), Evans (1966), Kendall and Skipwith (1969), Purser (1973), Purser and Loreau (1973), Scholle and Kinsman (1974), Schneider (1975), and Shinn (1983), to name a few. General sedimentation in the Arabian Gulf, including that on the tidal flats, is recorded by Purser (1973).

In addition to being the most extensive flats to form during the Holocene transgression, the Arabian Gulf example contains a plethora of sedimentary variations. Along the southern shore of the Gulf, the broad flats are several hundred kilometers long and in places more than 15 km wide. The prevailing winds and waves impinge almost at right angles to the flats. Along the north-south-trending eastern shore of the Qatar peninsula, however, wind and waves parallel the flats, causing the formation of a series of shelly beach ridges or spits similar to the cheniers of the Mississippi River delta (Shinn 1973a).

Other variations include the addition of wind-blown quartz and dolomite and the general lack of an extensively channeled intertidal belt, even though tidal fluctuation is 2 m or more. Tidal channels occur along the south shore but are widely spaced and many times larger than those of Andros Island. Some channels are more than 100 m wide near their mouths and as much as 15 m deep. Such channels generally lack the levees so common at Andros, but some small channels in localized areas have small levees composed of sandy sediment. Lack of levees is probably a result of dry climate. Any sediment above the capillary fringe is subject to deflation.

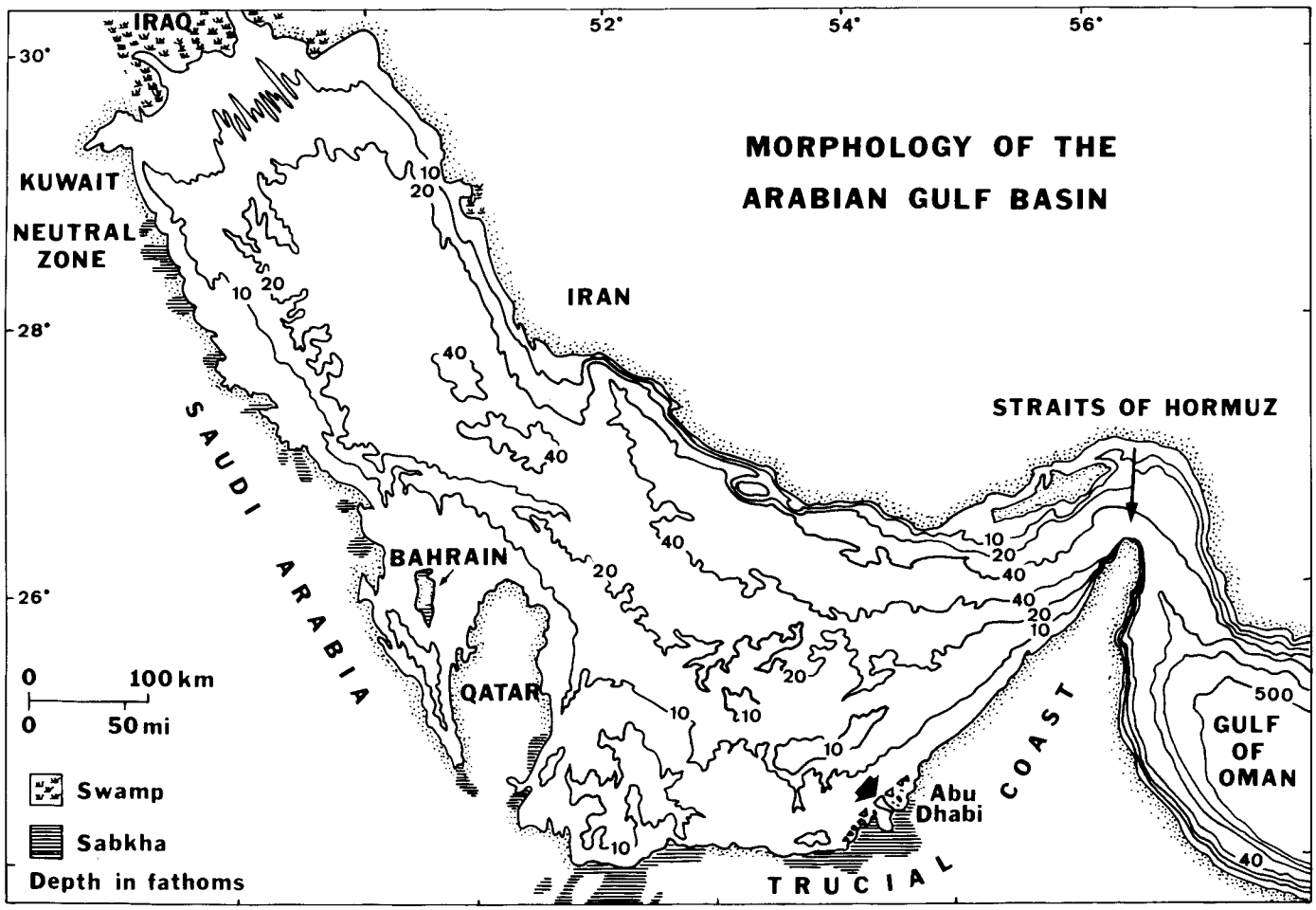

Figure 28.—Generalized map of Persian (Arabian) Gulf showing location of tidal flats, that is, sabkas, along the Trucial Coast and east coast of Qatar Peninsula. Water depth in meters. Modified from Purser and Siebold (1973).

In some respects the flats of the southern Gulf (Trucial Coast) are simpler than those of Andros, because they lack a complicated channeled intertidal belt. The flats build seaward to produce a regressive or offlap sequence. These flats also lack extensive mangroves, and vegetation of any kind is generally lacking on the supratidal flats.

Supratidal Zone

The supratidal zone of the Arabian Gulf is many times more extensive than the supratidal marsh of Andros and is generally referred to as a sabkha (figure 29). Although desiccation is the rule in this arid climate, mudcracks and mud polygons are surprisingly rare. These features are readily apparent on the surface, especially after a storm has deposited fresh sediment, but they do not appear to be abundant in cores or excavations. Once a mud polygon has formed in this dry climate, it is quickly eroded and removed by the wind. On Andros, however, mud polygons remain moist and an algal mat soon covers and protects them. Here, however, the climate is so dry that algal mats are prevented from growing in the supratidal zone, much of which is flooded infrequently and only during storm tides. Annual rainfall averages about 2 cm/year but tends to occur episodically every few years; some years rainfall is almost nonexistent. Large-scale V-shaped or prism cracks do form but are restricted almost entirely to algal mats of the upper intertidal zone.

Although mud cracks are rare in the supratidal sabkha, fenestral vugs form here and in places they are the only diagnostic indicators of supratidal conditions.

Although the sabkha does not contain evaporites everywhere, they are probably the most diagnostic feature when present. Because of slightly more rainfall, anhydrite does not form on the sabkhas of Qatar, but large gypsum rosettes are not uncommon. On the Trucial Coast, however, anhydrite occurs both as layers and as massive accumulations containing nodules separated by sediment and organic material, giving them a "chicken wire" fabric (figure 30). The layered anhydrite is generally contorted and forms small 30- to 40-cm-high diapirs (figure 30).

The sabkha, like the marsh at Andros, forms a wedge which thins landward on older rock of Tertiary age. Unlike Andros, however, this wedge tends to merge with quartz sand, and the transition is generally buried beneath large dunes of quartz sand. Migrating sand dunes, which cover the landward portion of the sabkha as it progrades seaward, are thought to be important for the preservation of the sabkha. They prevent desiccation and removal of sabkha sediment by wind (figure 31).

Beach ridges. The beach ridges along the Arabian Gulf are not as muddy as at Andros; they are sandy and have extensive beaches. Along the Trucial Coast, these beach ridges are analogous to the barrier islands of siliciclastic environments. These beach ridges may lie at the seaward edge of the flats or as distinct barrier islands separated from the flats by a shallow lagoon of variable width. Along the Trucial Coast, many of the barrier islands are so large (kilometers wide and tens of

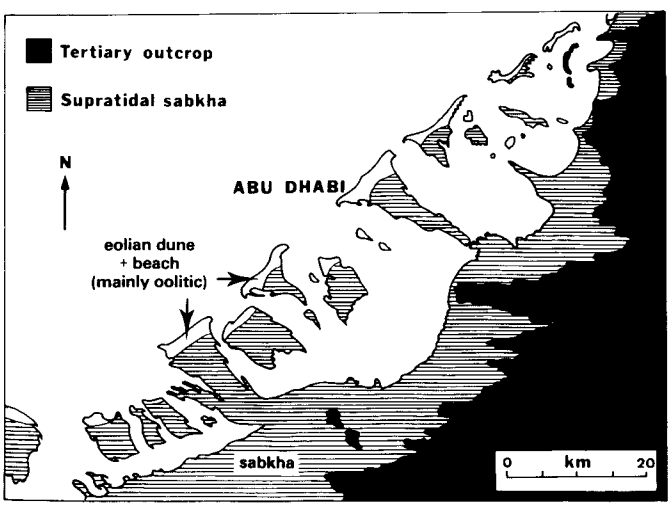

Figure 29.—Detail of classic tidal-flat area near Abu Dhabi on the Trucial Coast. Modified from Purser and Evans (1973).

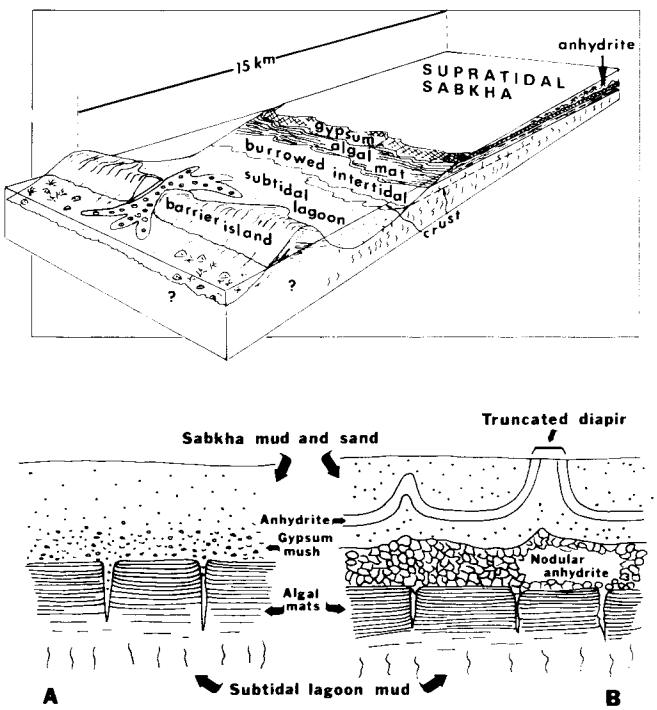

Figure 30.—Above: Major environments of Trucial Coast offlap (regressive) tidal flats. Note oolitic tidal delta between barrier islands and coral reefs seaward of barrier islands. Below: Detail sketches show relationship between algal mats, subtidal muds and evaporites obtained from a pit dug a few hundred meters landward of gypsum mush zone (A) and a pit dug 1,000 m or more from gypsum mush zone (B). Note gypsum has converted to nodular, banded, and enterolithic anhydrite. Note truncation of anhydrite diapir. Prism cracks in algal mat zone are filled with gypsum (at left) and mostly anhydrite (at right). (After Shinn 1983, reproduced with permission from AAPG.)

kilometers long) that they have well-developed tidal flats on their landward sides, facing the lagoon which separates the islands from the mainland tidal flats.

The sediments of the beach ridges and barrier islands consist of whole gastropod sand and gravel and skeletal sand derived from the breakdown of gastropods. The cerithid gastropods occur by the billions and are almost identical to the smaller variety at Andros.

Like the tidal flats themselves, the beaches tend to accrete seaward (figure 32). When they accrete, winds rework the sediment, forming small 1- to 2-m-high sand dunes. The small dunes are mostly plant-controlled and have a clump of small desert bushes or weeds at the seaward side.

The Trucial Coast barrier islands tend to shift laterally in step with large migrating tidal channels. Hook-shaped spits form at the ends of barriers adjacent to the channels. Longshore drift and the development of spits on the south coast are minor and nowhere approach the development of those that occur along the east coast of the Qatar peninsula.

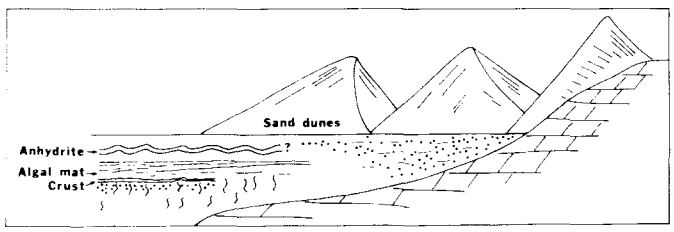

Figure 31.—Landward portion of sabkha showing vertical facies changes that result from offlap of depositional zones. Large quartz sand dunes commonly bury the sabkha deposits, thus preserving them from erosion.

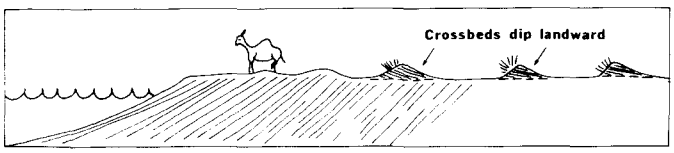

Figure 32.—A seaward-building barrier island. Note seaward dip of accretion beds in barrier deposit which is capped by small plant-controlled dunes with landward dipping beds.

Intertidal Zone

The intertidal zone is relatively narrow but contains features important for the identification of tidal flats. The intertidal zone occurs as a relatively simple belt parallel to the sabkha, seaward of the mainland flats and in places landward of the barrier islands (figures 33 and 34).

The upper part of the narrow intertidal flats is made visible by a black algal mat as much as 30 cm thick. These mats are extremely well-laminated. Individual laminae within the gelatinous mat consist of thin layers of wind-blown dust or storm-derived sediment brought in during flooding. Large V-shaped cracks form polygons a meter or more across. Some of the cracks are filled with sediment, but more commonly they are either healed by subsequent algal growth or infilled with gypsum (figure 35).

Toward the subtidal zone the algal mat gradually disappears and merges downward with gray, reduced muds or cemented skeletal sands. A gypsum mush consisting of individual crystals one to several millimeters across increases in thickness toward the sabkha in a landward direction. This mush can be as much as 30 cm thick and alters to anhydrite when buried beneath the sabkha.

The lower part of the intertidal zone lacks algae, due mainly to the presence of grazing cerithid gastropods. Algae are present, however, in the upper part of the intertidal zone due to exclusion of gastropods which avoid the hypersaline brines. Where they are of sand size, these lower intertidal sediments are generally cemented to form extremely hard crusts several centimeters thick (figure 36). Lagoonward, where the sediment is generally more muddy, cementation ceases and the sediment merges with burrowed subtidal sediment.

Initially, the algal mat section of the lower intertidal, as well as the upper part of the underlying subtidal lagoonal sediment, lacks evaporites. As the flats accrete seaward and become capped by supratidal sabkha sediments, evaporation becomes more important and large gypsum rosettes as much as several centimeters across precipitate within the algal mat and upper subtidal sediment. The gypsum mush above the mat converts to anhydrite and additional anhydrite, derived from occasional storm floodwater after evaporation, contributes to the expanding anhydrite zone.

Subtidal Zone

Subtidal sediments have variable grain size depending upon their position within the tidal-flat complex. Along the Arabian Gulf there are two dominant environments of subtidal sedimentation: within lagoons behind the barrier islands, and in front of or seaward of the barrier islands (figure 37).

The gray, fine-grained reduced muds are identical in gross appearance to the Andros Island subtidal muds and are restricted to the low-energy lagoons. As one would expect, the muddier sediments are in the deepest part of the lagoon, which generally is not more than 2 m deep. Subtidal sediments are more coarse grained in shallower water near the margins of the lagoon because they are exposed to more wind and wave action. Where there is shelter from waves, the sediment remains muddy.

In those areas where the lagoon is wide (1 km or more), there is sufficient fetch and wave action to winnow sediment in the upper part of the subtidal zone. These sediments are sandy but contain an admixture of mud. Such accumulations are thin, usually not more than 30 cm thick, and they are underlain by muddy subtidal lagoonal sediment. Almost invariably the upper 2-10 cm of this sand-sized sediment is cemented to form a hard pavement. This pavement invariably contains polygonal fractures produced by swelling. Swelling results in the formation of tepee structures. When seen from the air, the pattern of the tepees forms polygons tens of meters across (figure 38).

These relatively impermeable crusts become part of the sec-

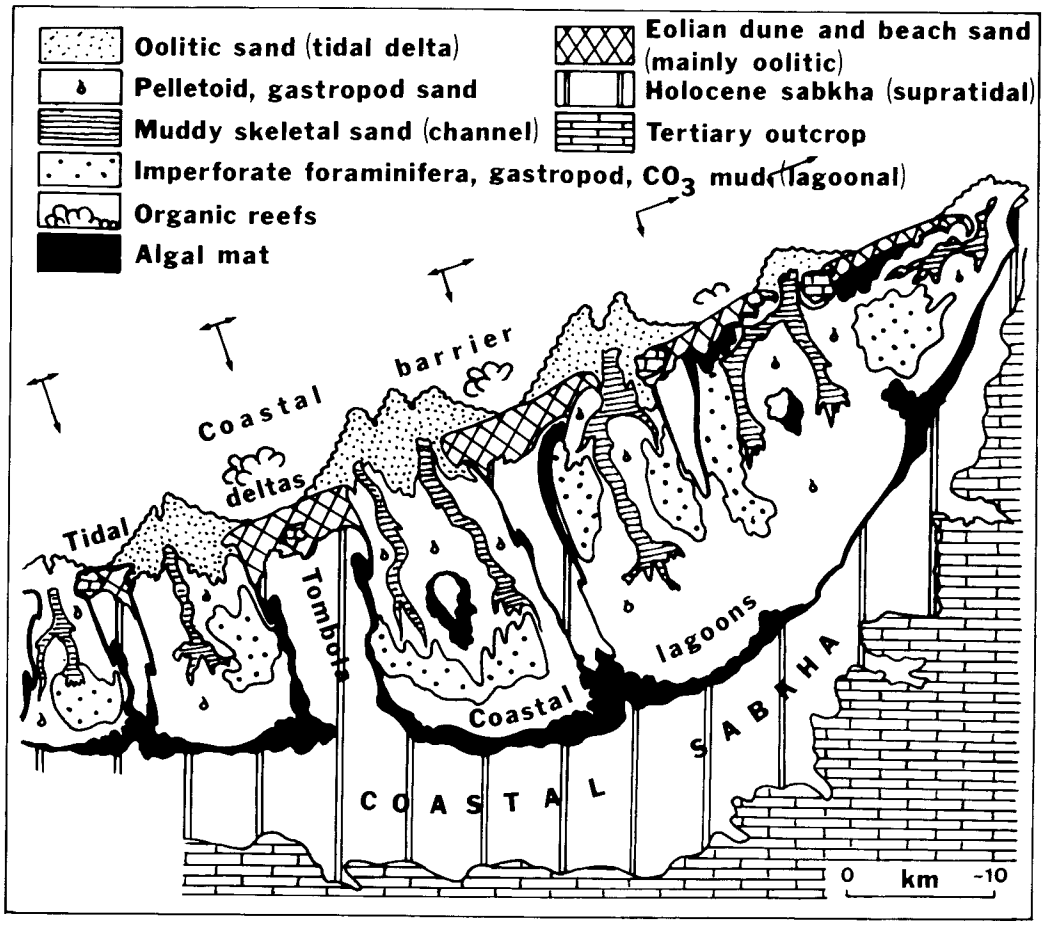

Figure 33.—Detailed depositional facies of Trucial Coast tidal flats near Abu Dhabi. Offshore arrows show degree and direction of longshore drift. Modified from Purser and Evans (1973).

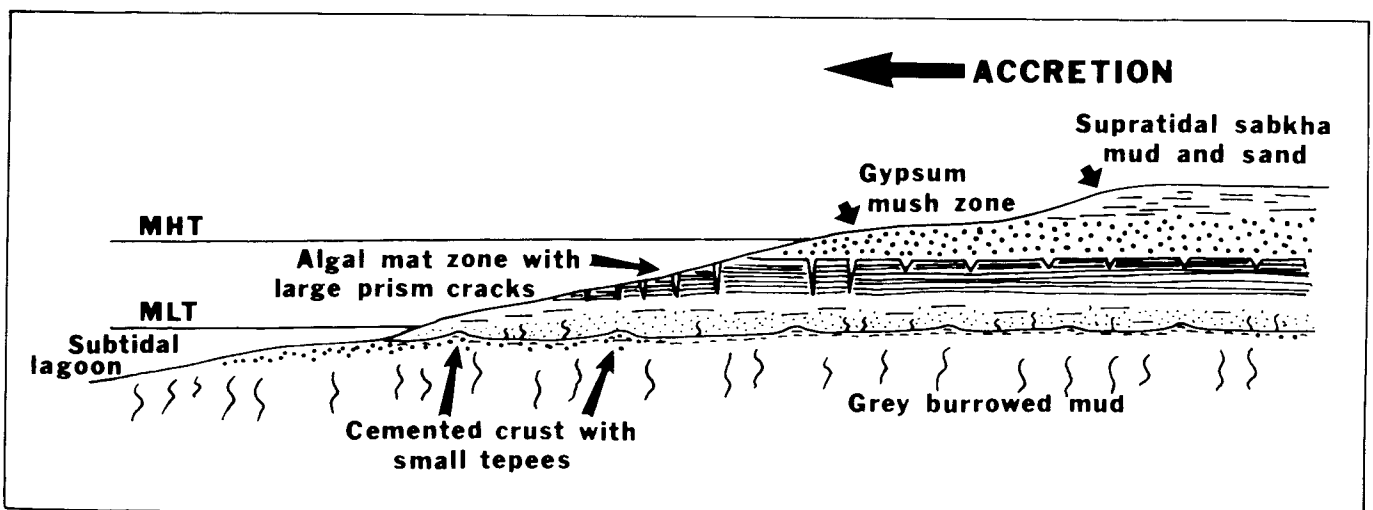

Figure 34.—Schematic cross section of accreting sabkha behind offshore barrier island system. Note sediment sequence in ascending order: (1) cemented subtidal sediment with tepee structures, (2) sand and muddy intertidal sediments, (3) accreting algal flat, (4) gypsum mush, and (5) supratidal mud and sand of the sabkha. Farther landward, gypsum grades into anhydrite. See details in sketch in figure 30. MHT = mean high tide; MLT = mean low tide.

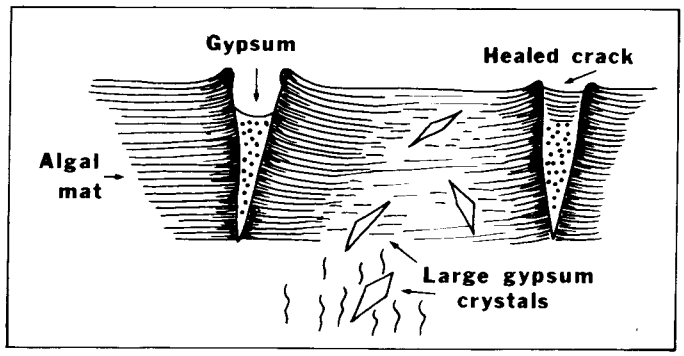

Figure 35.—Details of prism crack healing in algal mat zone. Large gypsum crystals several centimeters in length are preserved even after the gypsum mush within and above the prism cracks converts to anhydrite.

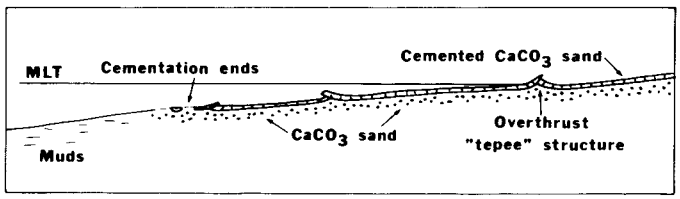

Figure 36.—Cross section showing detail of intertidal and subtidal cemented crust showing tepees and overthrust structures. Muddy sediment underlies coarser cemented sediment. Toward the lagoon, winnowed carbonate sand grades to mud which is not cemented. MLT = mean low tide.

tion as the flats accrete seaward and can form important barriers to the vertical movement of fluids. For example, a 10-m-long trench dug through the sabkha down to such a crust remained dry even though well below the water table. When a hole was made in the crust, water spurted up and the trench filled with water to a level approximately 40 cm above the crust (Shinn 1983) (figure 39).

Seaward of the barrier islands, within the Arabian Gulf itself, the sediment is sand size with coral reefs growing in numerous locations. The sediment is generally cemented. In this zone cementation is truly of submarine origin and extremely hard rock can form to a water depth of at least 30 m. The rock in this area is in the form of crusts 10-30 cm thick, and there are multiple crusts separated by 1 or 2 cm of uncemented sediment. Each crust is generally bored and slightly eroded on the upper surface; the surfaces are disconformable (figure 40).

Cementation of subtidal sediment produces a hard surface which is required for the establishment of corals; thus, distribution of most of the coral reefs in the Arabian Gulf is controlled by cementation. These offshore crusts and coral reefs exist in water depths ranging from the low-tide mark to as much as 30 m (figure 41). Generally, however, the zone between 0 and 5 m of water seaward of the barrier islands or beaches lacks the crusts or coral reefs, because storm waves continually disturb sediment and break up cemented crusts in that zone before they can form. Once beyond 5-m depths, crusts can be extensive and continue to much greater depths. Shinn (1969) estimated

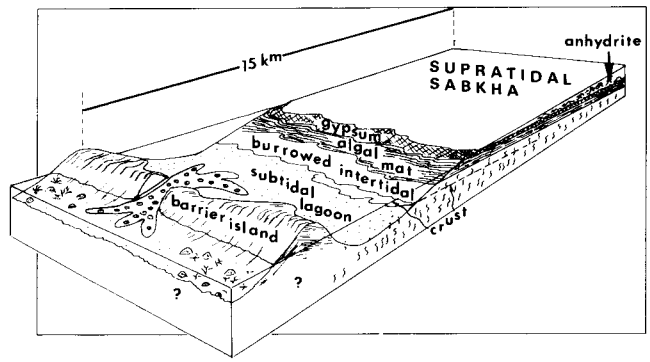

Figure 37.—Persian Gulf offlap model showing all major environments.

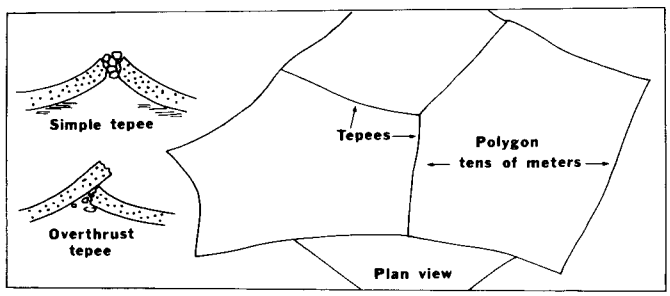

Figure 38.—Polygons (visible on aerial photographs) formed in cemented subtidal and intertidal carbonate sands by expansion, which results in tepees and overthrust structures.

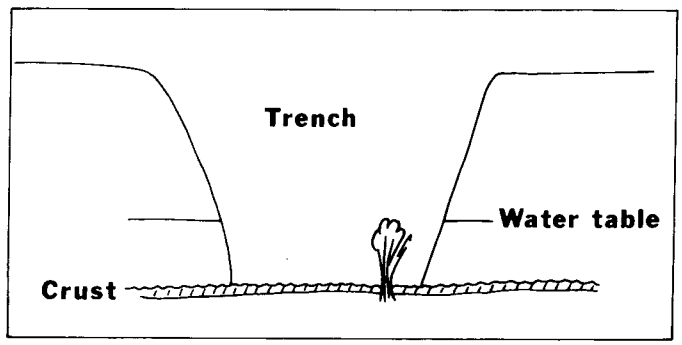

Figure 39.—Impermeable subtidal crust exposed in trench dug in sabkha. Note location of water table which caused water to spurt through hole hammered through crust. Color photograph of trench is shown in Shinn (1983, page 197, figure 41).

that individual layers of cemented sediment could be traced continuously for more than 100 km in the offshore environment of the Arabian Gulf.

If the tidal flats accrete seaward, then subtidal lagoon sediment along with its cemented crusts becomes buried beneath the intertidal and supratidal environments. If accretion continues, eventually the offshore sediments, including coral reefs, will be buried and become capped by the tidal-flat sequence. The offshore cemented crusts with their disconformable sur-

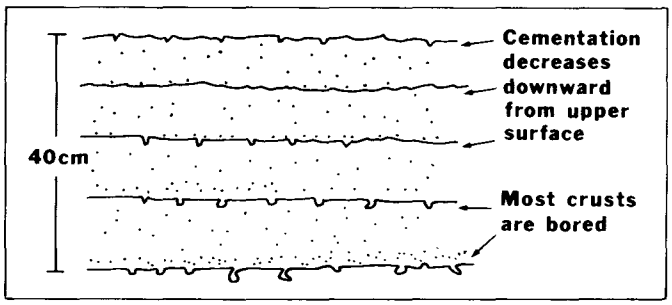

Figure 40.—Superimposed submarine crusts in offshore environment seaward of tidal-flat areas. Note bored upper surfaces and downward decrease in cementation in each crust.

faces will be overlain by barrier-island sands in the more seaward parts of the sequence, while similar crusts of the shallower lagoon will be capped by intertidal algal mats and supratidal sabkha deposits. This sequence of tidal flat building, modified from Purser (1973), is shown in figure 42.

Siliciclastic barrier islands may grow by jumps due to the development of offshore bars. In the carbonates of the Arabian Gulf, jumps might also be caused by the shoaling-upward of offshore coral reefs. It is expected, therefore, that the barrier-island beaches will not continue to accrete seaward and form broad sheet sands, but rather a new barrier island will spring up offshore. Such barrier island development will produce a new lagoon where tidal-flat sequences can begin to accumulate. Given stable sea level for a million years or more, continuation of this process will most likely result in a much more complicated mosaic of deposits than the simple model generally proposed. Nevertheless, one should expect the development of belts of porous, permeable sands parallel to the basin margin. The sequence of coral reef and barrier island accretion is shown in figure 43.

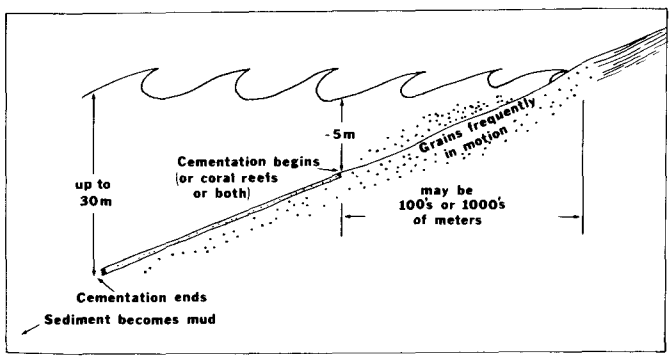

Figure 41.—Schematic distribution of cementation in the Arabian Gulf. On exposed coasts, grains are frequently moved and extensive cementation does not occur down to a depth of about 5 m. Carbonate sands are less frequently affected by wave energy below 5 m and cementation starts. Cemented crusts extend in places down to approximately 30 m of water depth, where sediment becomes muddier. Commonly several crusts are superimposed as in figure 40. Cementation is mainly restricted to sand-size sediment. Offshore cementation may extend parallel to shore for 100 km or more.

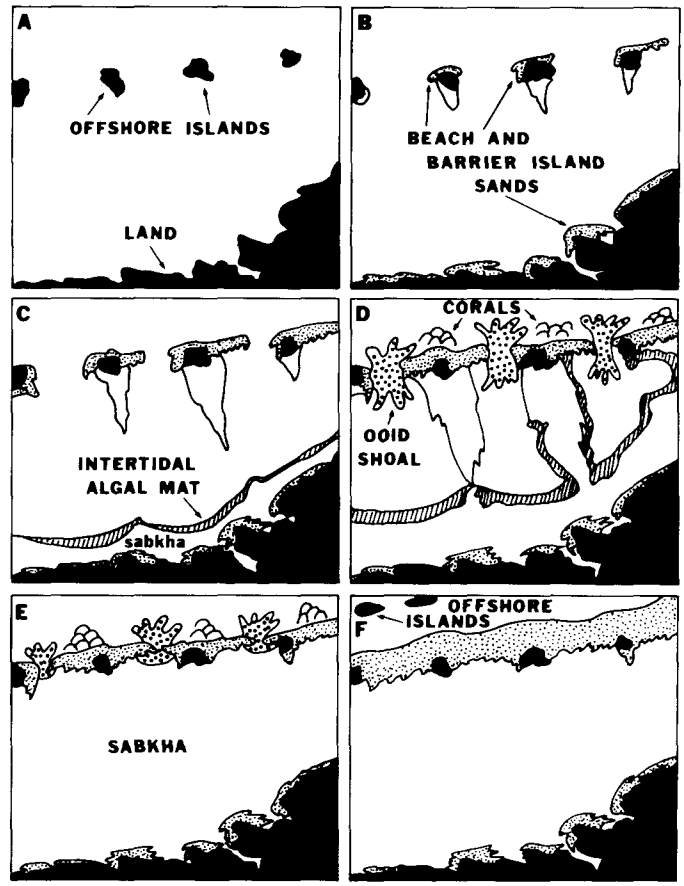

Figure 42.—Development and accretion of Trucial Coast sabkhas, barrier islands, oolitic tidal deltas and coral reefs. Modified from Purser and Evans (1973). (A) Offshore Pleistocene limestone islands (sea level approximately same as present). (B) Beaches form on seaward side of limestone islands and land, and sabkha begins to form in lee of islands. (C) Sabkha with intertidal algal mat begins to form in lagoon seaward of land and earlier beaches. Meanwhile, beaches build and are shaped by longshore currents as sabhka builds landward from offshore islands. (D) Previous processes continue with the addition of oolite shoals or deltas between barrier islands, and coral reefs begin accumulating seaward of barrier islands. This is essentially the situation at present. (E) In the future, sabkha will fill lagoonal area, creating an essentially straight shoreline with oolitic sand offshore of previous spaces between islands and reefs seaward of islands. (F) Eventually, more offshore islands begin and the process continues. Earlier deposits become buried in sabkha and eolian sand dune deposits.

Variations Caused by Longshore Drift

The tidal flats and barrier islands along the Trucial Coast face into the north-to-northwest prevailing winds for the most part. Longshore current and sediment transport, therefore, occur only locally. This lack of strong longshore current reduces the number and length of spits associated with barrier-island

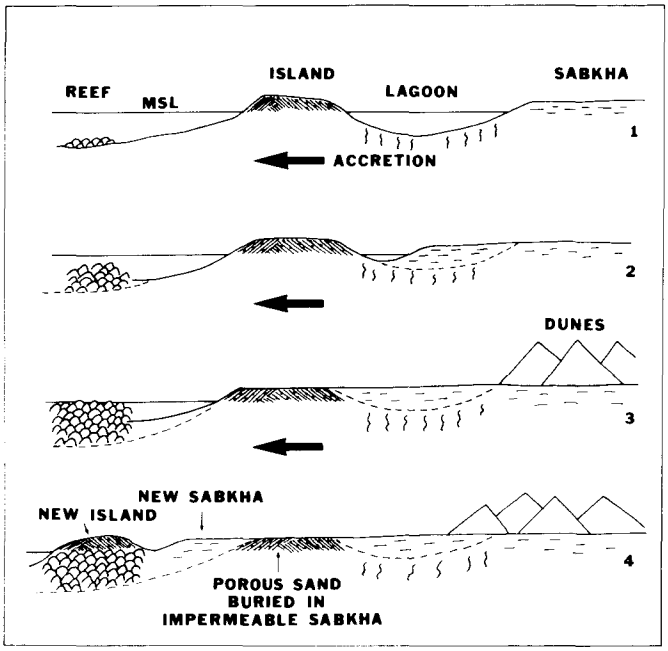

Figure 43.—Schematic drawings suggesting sequence of lagoonal infilling by accreting sabkha as reefs build up to create new offshore barrier island. Old barrier island is buried in sabkha, and eolian dunes march seaward to preserve sabkha and underlying deposits.

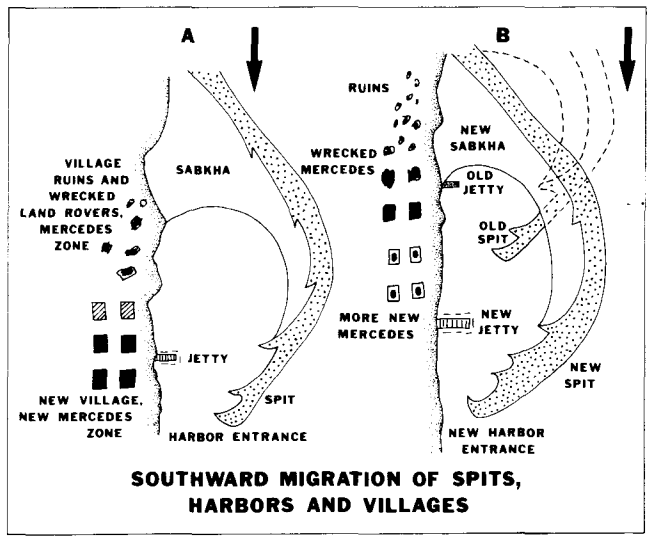

Figure 44.—Schematic of how spits along east side of Qatar Peninsula have migrated southward, creating and burying harbors. Ruins of several villages were observed by the author, indicating villages have migrated southward with harbors. Building materials and types of automobiles also reflect southward migration through time. Older village ruins predate introduction of Land Rovers. (Please note: remains of American cars are also mixed with Mercedes ruins!)

development. Hook-shaped spits occur, but tend to be accreted spit upon spit with few facies changes separating them. The situation is drastically different where there are strong longshore currents.

Strong longshore currents, especially during storms, exist along the north-south-trending east shore of the Qatar peninsula. On this shore numerous long, hook-shaped spits exist, many of which have isolated small bodies of water that serve as harbors and hence the location of fishing villages (figure 44). Historically, these spits and their harbors have marched southward in step with their associated lagoons, causing whole villages to migrate southward, leaving a rubble of mud and stone dwellings in their wake (figure 44). Near the northeast corner of the east shore, where the Tertiary bedrock is indented to form a large lagoon (between Ras Lafan and Khor), successive spits have formed by a series of seaward jumps (Shinn 1973a) (figures 45 and 46). Each individual spit, averaging about 12 km long, has served as a barrier to produce a muddy lagoon and accreting sabkha. The first such spit formed the largest lagoon which is now almost completely filled by upward-shoaling tidal-flat accumulation. During the lagoon-filling process, extensive tidal channels existed and each channel can be traced on the surface of the sabkha by minor changes in color caused by moisture content. These fossil channels can be traced to active tidal channels which originate at the lagoon/tidal-flat interface.

Since the formation of the first spit that allowed tidal-flat filling and channel scour of the lagoon, a series of additional spits has formed. Each spit (actually, long, narrow barrier islands or chenier-like features called "ribbon beaches") (Shinn 1973a) has produced another lagoon filled with a tidal-flat sequence (figure 46). The most seaward of these spits is currently growing southward. During the year and a half that this area was under study, the southern end of the spit accreted approximately 60 m (Shinn 1973a). Observations during a visit to the area in November of 1983, 16 years after the initial study, revealed several hundred meters of additional growth plus the development of an entirely new "hook" seaward of the one studied in 1967.

The net result of this kind of variation in tidal-flat sedimentation is a series of parallel porous and permeable "beach" deposits separated by relatively impermeable muddy subtidal, intertidal and sabkha sediments. Clearly, these bodies could serve as permeable conduits for fluids, including hydrocarbons, once buried in the subsurface. Explorationists should keep such variations and possibilities in mind when exploring for oil or gas in ancient tidal-flat sequences. Production geologists and engineers should especially be aware of these possibilities when exploiting existing tidal-flat oil fields or planning water-flood operations.

Quartz Sand in the Carbonate Tidal-Flat Environment

Along the southern part of the east shore of Qatar, a migrating dune field has spilled into the Gulf to produce a 40-km-long quartz sand sabkha more than 10 km wide and as much as 30 m thick (figures 47 and 48). This medium-to-coarse sand has completely smothered what was, 100 years ago, a carbonate environment. This sabkha is still expanding as 20- to 30-m-high

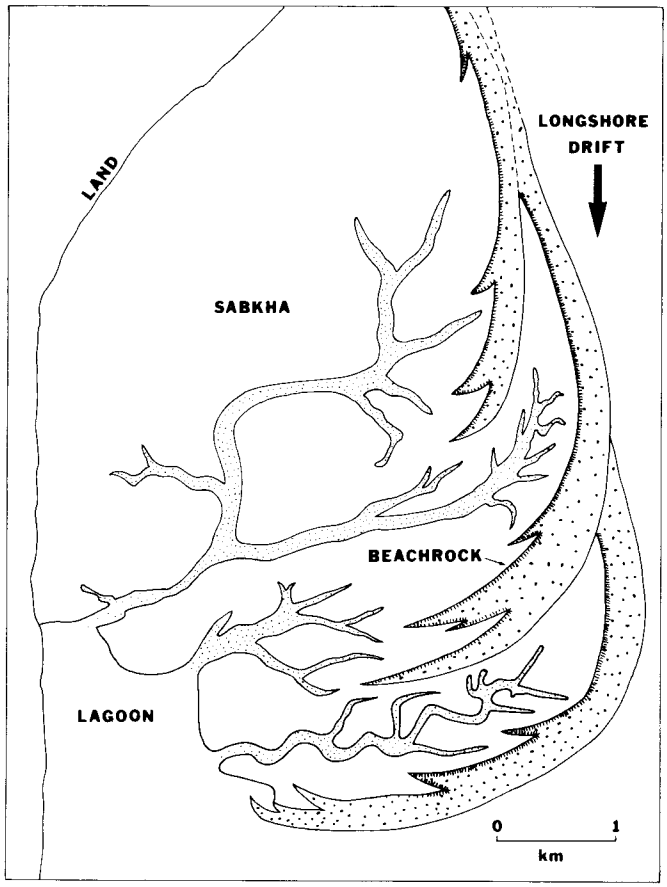

Figure 45.—Schematic of southward- and seaward-building of chenier-like carbonate sand spits and beaches which create quiet conditions favorable for sabkha development. Beach rock forms on back side of spits and beaches because grains are not in motion as on the seaward exposed side. Tidal channels extend between individual spits and beaches preserved in sabkha deposits. See figure 46 for documented example.

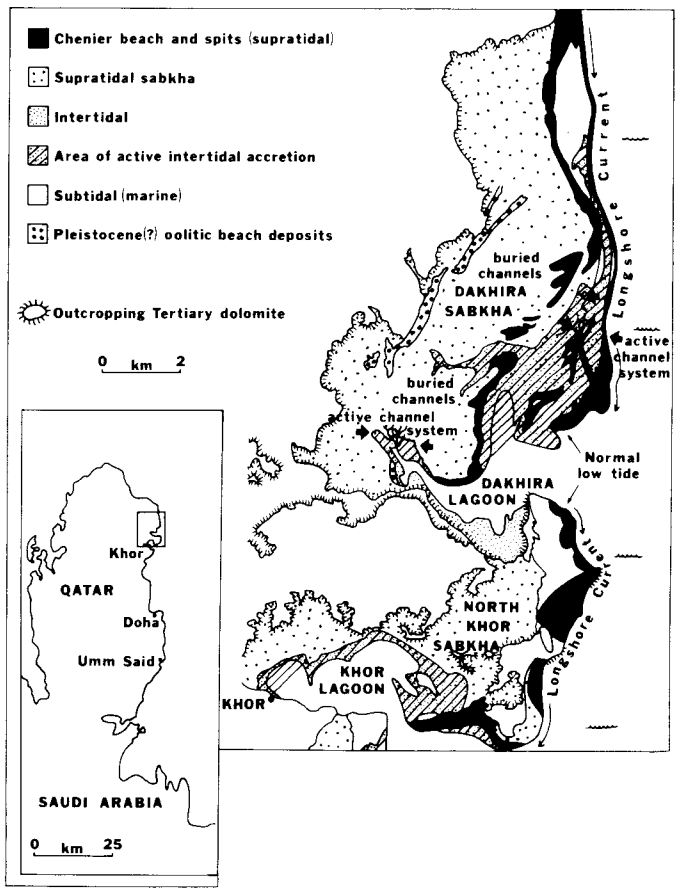

Figure 46.—Facies map of sabkha, chenier beach and sand spit area near village of Khor on east coast of Qatar Peninsula. Modified from Shinn (1973a).

barchan dunes march across the flats and spill into the sea. For a more thorough description of the area, see Shinn (1973b).

This quartz sand sabkha was revisited in November 1983, and it was found that barchans pictured by Shinn (1973b, figures 3, 4) had marched into the sea. It is therefore clear from the size of the remaining dune field and the rapidity of transport that within a few dozen years all the sand will be transported and deposited in the subtidal zone. Once the sand source is depleted, carbonate sedimentation will likely resume and a rather large, isolated quartz sand body will be completely surrounded by carbonates. Sedimentation caused by a combination of offshore winds and eolian transport of quartz sand represents another variation in the scheme of tidal-flat sedimentation.

The principal points to remember here are that, although sedimentation is marine, the supply line is eolian. Also, there are no sedimentary structures or features separating subtidal, intertidal and supratidal sedimentation. The source of such a large porous and permeable reservoir-sized body of quartz sand would be difficult to determine once buried in the subsurface. When the supply ends, the southwardly migrating carbonate spits, which previously existed and which still are active to the north, will continue migrating southward and will encase the seaward side of the quartz sand deposit.

The surface of the quartz sand sabkha (excluding the barchan dunes that march across it), like the carbonate sabkhas previously described, represent the flattest places on earth. In both cases the flatness is caused by interaction of capillarity and deflation of the surface. In arid climates the wind removes the sediment down to the permanently wet zone. Because wetness is due to upward movement of water by capillarity, the top of this zone can fluctuate slightly in response to fluctuating groundwater level. This quartz sand sabkha has formed by spilling of sand into water approximately 30 m deep, so the principal sedimentary structures consist of simple accretionary crossbedding. The major dip-direction is seaward, and individual, steeply inclined laminations may extend over a vertical distance of at least 20 m. The upper surface of each layer or bed is truncated at the top by the deflation surface (figure 49).

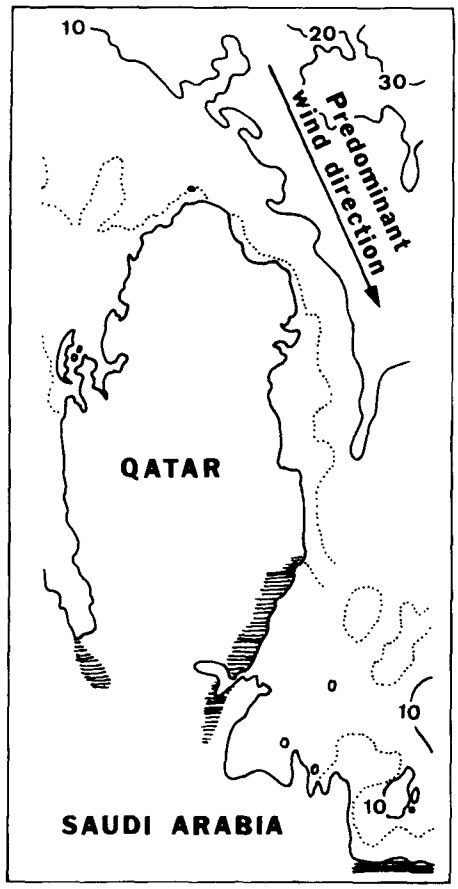

Figure 47.—Generalized bathymetry of offshore Qatar. Contours in meters.

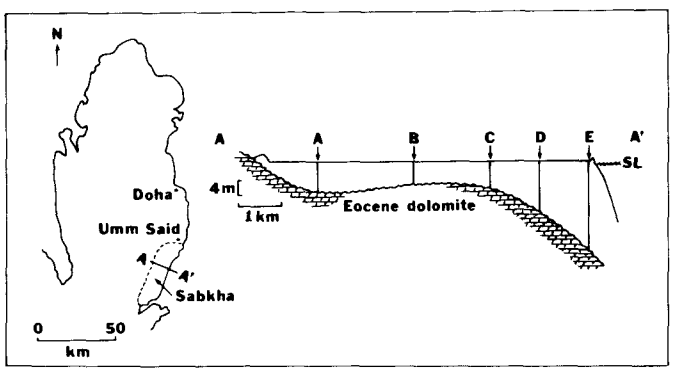

Figure 48.—Cross section interpreted from core holes drilled through quartz sand sabkha on southeast corner of Qatar Peninsula. Modified from DeGroot (1973).

Wind-Blown Dolomite

Dust storms are a common occurrence in arid climates such as the Arabian Gulf. The prevailing storm-wind direction is from the north. Dust from the Zagros Mountains in Iran several hundred kilometers away often reaches the southern part of the Gulf in such quantity that visibility is reduced to a few hundred meters and everything not moving becomes coated with yellow-brown dust. This dust contains about 65 percent silt-size dolomite rhombs, the remainder being clays and quartz silt.

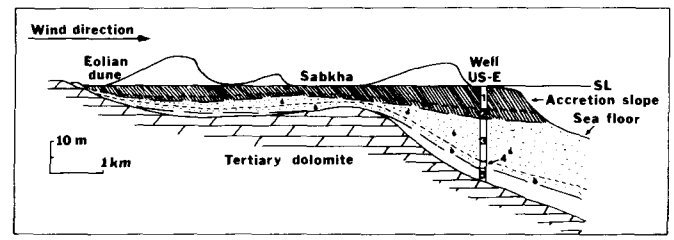

Figure 49.—Details revealed in core-hole transect shown in figure 48. Core US-E was oriented, revealing (1) a thick section of seaward-dipping sandstone beds, (2) moderately sorted fine-grained quartz sand, (3) poorly sorted fine-grained quartz sand and mollusks, (4) muddy (carbonate) quartz sand with bioturbation, mollusks and echinoids, and (5) lower regressive quartz sand. Modified from Shinn (1973b).

After each storm (several occur each year), algal mats in the intertidal zone act like sticky flypaper and become coated with as much as 1 mm of this dolomite-rich dust. Within 1-2 days, the wind-blown dust is overgrown and incorporated into the algal mats to form a distinct layer. Not only are the algal mats affected, but also virtually every environment where silt-sized material can settle is enriched with detrital dolomite and quartz.

DIAGENESIS AND ITS EFFECT ON SEDIMENTATION

Submarine Cementation (Hardgrounds)

Most submarine cementation is restricted to the offshore areas of the Arabian Gulf where it forms extensive continuous pavements. On the Bahama Banks submarine cementation is less active, has patchy distribution, and is restricted to special environments where the sediment is coarse grained and not frequently moved by waves and currents. There are no submarine hardgrounds forming seaward to the west of the Andros Island tidal flats, but they do exist northwest of the island.

Of special significance for the Arabian Gulf tidal flats is the submarine cementation that takes place in the upper subtidal and lower part of the intertidal zones. When the upper intertidal and supratidal zones migrate over these crusts, tidal channels rarely break through the crust; thus, these crusts limit the depth of channels and their deposits. Only very large main channels have cut through crust layers. On Andros, however, there is no such cementation and main channels generally erode down to the underlying Pleistocene bedrock. Importantly, the total tidal fluctuation on Andros is between 30 and 50 cm, whereas it is as much as 2 m in the Arabian Gulf. The tidal flats along the southern shore of the Arabian Gulf may be as much as 10 m thick; therefore, were it not for the rapid formation of sub-

marine hardgrounds just seaward of advancing tidal flats, channels would be much deeper.

The cement in Arabian Gulf crusts is of two types, both of which coexist. The most obvious cement is acicular aragonite like that which has been reported from many parts of the world (figure 50). The other cement is fine grained or mud textured high Mg-calcite. High Mg-calcite commonly fills in pores lined by acicular aragonite. It may form laminated geopetal fillings in voids, and range in color from light gray to white (figure 51). It is extremely hard and porcelain-like in appearance.

Submarine cementation is almost universally restricted to either sand-size sediment or porous reef frameworks except in the deep sea. No muds have been found to be cemented by this process, probably because in muddy environments permeability is extremely low (thus, cement-bearing waters cannot circulate freely) and because fine-grained sediment in shallow water is frequently resuspended by storm waves.

Sands, whether composed of carbonate or quartz, have very high permeabilities, thus allowing movement of supersaturated waters. The mechanisms that move water through these sediments are waves and fluctuating tides. Cementation is most thorough where storm-wave action is infrequent and sediment grains are allowed to lie undisturbed for long periods (Shinn 1969).

Submarine cementation is further enhanced by supersaturation of the overlying waters; thus, the process is much more active in the Arabian Gulf where the average salinity is about 45 parts per thousand and approximately 70,000 km of the subtidal zone has been affected.

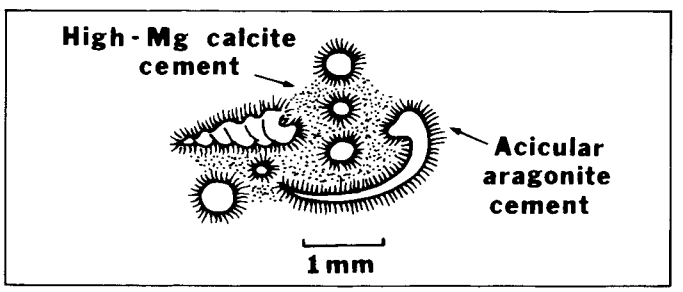

Figure 50.—Cemented carbonate grainstone showing acicular aragonite cement followed by muddy high-Mg calcite cement.

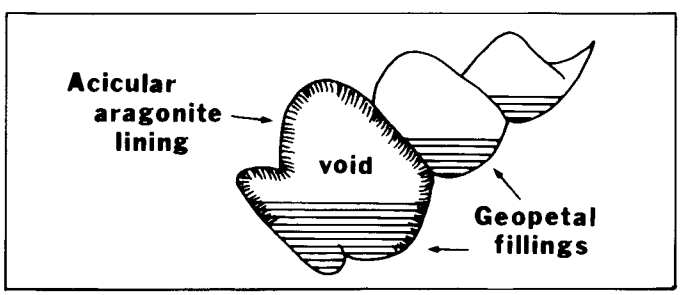

Figure 51.—Acicular aragonite lining interior of 1-cm-long gastropod followed by partial geopetal filling with laminated, fine-grained, high-Mg calcite cement.

Beach Rock

Intertidal beach rock cementation is common and restricted to sand-sized sediment wherever it remains immobile. Such cementation is extremely rapid in stabilized spits, that is, on the back side of barrier islands and beach ridges (figure 52). Cementation also occurs on the seaward side, but because of the general rapidity of sedimentation it becomes quickly buried and beyond the influence of circulating supersaturated waters.

Examination of aerial photographs showed that beach rock can form on the back sides of accreting spits in less than 10 years. Where beaches are unstable or being eroded, intertidal beach rock is eroded and redeposited as intraclasts within the beaches where they originated. Intertidal beach rock cementation, considered the same as submarine cementation, is enhanced because daily tidal fluctuation serves as an extremely efficient pump, causing large quantities off sea water to flow in and out of the beaches at a rapid rate. Although the cements and processes are similar to those of submarine cementation, the presence of air in the pores during low tide prevents cements from being isopachous and causes the formation of meniscus cement (Dunham 1970).

The cemented crust that forms in sand-size material in front of the advancing intertidal zone is in part "beach rock," although it would probably be impossible to distinguish it as such in the geologic record.

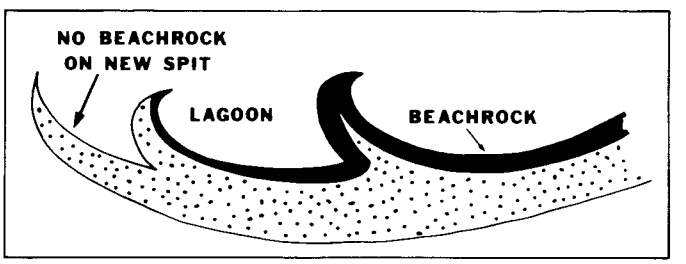

Figure 52.—Progression of beach rock cementation as revealed on typical accreting carbonate sand spit. Rock becomes progressively harder in older up-spit regions.

Evaporites

Gypsum and anhydrite. The most common evaporite in the arid Arabian Gulf is gypsum. On the humid flats of Andros traces of gypsum can be seen but only during dry periods. In this environment gypsum is quickly removed by rain water and storm flooding. Coring has shown that gypsum is not preserved at Andros, Abaco, or even Caicos where the climate is dry enough to support a solar salt industry.

Along the Trucial Coast of the Arabian Gulf, gypsum precipitates to form a "mush" that has the texture of ice cream salt. This mush forms at the most landward upper part of the intertidal zone and lower reaches of the supratidal zone where hypersaline lagoonal waters heat in the sun and concentrate even more. Generally, this zone lies at the top of the algal mat zone. As the intertidal and supratidal zones accrete into the lagoon, the mush zone is covered by the advancing supratidal sabkha. Eventually, after the zone of gypsum formation has moved on and comes to underlie supratidal sediment, evaporation continues. Surface temperatures between 40° and 50°C in this zone are not uncommon. Under these conditions gypsum dewaters and converts to anhydrite. In addition to the above process, infrequent storm flooding brings additional sea water, which evaporates to supplement the formation of anhydrite. It is probably this additional source which causes the anhydrite layers to swell and contort into folds and diapirs. The mechanism and rate of diapir formation are extremely complicated and not understood.

Thicker layers of anhydrite take on a nodular appearance similar to that found in the geologic record. As the nodules form and grow, sediment and organic matter are pushed aside and concentrated at the margins of interfering nodules. In cross section this material gives the anhydrite the so-called "chicken wire" appearance. The inferred sequence of gypsum to nodular anhydrite is shown in figure 53.

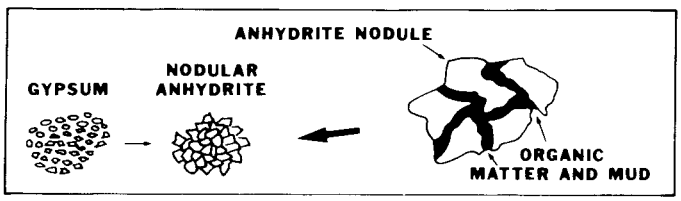

Figure 53.—Presumed stages in alteration of gypsum mush to nodular anhydrite. Because of observed expansion features in anhydrite, there must be continual addition of calcium sulfate because anhydrite is more dense than gypsum. Whether calcium sulfate is added in the form of anhydrite, or as gypsum later converted to anhydrite, is not known. Major portion of anhydrite is most likely derived by conversion of gypsum to anhydrite. Organic matter squeezed between growing nodules creates the classic chicken-wire texture.

Salt. Halite forms temporarily on the Arabian Gulf sabkhas but not on humid flats in the Caribbean. The salt forms layers several centimeters thick that are harvested by Arabs for food seasoning, but coring has failed to show that salt is preserved anywhere in the sabkha. Given an even more arid climate, salt might be preserved within the tidal-flat sequence. Groundwaters from the mainland flow through the most landward parts of the sabkha, converting anhydrite back to gypsum. Groundwater in the Gulf area is much fresher than sea water and certainly would remove any salt that might become buried within the sabkha.

Dolomite. The most important mineral formed on tidal flats is dolomite. Dolomite forms as thin centimeter-thick crusts on the Andros, Abaco and Caicos flats. It forms on the back sides of levees, on muddy beach ridges and to some degree on the seaward part of the supratidal marsh. According to Ginsburg and others (1977), dolomitic crusts form 20-25 cm above mean tide level where the sediment is exposed between 90 and 100 percent of the time, that is, a few centimeters above mean or normal high-tide level. The dolomite is poorly ordered, has a high calcium content, and is generally called proto-dolomite. Proto-dolomite content of these crusts is about 20-25 percent, but well cemented and leached crusts on the flanks of palm hammocks contain as much as 90 percent proto-dolomite (Shinn and others 1965).

In the Arabian Gulf dolomite forms in uncemented muds and can exceed a meter in thickness (Wells 1962; Illing and others 1965). Generally, the Arabian dolomite, which is more well ordered and more Mg-rich than the Andros dolomite, forms within and beneath the anhydrite zone of supratidal sabkhas. The separation of diagenetic and wind-blown dolomite mentioned earlier is difficult petrographically but can be readily identified by X-ray diffraction because the wind-blown material is well ordered (stoichiometric), and the magnesium content is close to 50 mole percent.

Diagenetic dolomite is forming in the landwardmost part of the quartz-sand sabkha described earlier. The rhombs measure 1-3 μm across, form a cement between quartz grains, and do not replace carbonate grains (figure 54). This dolomite forms by direct precipitation from hypersaline interstitial brines. For more information on this area and the dolomite, see Shinn (1973b) and DeGroot (1973). Similar dolomite cement in ancient sandstones is not uncommon.

Dolomitization may reflect reflux or downward seepage of hypersaline brines. This has been demonstrated in the porous and permeable quartz-sand sabkha at Qatar (DeGroot 1973). Water extracted from a 30-m-long core (core E in figures 55 and 56) showed hypersaline conditions in the subsurface beneath the shoreline. Groundwater salinity near the surface was the same as that of the offshore waters (figure 56). The only source for the hypersaline water was from the interstitial brine that exists in the sands several kilometers landward. This is probably the most clear-cut documentation of downward percolation of brines known in modern sediments.

Reflux may occur in the fine-grained carbonate sabkhas, but flow rates must be very slow because of extremely low permeabilities. There is good evidence for upward capillary movement stimulated by evaporation at the surface. Salinity profiles taken in carbonate sabkhas generally show a downward decrease in salinity, the opposite of what should be observed if reflux is occurring. Regardless of which process is most important

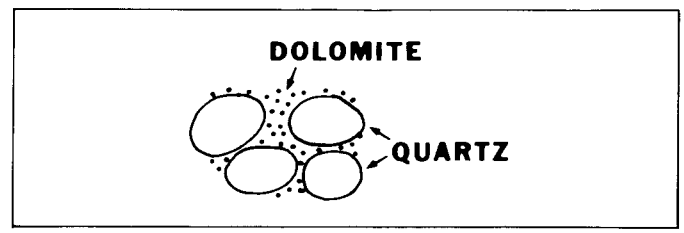

Figure 54.—Relationship of modern "primary" dolomite between quartz grains at location of core A in figures 55 and 56.

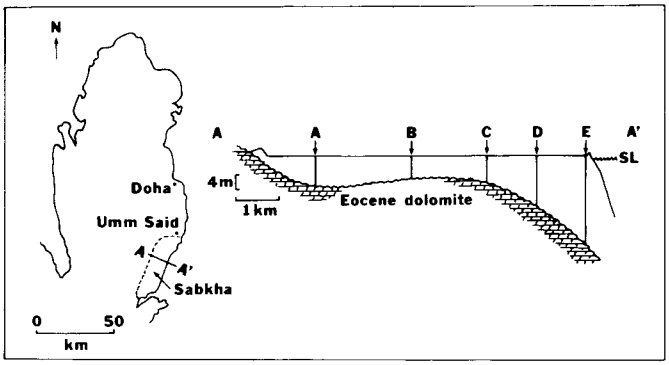

Figure 55.—Location of quartz sand sabkha core holes.

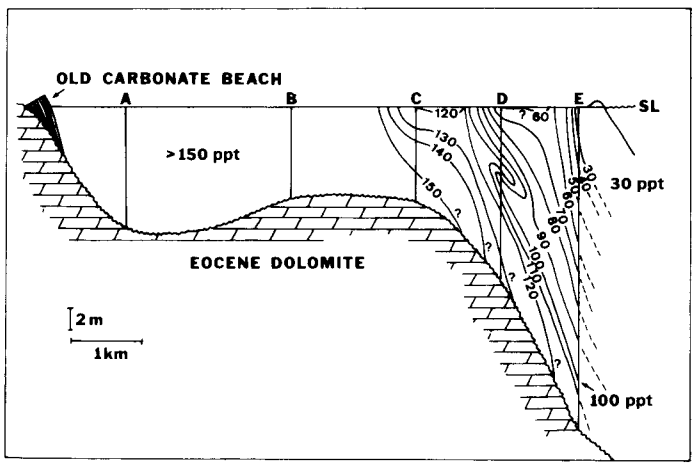

Figure 56.—Salinities of pore water from core holes in quartz sand sabkha expressed as grams chloride per liter. Increasing salinities in subsurface at location of core E indicates refluxing of brines beneath more normal salinity water.

for dolomitization, it should be emphasized that similar rocks, especially those in the oil-bearing Permian of west Texas and New Mexico, are invariably completely dolomitized, and the size of individual dolomite rhombs is small (5-10 μm) although larger than those in the Holocene.

Marine Caliche and Pisolites

At numerous locations within the spray zone along the southern shore of the Arabian Gulf, laminated crusts and spherical concretions analogous to the well known Permian age pisolites exist. These features occur in the supratidal zone but only where they are close to the lagoons or open Gulf. The supratidal sediment is also generally sand sized and usually cemented by beachrock-type cement.

These crusts and spheroidal pisolites are tan to brown in color and are composed both of aragonite and high Mg-calcite. For further details and petrography, see Purser and Loreau (1973) and Scholle and Kinsman (1974) (figure 57).

Similar spherical pisoids were described by Shinn (1973b)

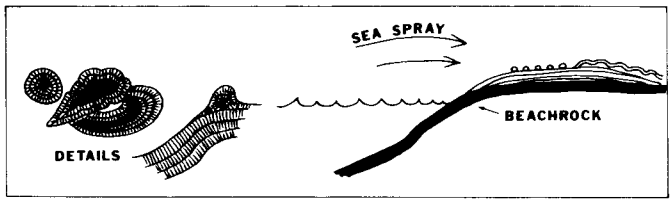

Figure 57.—Details of pisoid and pisolitic coatings in spray zone of certain areas of the Arabian coast. Individual pisolites occur in quartz sand on the surface of sabkha near core hole E (see figure 56). Coatings and pisoids, such as shown in drawing to right, occur on the Trucial Coast.

from the uncemented quartz sand sabkha in southeast Qatar discussed earlier. At Qatar their distribution was restricted to a zone extending no more than 100 m from shore. They occur as coatings around gastropod shells and fragments within a centimeter of the surface, and they "float" within a matrix of quartz sand. The coatings are restricted to gastropod shells, probably because they are the only carbonate grains in the quartz sand. Apparently, a carbonate substrate exposed to capillary water concentrated by evaporation will become preferentially coated with carbonate before a quartz substrate.

Scholle and Kinsman (1974) pointed out that these features are essentially the same as freshwater caliche or tufa, but in this case the waters are marine. Their restriction to locations adjacent to a source of marine water and sea spray could have useful applications in ancient rocks.

Similar caliche-like crusts and pisoids have not been detected in the humid tidal flats previously described, suggesting that an arid climate is necessary for them to form.

Additional evidence that arid conditions are necessary comes from descriptions of similar crusts and spheroids in the hypersaline inland sabkhas and salinas of southern Australia (Warren 1982). The author recently observed them in dolomitic crusts surrounding the Pekelmeer (salt ponds) at Bonaire in the Netherlands Antilles. The ponds and dolomite crusts at Bonaire were described by Deffeyes and others (1965) as supporting evidence for reflux dolomitization. The presence of these features in ancient rocks can be useful indicators not only of climate but also as a key to location relative to the basin. For example, in the Permian rocks of west Texas and New Mexico, pisolites and pisolitic crusts are associated with the well-known backreef tepee structures that appear to be restricted to a belt within approximately 2 km of the ancient Delaware basin shoreline. They are generally composed of dolomite, but calcitic examples also exist. Those composed of dolomite are probably more similar to the present-day arid sabkha examples than those composed of calcite.

PRACTICAL APPLICATIONS— THE FUTURE PREDICTED FROM THE PRESENT EQUALS THE PAST: MAYBE!

To make Holocene examples more useful for interpreting older rocks, it is necessary to consider the variations that might

result if present processes are allowed to continue for several thousands or millions of years.

ANDROS TIDAL FLATS

The development of a regressive sequence is most likely to continue at southwest Andros as it has during the past few thousand years. The northwest coast, however, will likely continue to experience erosion and onlap (transgressive sequence) for some time. It should be noted that both flats at Andros have experienced the same relative rise in sea level, yet one is producing a transgressive sequence while the other is depositing a regressive sequence. These two diametrically opposed sequences of sedimentation are the result of exposure and variations in sediment supply.

The seaward-accreting flats of southwest Andros lack extensive and active channel systems, whereas the retreating flats of northwest Andros possess an extensive and active tidal channel system. Shinn (1983) proposed that tidal channels are erosive features characteristic of onlap or transgressive sequences and that under offlap conditions, which require an unlimited supply of sediment, previously formed channels become choked and filled and new channels simply do not form. In the rock record, transgressive sequences are thin and probably produce only thin sedimentary records. What we generally see in the record are the regressive sequences which build thick units in subsiding basins where they are less likely to be removed by erosion. This may explain why tidal channels are so difficult to detect in outcrops of ancient tidal flats.

Why have the northwest Andros tidal flats experienced erosion and retreat when coring has shown that the supratidal marsh unit once extended well beyond the present flats? Sea-level rise during the Holocene has been rapid. The rapid relative rise drowned the reefs and sediment-covered flats northwest of Andros a few thousand years ago. As the shallows of the northwest Bahama Bank became deeper, larger waves caused by seasonal winter storms began to impinge on an area previously protected by offshore shallows. Much of the muddy source material offshore was removed and the shoreline of the flats (beach ridges) began to retreat landward. Channels formed in response to the lessening supply of sediment and provided a pathway for sediment to reach the supratidal marsh and other environments. The entire unit thus began to onlap the land as the sea rose.

If sea level remains stable for a few thousand years, it is likely that reefs will build up to sea level. At the same time, the various sedimentary environments (mainly hard pellet sand and ooid shoals) on the vast expanses of the Bahama Bank will build up to near sea level. When this happens, water circulation will be retarded and evaporation of bank water may enhance precipitation and transport of carbonate muds onto the tidal flats.

The reduced wave action that will result from the shallowing of offshore environments should reduce or stop shoreline erosion, and the flats will begin to accrete seaward, probably in a series of jumps similar to those that have occurred on the flats of southwest Andros. Consider what will happen to the entire tidal flat when the flats begin to accrete seaward. First, the channels will probably become choked with fine-grained sediment, allowing the preservation of a channel system with its more porous and permeable basal deposits; thus, the entire channeled intertidal belt as we see it today may be frozen in place. Second, levees will stop forming, but the existing ones would be preserved probably as a complicated mosaic of 20- to 40-cm-thick lenses of distinctly laminated sediment underlain and surrounded on their tapering sides by burrowed intertidal and pond sediments.

Given a little subsidence and a continued supply of sediment, the supratidal marsh will begin to build seaward and will cap the complex mosaic of channels, levees, intertidal and pond sediments. Meanwhile, the beach ridges would build outward in a series of jumps. The net result of these processes would be an enormous tidal flat containing a frozen system of porous and permeable channel deposits oriented more or less perpendicular to the basin, and seaward the beach ridges would leave a series of porous and permeable deposits parallel to the basin margin. Given repeated sea-level rises and falls superimposed on continual subsidence, the above sequence of events might be repeated many times. Beach ridges would tend to be concentrated as individual parallel deposits in the most basinward part of the system, while channeled belts would come to overlie each other in the more landward parts of the system. Supratidal marsh sediments would form seaward-extending wedges separating the individual products of transgression and regression. The fact that similar processes have occurred in the past is inescapable, but the fine-tuned details of these processes are almost impossible to decipher on outcrop and certainly impossible in the subsurface. It is important, however, to be aware of the possibility of these variations. For purposes of subsurface exploration, one must lump and generalize, and, with luck, drill into a permeable beach ridge or channel deposit. Either facies is likely to drain a large area, and exploitation geologists and engineers especially should be aware of this possibility.

Because of the unlikelihood of predicting the exact location of a channel or beach ridge in the subsurface, it is important to look for areas where these facies may be concentrated and stacked through time. Many tidal-flat sequences are thick, some even hundreds of meters. Given a fairly stable but subsiding basin axis, one would expect the concentration of parallel beach ridges in a more basinward location and tidal channels in a more landward position. Even farther landward, the supratidal marsh sediments may simply stack to produce an extremely thick monotonous sequence. Seaward extensions of this facies could produce the seals for stratigraphic traps. Thus, for exploration purposes, it may be necessary to identify only three major facies: the supratidal marsh or sabkha (the seal), the combined intertidal channeled belt sediments, including beach ridges and levees which would interfinger with the supratidal marsh sediments, and the marine sediments that may contain everything from gray burrowed muds to ooids and reef-buildups. Once a field has been discovered and numerous wells drilled, it may then be possible to recognize and exploit individual facies such as channels, beach ridges, ooid shoals and reefs. Traditionally, exploration geologists have been aware of variations and possibilities, but they lack the necessary well data to make accurate predictions. Production geologists and engineers who have ac-

cess to more well data than the wildcat explorationists traditionally do not study the rocks other than to measure porosity and permeability. It may be fruitful, therefore, for the exploration geologist to participate with production engineers in field development.

PERSIAN GULF

Similar predictions can be deduced from the Arabian Gulf examples and these "models" are probably more applicable to the ancient sequences than those at Andros Island. The various Arabian Gulf arid "models" are almost exact analogs of the Permian age tidal flats in the Permian basin of west Texas and New Mexico.

What makes the arid models so important are the sabkha evaporites. Similar evaporites are present in the Permian tidal flats, and because of anhydrite, permeability is so low this facies can form an effective seal. Because evaporite minerals deform and flow under stress rather than fracture as do limestone and dolomite, the trapping facies that contain evaporites are less likely to leak.

All tidal flats examined in the Arabian Gulf thus far are building seaward to form regressive sequences. It is thought that the abundance of sediment necessary for seaward accretion reduces the likelihood of extensive channel development. Those channels that do exist there are widely spaced, broad and deep. Predicting their existence and tracing them in the subsurface seems much more feasible than locating the smaller complicated types such as those at Andros. As shown by Shinn (1973a, 1983), the Arabian Gulf tidal channels are ultimately filled with very porous and permeable wind- and storm-driven sands as the sabkhas advance seaward. As in the Andros example, they trend approximately perpendicular to the basin margin or shoreline, but they are much wider and longer.

Beach ridges in the Arabian Gulf are generally broad and thick, and they are composed entirely of coarse gastropod gravels and sands. Many of the young beach ridges have already reached a size large enough to be considered good reservoirs if they were buried in the subsurface. Their trend is parallel to the basin margin or shore, and they are located toward the most basinward part of the tidal-flat system.

The preserved beach ridges (ribbon beaches) in the north-south-trending Qatar example are very narrow (50 to 75 m wide) and separated by relatively impermeable muds. Many of the channels in this area snake between the beach ridges, and thus they too are more or less parallel to the coast, unlike the perpendicular ones along the southern Trucial Coast. It should be noted that all the narrow beach ridges are joined together to the north where they originate. If these beaches remained permeable after burial, then a single well has the potential to drain the entire beach ridge system. The same is true of many of the channels. Perhaps, then, there are ancient oil-bearing beach ridges that are interconnected.

Along the southern Trucial Coast, ooid deltas have developed in tidal passes between many of the barrier islands. Many of these few thousand-year-old ooid deltas are of reservoir size. Continued outward accretion of the impermeable sabkha will cause burial of these ooid deposits, even if there is no subsidence or rise in sea level. The barrier islands, on the other hand, extend well above sea level and thus cannot be buried until there is subsidence or a relative rise in sea level.

There are also coral reefs seaward of most Arabian Gulf tidal flats and they are especially well developed seaward of the barrier island along the south shore. These reefs, like the ooids deltas, are below sea level and are subject to burial beneath the advancing sabkha. Alternatively, many of these reefs may build to sea level and give rise to islands. Islands initiated this way are likely to evolve into new barrier islands. When the present lagoons have been filled and the sabkha advances to the present shoreline, the development of new offshore barrier islands and a new phase of tidal-flat sedimentation seems inevitable.

In the final analysis, it should be clear that this style of tidal-flat sedimentation will produce many permeable reservoir-size bodies and trends, and the ultimate seal will be the anhydrite-rich dolomitic supratidal sabkha which will advance seaward and cover all other facies including coral reefs. The numerous cemented hardgrounds which may be incorporated into this package will form vertical seals; however, they are brittle and ultimately may fracture and leak. These hardgrounds have bored and eroded upper surfaces similar to subaerially exposed limestones, and it should be kept in mind that they are not subaerially formed and thus do not imply sea-level fluctuations.

The Arabian Gulf has much in common with ancient epeiric seas and apparently is experiencing gradual subsidence with the tectonic "hinge line" located in the vicinity of the south shore. Given sea-level fluctuations superimposed on gradual subsidence, many transgressive-regressive sequences should result (figure 58).

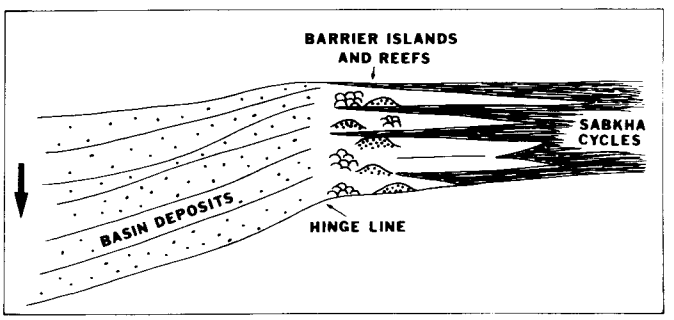

Figure 58.—Proposed development of porous carbonate sand and coral reef zones within regressive cycles developed during subsidence or relative rise in sea level. See text for discussion.

Hinge lines are common in subsiding basins, and it seems likely that their location would tend to terminate seaward accretion of an accreting tidal flat.

It is likely that basin-parallel barrier islands, associated ooid deltas and reefs would concentrate along the tectonic hinge. Thick tidal-flat sequences, made up of numerous individual transgressive and regressive sequences, may thus concentrate near or stack vertically along such a trend. Exploration or exploitation of these deposits would require a different philosophy than a search for tidal channels or updip traps beneath the sabkha seal.

The quartz sand sabkha resulting from wind-blown dunes, as described earlier, represents a unique situation. Although

this is the only known example of Holocene age, it seems feasible that similar deposits formed in the past. Unlike exploration in carbonate tidal flats, the quartz-sand accumulation in an otherwise carbonate province cannot be predicted or anticipated. However, well processed seismic data may detect accretionary bedding and the general shape of such a deposit. Recognition of the nature of such an accumulation once found by drilling would be very important. Without a model such as this in mind, one might misinterpret the accumulation for a deltaic deposit. Such an interpretation might suggest exploration for an upland source and a river or wadi deposit which does not exist. It is important, therefore, that such a deposit not be misinterpreted as a delta.

Most ancient tidal flats are dolomite and in many, such as those in the Permian basin, even the marine and intertidal facies have been dolomitized. In the latter case, thorough dolomitization may have been caused by (1) sea waters with a different chemistry than exists today, that is, more magnesium may have been available; (2) reflux of hypersaline brines from back-barrier or backreef lagoons or the sabkha itself; (3) abundant influx of wind-blown detrital dolomite; or (4) gradual drying up of the basin and production of huge quantities of hypersaline brines, which may dolomitize subtidal slope and basin sediments.

Regardless of which process dominated, it has been observed in many instances that supratidal dolomite is finer grained (5-10 μm) than that found in intertidal or subtidal facies (10-100 μm). The coarser grained dolomite also has higher permeability and is generally the one that produces oil and gas, whereas the finer grained dolomite of the sabkha, along with its evaporites, does not produce and usually forms effective seals.

Color is regarded as an important attribute of tidal-flat sediments. Intertidal and supratidal sediments are oxidized to a light tan color, whereas subtidal sediments are gray. In Permian tidal flats, these color changes are also generally present. While logging cuttings from a Permian tidal flat in west Texas, the author consistently noted similar color variations. Within a field with adequate well control, such color changes correlated with electric log responses could be very useful for correlation and facies prediction, even when only cuttings are available.

In summary, given continual subsidence, opportunity exists for numerous variations and cycles within an area of continued tidal-flat sedimentation, whether a hinge line is present or not (figure 59). The style of tidal-flat sedimentation, however, basically produces permeable sands or reefs parallel to the basin margin and permeable tidal-channel sands perpendicular to the basin margin. Given dolomitization, even muddy intertidal and marine deposits may develop good reservoir-quality permeability. The sabkha, in contrast with its evaporites and fine-grained dolomite or the marsh with its fine-grained sediments and thick stromatolitic laminations, should be relatively impermeable and should produce seals. Fingers of permeable intertidal and subtidal sediments interconnected by permeable channel sands wedging out between basinward-extending sheets of sabkha or

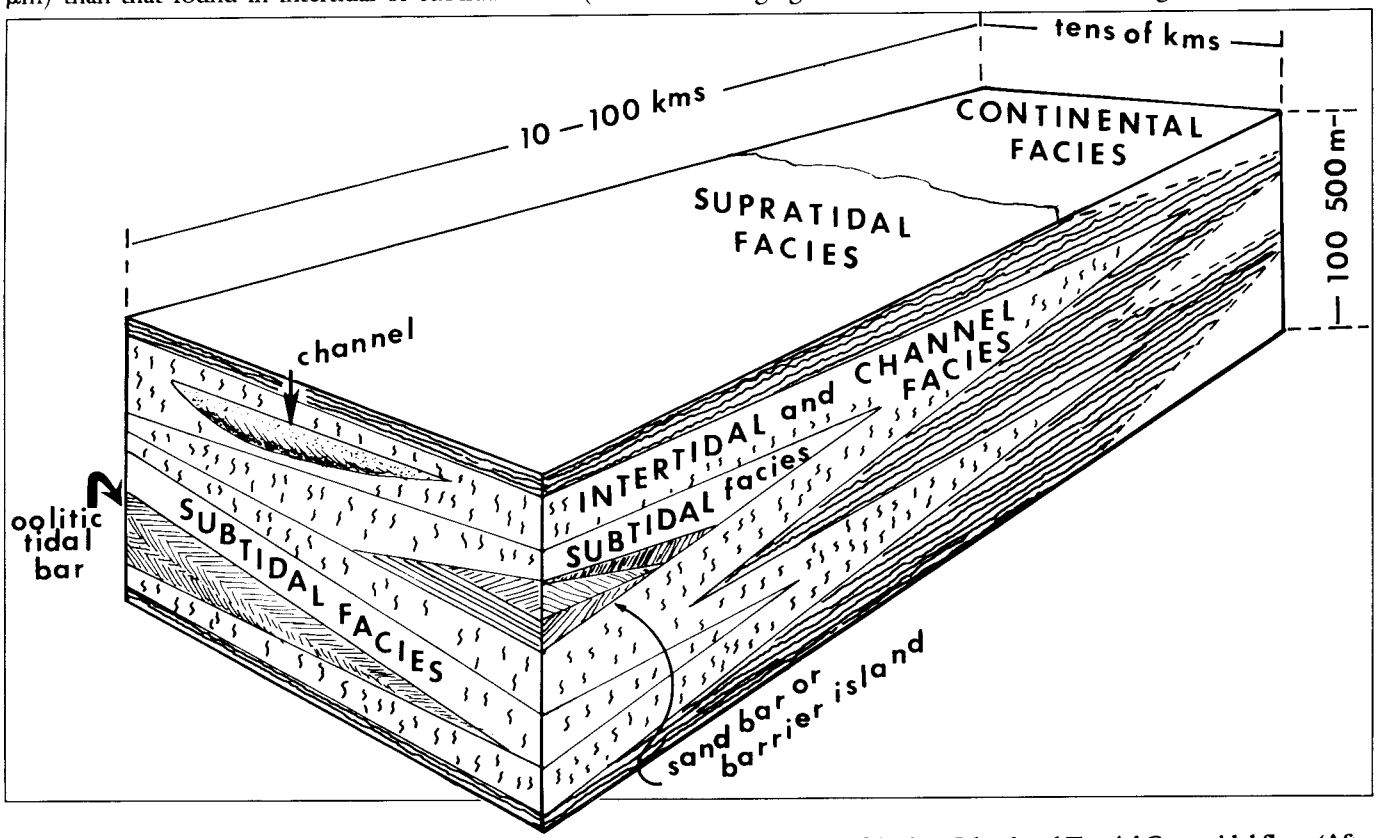

Figure 59.—Possible kinds of porous and permeable deposits that may be developed over time by repeated onlap and offlap, combining elements of Andros Island and Trucial Coast tidal flats. (After Shinn 1983, reproduced with permission from the AAPG.)

marsh units could form productive stratigraphic traps. Such traps would be even more attractive in a basin which subsided faster near the basin axis. The basinward tilting would result in updip migration and import of hydrocarbons from the adjacent downdip basinal sediments.

The key to exploiting such tidal flats lies first and foremost in their recognition. Recognition hinges both on correct interpretation of sedimentary structures, and, equally important, on the sedimentary sequence. The following illustrations attempt to tabulate the diagnostic sedimentary features of each subenvironment which will aid tidal-flat recognition (figures 60 and 61). It should be emphasized that, as with most cyclic accumulations, the perfect cycle will seldom exist. Erosion of earlier cycles during each new transgression or regression will commonly remove units before deposition of the next. Once identification of tidal-flat features has been made in an ancient deposit, it is hoped that some of the observations and ideas presented here will aid explorationists in making creative predictions about where to drill for the more permeable units.

REFERENCES

Black, M., 1933, The algal sediments of Andros Island, Bahamas: Philosophical Transactions of the Royal Society, London, Series B, volume 222, pages 165-192.

Butler, G.P., 1965, Early diagenesis in the recent sediments of the Trucial Coast of the Persian Gulf: London University, Ph.D. dissertation, 251 pages.

Deffeyes, K.S., Lucia, F.J., and Weyl, P.K., 1965, Dolomitization of Recent and Plio-Pleistocene sediments by marine evaporite waters on Bonaire, Netherlands Antilles, *in* Dolomitization and limestone diagenesis: Society of Economic Paleontologists and Mineralogists Special Publication 13, pages 71-88.

DeGroot, K., 1973, Geochemistry of tidal flat brines at Umm Said, southeast Qatar, Persian Gulf, *in* Purser, B.H., editor, The Persian Gulf—Holocene carbonate sedimentation and diagenesis in a shallow epicontinental sea: Heidelberg, Berlin, Springer-Verlag Publishing Company, pages 377-394.

Dunham, R.J., 1970, Meniscus cement, *in* Bricker, O., editor, Carbonate cements: Johns Hopkins University Studies in Geology, number 19, pages 297-300.

Evans, G., 1966, The recent sedimentary facies of the Persian Gulf region: Philosophical Transactions of the Royal Society, London, Series A, volume 259, pages 291-298.

Garrett, P., 1970, Phanerozoic stromatolites—non-competitive ecologic restriction by grazing and burrowing animals: Science, volume 169, pages 171-173.

Gebelein, C.D., 1974, Modern Bahamian platform environments, a guidebook for the 1974 annual GSA meeting, Miami Beach, Florida, 106 pages.

Ginsburg, R.N., and Hardie, L.A., 1975, Tidal and storm deposits, northwestern Andros Island, Bahamas, chapter 23, pages 201-208, *in* Ginsburg, R.N., editor, Tidal deposits, a casebook of recent examples and fossil counterparts: New York, Springer-Verlag Publishing Company.

Ginsburg, R.N., Hardie, L.A., Bricker, O.P., Garrett, P., and Wanless, H.R., 1977, Exposure index—a quantitative approach to defining position within the tidal zone, chapter 3, *in* Hardie, L.A., editor, Sedimentation on the modern carbonate tidal flats of northwest Andros Island, Bahamas: Baltimore, The Johns Hopkins University Press, The Johns Hopkins University Studies in Geology, number 22, 202 pages.

Hardie, L.A., 1977, Sedimentation on the modern carbonate tidal flats of northwest Andros Island, Bahamas: Baltimore, The Johns Hopkins University Press, The Johns Hopkins University Studies in Geology, number 22, 202 pages.

Illing, L.V., Wells, A.J., and Taylor, J.C.M., 1965, Penecontemporary dolomite in the Persian Gulf, *in* Pray, L.C., and Murray, R.C., editors, Dolomitization and limestone diagenesis—a symposium:

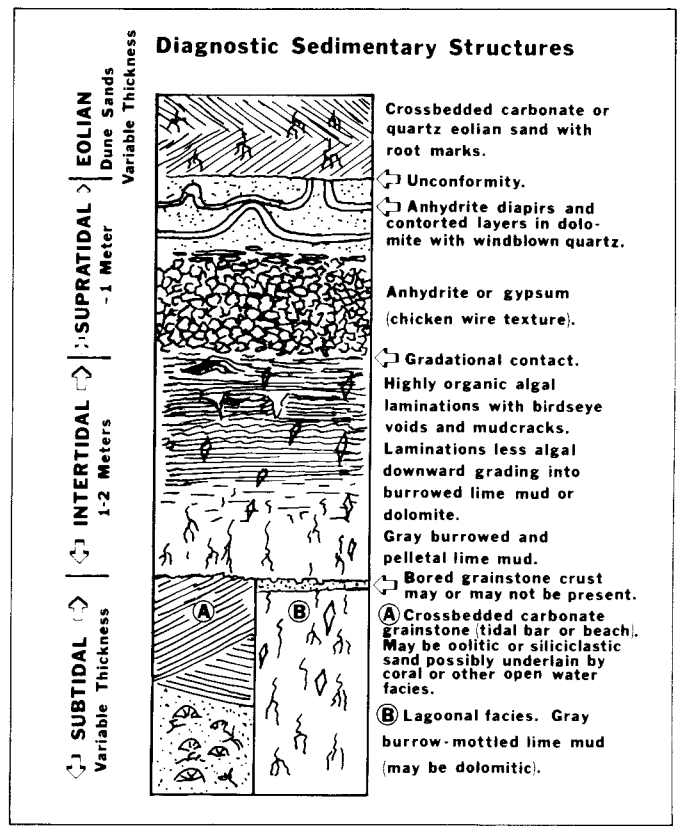

Figure 60.—Ideal offlap sequence based on the Persian Gulf examples described in the literature and observed by the author. Such a complete sequence is unlikely in the geological record due to the potential for subaerial erosion interrupting deposition. In addition, several variations are possible. First, notice that eolian sands above the supratidal zone are likely, and where they occur, these sands probably blanket and preserve sabkha facies. Such sands commonly migrate over the supratidal zone during and soon after deposition in arid climates. This movement and protection by eolian sands is common on modern tidal flats in the Persian Gulf. Second, notice that subtidal facies can range (depending on local conditions) from crossbedded carbonate sands, often oolitic, to coral reefs. In the geological record, corals might be replaced by stromatoporoids, rudistids or other reef builders, but oolitic facies are common. Subtidal facies may also be composed of pelleted and burrowed muds. Cemented crusts with bored and eroded upper surfaces may occur both within and at the top of subtidal facies. The most diagnostic facies, however, is the desiccated algal stromatolite zone and the nodular or chicken-wire anhydrite zone. (After Shinn 1983, reproduced with permission from AAPG.)

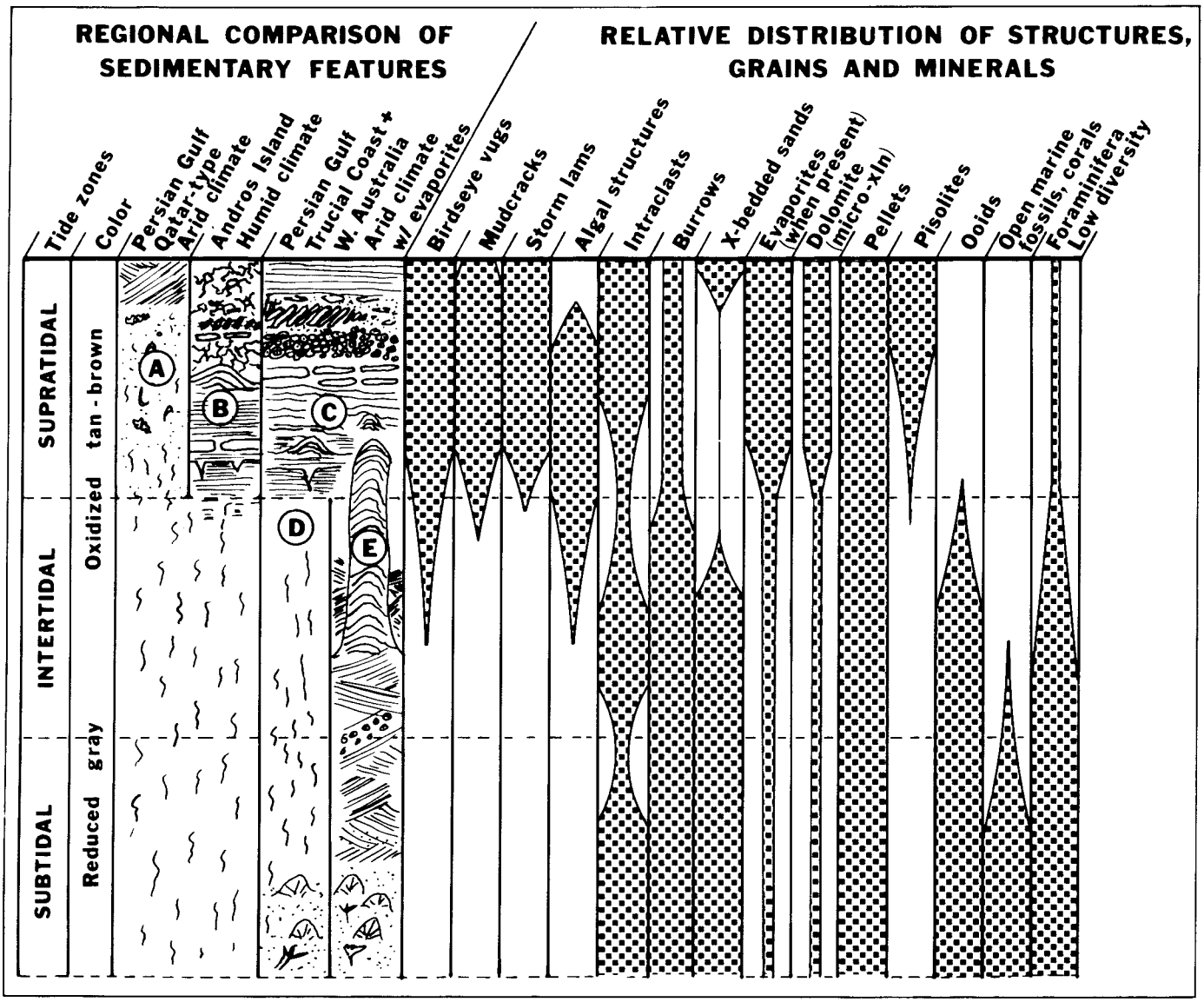

Figure 61.—An attempt to compile all commonly accepted facets of facies variations associated with carbonate tidal-flat accumulations. Column (A) shows the sequence on tidal flats around the Qatar Peninsula in the Persian Gulf. Note lack of a well-developed algal mat or anhydrite zone due to slightly higher rainfall than on the Trucial Coast. Column (B) shows sedimentary structures, such as soil clasts, current-deposited intraclasts, minor algal heads, and domes, mud polygons and mud cracks developed in humid climates, such as at Andros Island in the Bahamas. Column (C) shows the sedimentary features associated with arid tidal flats, such as on the Trucial Coast in the Persian Gulf or in the Shark Bay region, Western Australia. Note that the major difference in the last case is the presence of nodular or chicken-wire anhydrite. The intertidal zones can range from oxidized muds to coral reefs (column D) to rippled crossbedded sands containing large club-shaped algal structures (column E). Growing club- or columnar-shaped stromatolites extend to a water depth of at least 3 m at Shark Bay, and similar stromatolites up to 2 m high have recently been discovered in water 6-7 m deep in the Bahamas. These stromatolites therefore cannot be considered exclusive of intertidal deposition. The right-hand portion indicates expected relative abundances of various sedimentary structures, grain types, minerals and fossils, based on the literature and personal observations of modern and ancient sequences. No geologic example is likely to show exactly all the features illustrated here. (After Shinn 1983, reproduced with permission from AAPG.)

Society of Economic Paleontologists and Mineralogists Special Publication 13, pages 89-111.

Kendall, G. St. C., and Skipwith, P.A. D'E., 1969, Holocene shallow-water carbonate and evaporite sediments of Khor al Bazam, Abu Dhabi, southwest Persian Gulf: American Association of Petroleum Geologists Bulletin, volume 53, pages 841-869.

Kinsman, D.J.J., 1964, The recent carbonate sediments near Halat el Bahrani, Trucial Coast, Persian Gulf, *in* Deltaic and shallow marine deposits—developments in sedimentology, volume 1: Amsterdam, Elsevier Scientific Publications, pages 185-192.

Pratt, B.R., 1982, Stromatolite decline—a reconsideration: Geology, volume 10, pages 512-515.

Purser, B.H., 1973, The Persian Gulf—Holocene carbonate sedimentation and diagenesis in a shallow epicontinental sea: Heidelberg, Berlin, Springer-Verlag Publishing Company, 471 pages.

Purser, B.H., and Evans, G., 1973, Regional sedimentation along the Trucial Coast, southeast Persian Gulf, *in* Purser, B.H., editor, The Persian Gulf—Holocene carbonate sedimentation and diagenesis in a shallow epicontinental sea: Heidleberg, Berlin, Springer-Verlag Publishing Company, pages 211-231.

Purser, B.H., and Loreau, J.P., 1973, Aragonitic, supratidal encrustations on the Trucial Coast of the Persian Gulf, *in* Purser, B.H., editor, The Persian Gulf—Holocene carbonate sedimentation and diagenesis in a shallow epicontinental sea: Heidelberg, Berlin, Springer-Verlag Publishing Company, pages 343-376.

Purser, B.H., and Seibold, E., 1973, The principal environmental factors influencing Holocene sedimentation and diagenesis in the Persian Gulf, *in* Purser, B.H., editor, The Persian Gulf—Holocene carbonate sedimentation and diagenesis in a shallow epicontinental sea: Heidelberg, Berlin, Springer-Verlag Publishing Company, pages 1-9.

Schneider, J.F., 1975, Recent tidal deposits, Abu Dhabi, United Arab Emirates, Arabian Gulf, *in* Ginsburg, R.N., editor, Tidal deposits, a casebook of recent examples and fossil counterparts: New York, Springer-Verlag Publishing Company, pages 209-214.

Scholle, P.A., and Kinsman, D.J.J., 1974, Aragonitic and high-Mg calcite caliche from the Persian Gulf—a modern analog for the Permian of Texas and New Mexico: Journal of Sedimentary Petrology, volume 44, number 3, pages 904-916.

Shinn, E.A., 1968, Selective dolomitization of Recent sedimentary structures: Journal of Sedimentary Petrology, volume 38, number 2, pages 612-616.

Shinn, E.A., 1969, Submarine lithification of Holocene carbonate sediments in the Persian Gulf: Sedimentology, volume 12, pages 109-144.

Shinn, E.A., 1973a, Carbonate coastal accretion in an area of longshore transport, northeast Qatar, Persian Gulf, *in* Purser, B.H., editor, The Persian Gulf—Holocene carbonate sedimentation and diagenesis in a shallow epicontinental sea: Heidelberg, Berlin, Springer-Verlag Publishing Company, pages 179-191.

Shinn, E.A., 1973b, Sedimentary accretion along the leeward, southeast coast of Qatar Peninsula, Persian Gulf, *in* Purser, B.H., editor, The Persian Gulf—Holocene carbonate sedimentation and diagenesis in a shallow epicontinental sea: Heidelberg, Berlin, Springer-Verlag Publishing Company, pages 199-209.

Shinn, E.A., 1983, Recognition and economic significance of ancient carbonate tidal flats—a comparison of modern and ancient examples, *in* Scholle, P.A., editor, Recognition of depositional environments of carbonate rocks: American Association of Petroleum Geologists Memoir 33, pages 172-210.

Shinn, E.A., Ginsburg, R.N., and Lloyd, R.M., 1965, Recent supratidal dolomite from Andros Island, Bahamas, *in* Pray, L.C., and Murray, R.C., editors, Dolomitization and limestone diagenesis—a symposium: Society of Economic Paleontologists and Mineralogists Special Publication 13, pages 112-123.

Shinn, E.A., Lloyd, R.M., and Ginsburg, R.N., 1969, Anatomy of a modern carbonate tidal flat, Andros Island, Bahamas: Journal of Sedimentary Petrology, volume 39, pages 1202-1228.

Tebbutt, G.E., Conley, C.D., and Boyd, D.W., 1965, Lithogenesis of a distinctive carbonate rock fabric: University of Wyoming Contributions to Geology, volume 4, pages 1-13.

Wanless, H.R., and Dravis, J.J., 1984, Comparison of two Holocene tidal flats—Andros Island, Bahamas, and Caicos, British West Indies (abstract): American Association of Petroleum Geologists Annual Meeting Book of Abstracts.

Warren, J.K., 1982, The hydrological significance of Holocene teepees, stromatolites, and boxwork limestones in coastal salinas in south Australia: Journal of Sedimentary Petrology, volume 52, number 4, pages 1171-1201.

Wells, A., 1962, Primary dolomitization in Persian Gulf: Nature, volume 194, number 4825, pages 274-275.

ANCIENT CARBONATE TIDAL-FLAT DEPOSITS

Lawrence A. Hardie

Method of Approach

The basic method of recognizing ancient carbonate tidal-flat deposits in the geologic record is that of comparative sedimentology, using the diagnostic sedimentary features outlined in the preceding section. The method is best used in a stratigraphic framework by careful measurement of vertical sections in outcrop or core. The fundamental unit of measurement is the subfacies, which is the rock record of a subenvironment. Modern tidal-flat environments consist of an areal mosaic of genetically linked subenvironments; for example, the channeled belt of the Andros Island tidal flats is made up of a complex of interdependent channels, levees and tidal ponds (figure 62). Each subenvironment is a mappable part of the environment (figure 62) that has a distinctive physiography, distinctive surface features (both physical and organic), and in which a distinctive set of physical, biological and chemical processes operate (Reinhardt and Hardie 1976; Hardie 1977). The sedimentary record of a subenvironment is, therefore, characterized by a distinctive set of depositional, biological and diagenetic features (as, for example, observed on the Andros Island tidal flats; Hardie 1977, table 15). This set of features is the key to the application of the comparative sedimentology approach. Using the features found in modern carbonate deposits as a guide, the stratigraphic sequences are divided into subfacies identified by their distinctive assemblages of sedimentary structures, biota, early diagenetic features, etc. The terminology used here is not purely a descriptive one, but carries a direct genetic link between the basic rock unit and its presumed depositional setting, that is, subfacies = subenvironment. The prefix "sub-" is used because in modern depositional settings the mappable environment units, such as channels, levees, tidal ponds, marshes, etc., are not independent environments, but are interdependent components of a larger parent system, in this case the tidal flat as a whole. The terms used here are:

Environmental Unit		Rock Unit
Subenvironment (e.g., supratidal marsh subenvironment)	=	Subfacies (e.g., supratidal marsh subfacies)
Environment (e.g., tidal-flat environment)	=	Facies (e.g., tidal-flat facies)

Despite the obvious dangers of using a rock terminology that is directly linked to the interpretation of rock origin, the advantages are that it goes directly to the question of the genesis of the rock sequence, and forces asking critical questions about the significance of each observation. The definitions of facies and subfacies used here differ significantly from those employed for siliciclastic deposits (see Miall 1978; Walker 1984). A number of workers in siliciclastics essentially equate the record of an individual sedimentary structure, such as ripple-drift cross-lamination, with a facies. But a sedimentary structure is the result of a sedimentary process (as in migration of current ripples during bed-load transport) that may occur in many different depositional environments. Therefore, such structures (and there are many) by themselves may not be environmentally diagnostic. Also, some vertical successions of sedimentary structures (for example, Bouma sequences or other waning-current sequences) may be deposited from the same flow and so certainly do not signify the stratigraphic superposition of the deposits of different environments. Thus, the complexities introduced by considering individual sedimentary structures as facies can thoroughly obscure the basic picture of the paleoenvironment relations in space and time. It is only the whole set of interacting processes operating in a single subenvironment (for example, a sabkha) that leaves a diagnostic environmental re-

0163-9153/86/8101-0037 $00.20/0

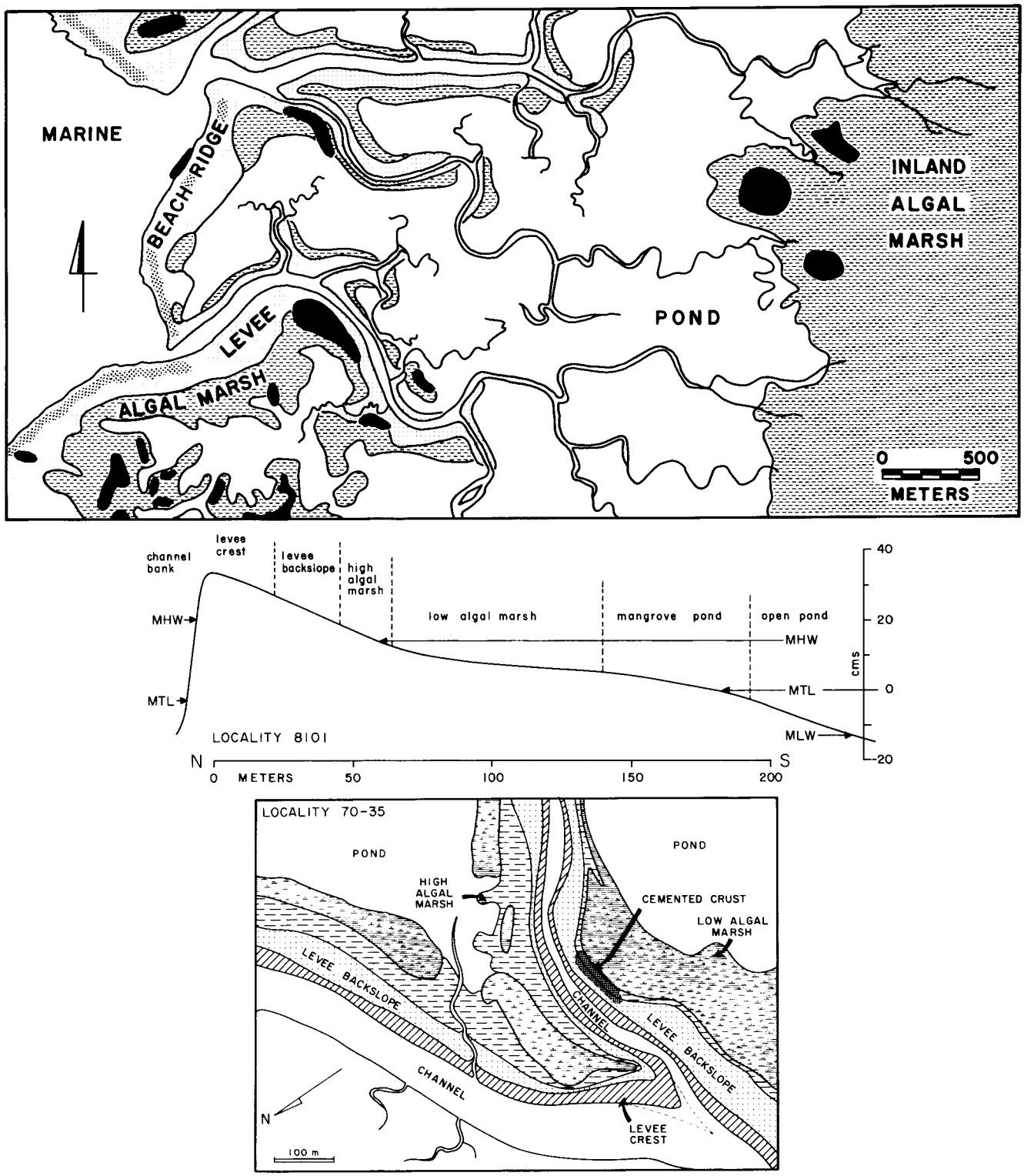

Figure 62.—Tidal flats as a mosaic of interdependent subenvironments, as exemplified by the northwest Andros Island tidal flats. Upper panel shows the basic areal arrangement of subenvironments (Hardie 1977, figure 6B); dark patches are areas of dolomitic surface crusts. Middle panel is a typical cross-sectional profile showing how subenvironments change with small differences in elevation measured in centimeters (Hardie 1977, figure 9A). Lower panel shows the detailed areal distribution of subenvironments (Hardie 1977, figure 10).

cord in the rocks: this is the rationale for the present approach.

At the first level of interpretation in the present approach, the tidal-flat sections within a carbonate sequence are recognized by:

(1) The presence of subfacies carrying unequivocal evidence of subaerial exposure (mudcracks, prismcracks, sheetcracks, caliche and other soil features, etc.) that would signal supratidal processes; and

(2) Interbedding at a meter scale of these supratidal subfacies with a variety of other shallow-water subfacies. This latter point follows because on tidal flats, more than any other environment, small changes in relative sea level will drastically change the succession of subfacies.

At the second level of interpretation, using the supratidal subfacies as markers, the succession of subfacies is analyzed to identify the associated intertidal and subtidal units and their stratigraphic relationships. Repetitive vertical packages of subfacies, with a supratidal over intertidal over subtidal motif 1-10 m thick, are typical, although not invariable, stratigraphic patterns in ancient carbonate tidal-flat sequences.

At the third level of interpretation, a detailed comparison of the specific features of each subfacies with the array of modern counterparts should allow precise reconstructions of the type of tidal flat on which the sediments were originally deposited. At this level the "building block" approach (Hardie 1977, pages 188-189) can be used to advantage.

A fourth level involves constructing three-dimensional facies and subfacies mosaics by correlating a series of measured sections. This aspect—facies stratigraphy—is addressed in the next chapter.

ILLUSTRATIVE EXAMPLES OF ANCIENT CARBONATE TIDAL-FLAT DEPOSITS

Ancient counterparts of modern carbonate tidal-flat deposits have been reported from the Proterozoic to the Quaternary (for example, Lucia 1972; Ginsburg 1975; Wilson 1975; Shinn 1983a; James 1984). The variety of types of deposits described is extremely wide, but a few particular examples from different geologic periods will illustrate some of the variations observed, as well as demonstrate the use of the vertical-sequence approach.

I. Precambrian

Algal stromatolites, presumed to be formed mainly in shallow water, are known from rocks as old as 3,500 m.y. (Lowe 1980; Walter and others 1980), but their heyday was the Proterozoic. In the absence of browsers and burrowers (Garrett 1970), algal stromatolites occupied all niches on Proterozoic carbonate platforms (Hoffman 1974, 1976) and developed a spectacular array of shapes and sizes (Raaben 1969, Hofmann 1973). Tidal flats in these Proterozoic carbonate platforms were no exception to this rule, and their sedimentary record is dominated by algal stromatolites throughout the tidal range (Hoffman 1976; Donaldson 1966, 1976; Eriksson and Truswell 1974; Cecile and Campbell 1978). The application of the method of comparative sedimentology to these Proterozoic tidal-flat carbonates is complicated by this environmental range of stromatolites. Modern analogs of subaqueous algal stromatolites, both sediment-trapping and precipitated tufa types, have been described only from hypersaline settings, and, at the other extreme, from freshwater settings. Very recently subtidal algal bioherms have been found in normal marine subtidal environments in the Bahamas, but apart from Dravis' (1983) short report, full descriptions of their characteristics have not been published as of this writing. In regard to the comparative sedimentology of stromatolites, it is interesting that Black's (1933) pivotal study on modern algal-laminated sediments on Andros Island, Bahamas, was quickly applied by Young (1935) to the Proterozoic stromatolites of the Transvaal System, South Africa, but both works remained unappreciated until Ginsburg (1955) reintroduced Black's blue-green algae model for stromatolite genesis.

The Rocknest Formation (Lower Proterozoic) Northwest Territories, Canada. A sequence of shallow-water carbonates forms part of the 1.8-2.2 b.y. old Epworth Group of the Coronation geosyncline, Northwest Territories, Canada (Hoffman 1973), and has been described briefly by Hoffman (1975, 1976) and recently in detail by Grotzinger (1985). This carbonate sequence, the Rocknest Formation, lies between a lower quartz arenite-mudstone sequence (the Odjick Formation) and an upper turbiditic sequence (the Recluse Formation) (figure 63). It is up to 1 km thick and covers an outcrop area of 20,000 km^2. The inner shelf sequence consists mainly of "shoaling-upward shale-to-dolomite cycles" that range from 1 to 15 m thick. The most common of these meter-scale cycles consist, from bottom to top, of (figure 63):

(1) A thin basal intraclast packstone (5-30 cm).

(2) A thick unit of red-brown to black laminated shale with scattered dololutite laminae and graded thin beds of dolarenite. The shale contains halite casts and sediment-filled mudcracks interpreted by Hoffman and Grotzinger as syneresis cracks. The dolomitic layers become more abundant upward and pass

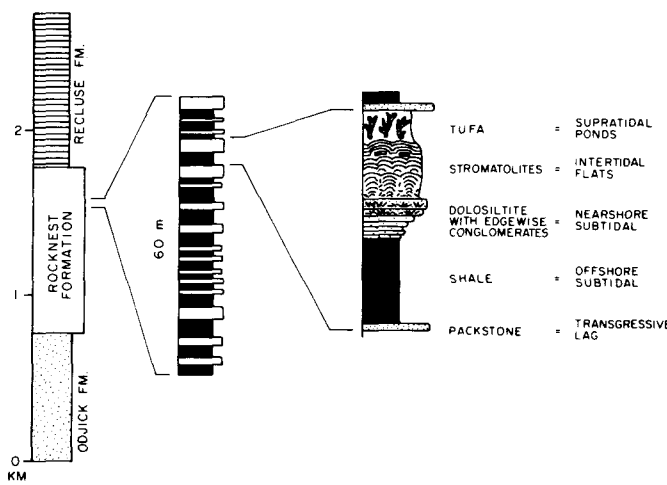

Figure 63.—Shallowing-upward sequences of the Lower Proterozoic Rocknest Formation, Northwest Territories, Canada (from Hoffman 1975, and Grotzinger 1985).

into thick-laminated dolosiltite with edgewise conglomerates.

(3) A unit of gray stromatolitic dolomite in which the stromatolites are vertically zoned and of LLH-type (laterally linked hemispheres) with elongate domal structures at the base, branched columns in the middle, and stratiform sheets with oncolites at the top.

(4) A cap of black, cherty dolomitic tufas made up of thin beds of tiny arborescent stromatolites (algal filaments are preserved in chertified stromatolites). The distinctive Precambrian stromatolite *Conophyton* is present in this unit in some cycles.

Hoffman (1975) interpreted these cycles in the Rocknest Formation as shallowing-upward sequences that originated by progradation of carbonate tidal flats over a muddy subtidal shelf. His evidence for a tidal-flat environment is:

(1) shoal-water grainstones; (2) flat-pebble conglomerates as "surf indicators;" (3) elongate, domal stromatolites shaped by wave scour (the significance of modern analogs in Shark Bay, Western Australia, was first recognized by Hoffman—see Logan and others 1974); and (4) arborescent stromatolites, which Hoffman interprets as tufa precipitated by algae in freshwater supratidal marshes similar to those on the modern Andros Island tidal flats (Monty and Hardie 1976; Hardie 1977). Grotzinger (1985) offered essentially the same interpretation of these cycles.

There are several somewhat unusual features about this fascinating and beautifully exposed cyclic carbonate sequence: (1) there is a paucity of unequivocal evidence of exposure in the inter- and supratidal subfacies; (2) there is a lack of subtidal stromatolites, which contrasts strongly with the abundance of such features in the 1.8 b.y. old Pethei Group in the Great Slave basin to the south of the Epworth basin (Hoffman 1974); (3) the mud cracks in the laminated shale subfacies are interpreted, not as subaerial features, but as syneresis cracks formed by compaction dewatering (Grotzinger 1985, page 138). The interpretation of these mud cracks is pivotal to the whole interpretation of the cycles. If these are not compactional dewatering cracks but instead are subaerial mud cracks (as is possible from their V-downward shapes, layered sediment fills, see Hoffman 1975, figure 30-6, and associated halite casts), then the origin of the Rocknest shale-based cycles will need to be completely re-evaluated; (4) the offshore, with a siliciclastic mud bottom, could not have been the "carbonate factory" for the carbonate tidal flats, a situation very different from modern lime sediment peritidal environments. As a result, the classic progradation mechanism for tidal-flat seaward growth (see next chapter) cannot be applied to the origin of the Rocknest cycles.

II. Lower Paleozoic

The Cambro-Ordovician was a time of extensive carbonate deposition, particularly in North America, which was rimmed by broad, carbonate shelves that ran the length of the Appalachians in the east and the length of the Rockies in the west (Dott and Batten 1971, figures 9-15, 9-16, 9-17 and 9-23). Valuable studies of the depositional environments in which these North American Cambro-Ordovician platform carbonates were deposited are those of Sarin (1962), Root (1964, 1968), Aitken (1966, 1967), Roehl (1967), Matter (1967), Braun and Friedman (1969), Mukherji (1969), Ahr (1971), Walker (1972), Walker and Ferrigno (1973), Reinhardt (1974, 1977), Halley (1975), Reinhardt and Hardie (1976), James and Kobluk (1978), Grover and Read (1978), Read (1980), Pfeil and Read (1980), Demicco and Mitchell (1982), Demicco (1983, 1985), and Mitchell (1985), among others.

During the Silurian in North American, extensive but much thinner carbonate shelves persisted in the West and Midwest while in the East shelf-carbonates were restricted to intracratonic basins, such as the Michigan and Illinois basins (Dott and Batten 1971, figure 11-11). Useful works describing Silurian carbonate tidal-flat deposits in North America are those of Roehl (1967), Tourek (1970), Smosna and others (1977), and Smosna and Warshauer (1981).

Three deposits from the Appalachians will be used as examples of carbonate tidal-flat deposition during the Lower Paleozoic.

Conococheague Limestone (Upper Cambrian), Central Appalachians. The Conococheague Limestone is part of a very thick succession of platform carbonates in the Appalachians that records continuous deposition at or near sea level from the Middle Cambrian to the Middle Ordovician, a time-span more than one-sixth the entire Phanerozoic. This Appalachian Cambro-Ordovician platform is a wedge of carbonates over 3000 km long, more than 300 km wide and up to 3.5 km thick (Colton 1970), and it constitutes one of the largest accumulations of carbonates in the geologic record. In the central Appalachians the Conococheague Limestone is 750 m thick and consists primarily of coarse-grained shelf-lagoon facies, but two separate sequences of tidal-flat facies interrupt this pattern (figure 64; Demicco and Hardie 1981; Demicco and Mitchell 1982; Demicco 1985). The shelf-lagoon facies are characterized by cross-stratified ooid-peloid grainstones, thrombolitic mounds (Demicco and others 1982; Demicco 1985) and thin-bedded, wave-rippled "ribbon rocks" (Demicco 1983). The tidal-flat facies, each about 50 m thick, consist of a succession of meter-scale asymmetrical cycles that are capped by mud-cracked laminites.

A typical tidal-flat cycle in the Conococheague Limestone in western Maryland (Reinhardt and Hardie 1976; Demicco and Mitchell 1982; Demicco 1981, 1983, 1985) is a well-defined sequence (figure 64), organized vertically as follows:

(1) A basal subfacies complex of cross-stratified ooid-peloid grainstones, flat-pebble conglomerates and thrombolitic mounds;

(2) A thin bedded, wave-rippled and burrowed "ribbon rock" subfacies that grades up into (3);

(3) A prism-cracked, wavy laminite subfacies; and

(4) A cap of mud-cracked dololaminite subfacies.

Lower and upper boundaries of each sequence are sharp and easily located in the field but internal boundaries between subfacies are most commonly gradational, especially between (2) and (3), and between (3) and (4). The lower cyclic tidal-flat facies consists of eight sequences that range from 2-20 m thick, while the upper cyclic tidal-flat facies is comprised of fifteen sequences that range from 1-12 m thick. Individual cycles can be correlated across depositional strike of the outcrops for a

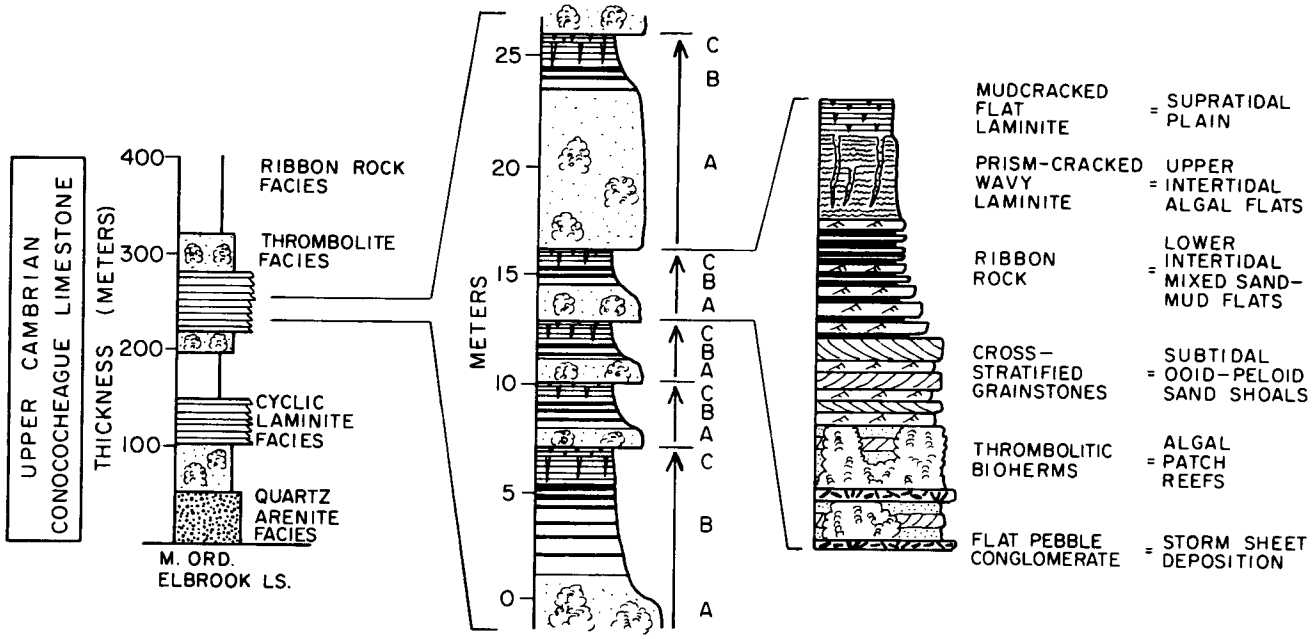

Figure 64.—Shallowing-upward tidal-flat sequences of the Upper Cambrian Conococheague Limestone, Maryland (from sections measured by Demicco 1981).

distance of at least 25 km (about 50 km on a palinspastic restoration) (Demicco 1981; Demicco and Mitchell 1982).

Each cycle is interpreted as a shallowing-upward sequence produced by progradation of broad tidal flats over a "high energy" sandy shelf-lagoon covered with algal patch reefs (figure 64; Reinhardt and Hardie 1976; Demicco 1981; Demicco and Mitchell 1982; Demicco 1983, 1985). The evidence for periodic exposure abounds in the upper subfacies of each cycle, as follows:

(1) Mud cracks V-downwards from common bedding surfaces and are filled with sediment from the overlying layer or layers.

(2) Wavy laminites with deep prism-cracks which have ragged edges draped by small "heads" of peloidal laminae that defy gravity in classic Black-type algal "stick-on" fashion (Hardie and Ginsburg 1977). These prism-cracked laminites are interpreted as desiccated cryptalgal laminites of the upper intertidal-lower supratidal zone analogous to those in the modern Persian Gulf (Shinn 1983a, figure 9A and B; Kinsman and Park 1976, figure 8).

(3) Mud cracks and prism-cracks may show reactivation several times along the same fracture as is manifested by multiple cracks with several generations of sediment fills. This characteristic, together with features (1) and (2), demonstrates that sedimentation and mudcracking were contemporaneous and recurrent, as most typically occurs in ephemeral settings such as tidal flats and playas where deposition of a sediment layer is followed by subaerial desiccation and polygonal mudcracking (see Smoot 1983, for a discussion of subaerial versus syneresis cracks).

(4) "Jelly-roll" structures in prism-cracked peloidal laminites (Demicco 1985, figure 10B) indicate that disrupted algal mats were rolled over at the surface.

(5) Pockets of intraclast chips associated with mud-cracked laminites are presumed to be eroded fragments of mud-crack polygons.

(6) Isolated, displacive nodules of sparry calcite in the uppermost mud-cracked dololaminite subfacies once may have been anhydrite nodules formed in the supratidal zone. This, in turn, suggests that the climate in Conococheague time was dry enough to produce some growth of evaporite minerals within the supratidal sediments but not arid enough to accummulate a cap of sabkha evaporite deposits. Much farther south in southern Virginia the equivalent age Nolichucky Formation has exactly the same type of tidal-flat cycles except that nodules, presumed to be anhydrite originally, are more abundant in the supratidal cap (Markello and others 1979).

Evidence for a tidal influence is present in the "herring-bone" cross-beds of the ooid-peloid grainstones, which in places have 180° opposed foresets (true dip) in the same cross-bed set. Also, the "ribbon rocks," which grade upwards into prism-cracked cryptalgal laminites, characteristically have wavy, lenticular and flaser bedding structures analogous to those in the sediments of the mixed sand-mud intertidal flats of the North Sea (Demicco 1983). If the "ribbon rocks" are interpreted as the deposits of intertidal flats, then the thickness of the "ribbon rock" subfacies in each cycle can be used to estimate the tidal range (Klein 1971). This yields a range of about 2-5 m on the average, making the Conococheague environment a mesotidal to macrotidal system. With such a tide range, barrier bars separating the tidal flats from the open shelf-lagoon are unlikely to have been present. This is consistent with the transitional relationship between the ribbon rock subfacies and the underlying grainstone-thrombolite subfacies, which is interpreted to have been deposited in an open shelf-lagoon. This latter interpretation follows from the fact that the grainstone-thrombo-

lite subfacies of the tidal-flat facies are exactly like those of the thick shelf-lagoon facies that characterizes the Conococheague succession overall. Cross-bedded and hummocky cross-stratified ooid-peloid grainstones are interpreted to be the record of an extensive sandy lagoon bottom covered with shoals and agitated by waves and tidal currents, as occurs today over large areas along the margins of the Great Bahama Banks (Ball 1967). This sedimentological analogy can be carried further because the flat-pebble conglomerates associated with the grainstone in the Conococheague consist of pebbles made of cross-stratified grainstone intraclasts with early marine cement fabrics (see James and Choquette 1984). The Bahamian ooid shoals are undergoing penecontemporaneous cementation beneath the surface of even active sand waves (Ball 1967; Harris 1979), and erosion and migration of these patchily cemented shoals is producing rounded ooid-grainstone clasts similar to those of the Conococheague flat-pebble conglomerates in the grainstone subfacies. The thrombolites interbedded with the grainstones in the Conococheague are very much like those first described by Aitken (1967) from equivalent rocks in the Canadian Rockies. The Conococheague thrombolites are meter-scale mounds made up of clusters of small digitate stromatolites bound by encrusting *Renalcis, Girvanella,* and micrite rinds (see Pratt and James 1982). These thrombolitic mounds have been interpreted as algal patch reefs scattered across the sandy, well-circulated shelf-lagoon of the Conococheague platform (Demicco and Hardie 1981; Demicco and others 1982; Demicco and Mitchell 1982; Demicco 1981, 1983, 1985).

The Conococheague tidal-flat facies contain a range of beautifully preserved primary features too numerous to describe here, but a full account is given by Demicco (1981). In summary, noteworthy features of the Conococheague tidal-flat facies, some of which may serve as patterns for carbonate tidal-flat sequences in general, follow:

(1) The facies consists of a stack of meter-scale shallowing-upward sequences, most of which are asymmetrical A-B-C, A-B-C, etc.

(2) Upper and lower contacts of each sequence are sharp.

(3) Internally, boundaries between component subfacies are gradational.

(4) Individual sequences can be correlated laterally across strike in a layer-cake stratigraphy.

(5) Supratidal subfacies are easily identified by their unequivocal evidence of exposure, mainly in the form of desiccation cracks.

(6) Intertidal subfacies carry evidence of on-off currents in the form of wavy, lenticular and flaser bedding that reflect tidal and storm activity.

(7) Sandy subtidal subfacies carry evidence of tidal-current reversals in the form of "herring-bone" cross-bedding.

(8) Thickness of the intertidal subfacies indicates a mesotidal to macrotidal range, which in turn implies that the tidal-flat shoreline had few or no barriers, much like the huge modern macrotidal flats of the northwest Gulf of California (Thompson 1968). This implication is consistent with the transitional boundaries between the subtidal and intertidal subfacies in the Conococheague cycles.

(9) Sequences are fining-upward with sandy subtidal subfacies grading upward to peloidal mud supratidal subfacies.

(10) Algal lamination is confined mainly to the zone above mean high water.

(11) In the upper Cambrian of the Appalachians, Conococheague type tidal-flat cycles (figure 64) are present from Pennsylvania (Root 1964, 1968) to southern Virginia (Markello and others 1979), so that the tidal-flat belt covered a restored area of at least 40,000 km^2, a scale that prompted Ginsburg (1982) to question our actualistic models of carbonate deposition based on small modern systems.

St. Paul Group (Middle Ordovician), Central Appalachians. The St. Paul Group of Chazyan age lies near the top of the Cambro-Ordovician carbonate succession in the central Appalachians. This 150-200 m thick group of platform carbonates carries tidal-flat facies that are markedly different from those of the just described Conococheague Limestone of the same area.

The St. Paul carbonates in western Maryland and southern Pennsylvania are organized into five facies (Mitchell 1982, 1985; Demicco and Mitchell 1982) in each of which the predominant component is lime mud and peloidal lime mud. These facies are (figure 65):

(1) Restricted shelf-lagoon facies (burrowed micrite with a very low diversity fauna);

(2) Semi-restricted shelf-lagoon facies (burrowed micrite with a low to moderate diversity fauna);

(3) Open shelf-lagoon facies (burrowed wackestones, packstones, minor peloid-skeletal grainstones, and a diverse fauna that includes bryozoans and tabulate corals);

(4) Tidal-flat facies (burrowed micrites, thin beds and mudcracked laminites); and

(5) Coastal freshwater lake facies (thin beds, laminites and LLH-stromatolites).

These five facies are arranged vertically in a succession that records transgression-regression-transgression on a megacycle scale, with the coastal freshwater lake facies marking the peak of the regressive phase (figure 65).

The tidal-flat facies and associated coastal freshwater lake facies are about 150 m thick in the west and thin to less than 100 m over a distance of 8 km (about 16 km restored distance) to the east, the seaward side of the St. Paul platform. The tidal-flat facies consists of four main subfacies interbedded in a complex fashion. These subfacies are:

(1) Unlayered micrite subfacies (0.1 - 3 m), which is a lime mudstone with a small component of skeletal debris of low diversity (mainly ostracodes) and characterized by innumerable mm-scale tubular burrows;

(2) Coarse packstone subfacies (0.3 m) of sand to pebble size peloids and micrite intraclasts with micrite matrix, internal sediment or calcite spar void fillings, and large tubular burrows (15 - 20 mm diameter) which have disrupted what appears to have been a primary cross-bedded peloidal grainstone;

(3) Laminite subfacies (0.2 - 1 m), which carries an array of laminite types such as planar laminites, wavy fenestral laminites, mudcracked laminites, etc., all of which are micritic and peloidal in texture; and

(4) Thin-bedded micritic subfacies (1 m), which is an as-

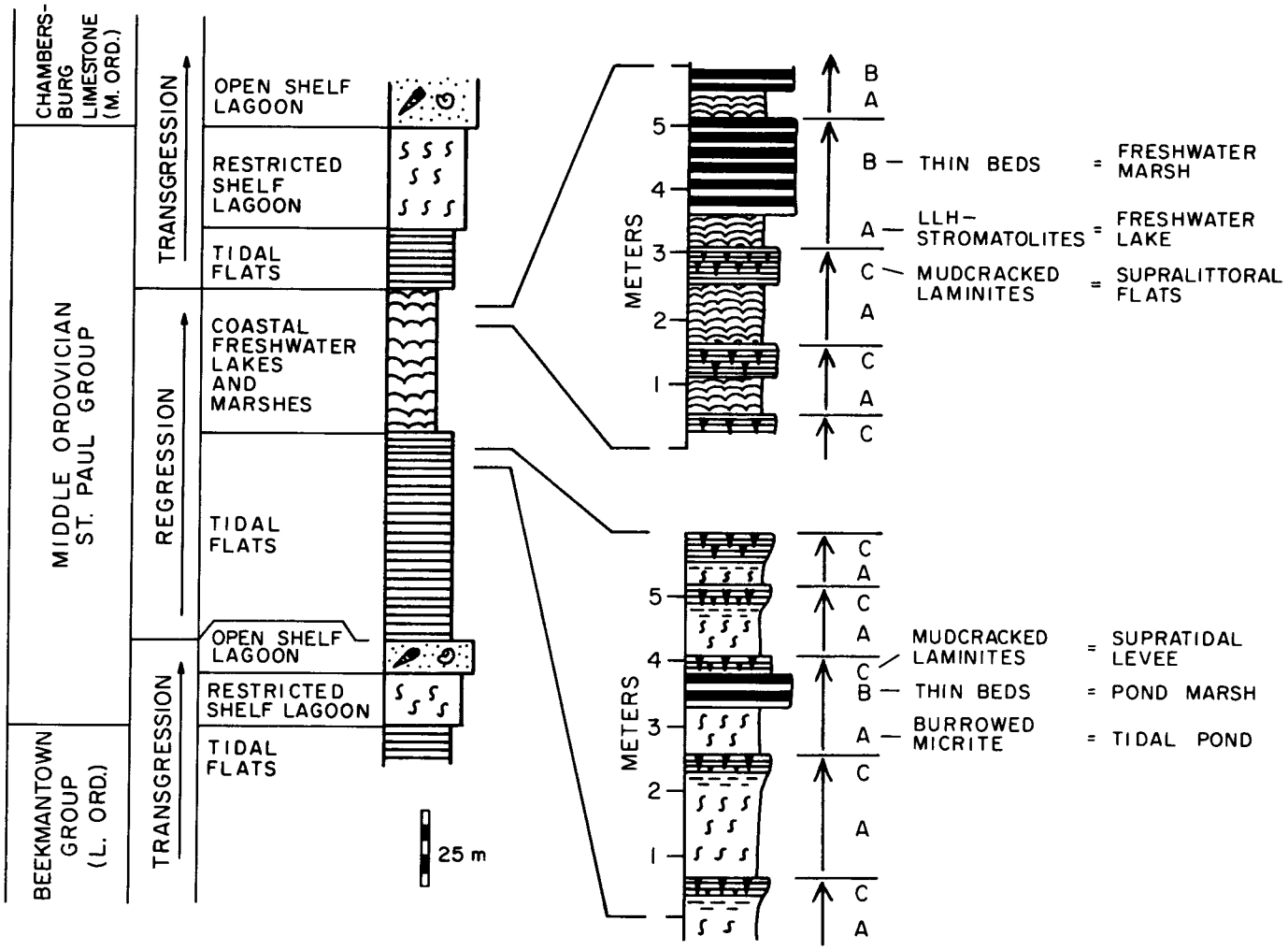

Figure 65.—Shallowing-upward peritidal sequences of the Middle Ordovician St. Paul Group, Maryland (from sections measured by Mitchell 1981).

semblage of unfossiliferous micrites containing algal filament tubes (algal tufa), micritic LLH-stromatolites and intraclast packstones.

Mitchell (1981, 1985; Demicco and Mitchell 1982), following the path of Matter (1967), made a careful study of the St. Paul carbonates and concluded that the closest modern counterpart of the tidal-flat facies is the Andros Island, Bahamas, system. The abundance of lime mud, absence of ooid grainstones and algal patch-reef mounds, the restricted fauna, and the dominance of bioturbated micrite and laminite subfacies make a convincing case. From a detailed comparison of the St. Paul rocks and the Andros Island sediments, Mitchell arrived at the following equations:

St. Paul Subfacies		Andros Island Subenvironment (Hardie 1977)
1. Bioturbated micrite subfacies	=	Intertidal ponds
2. Coarse packstone subfacies	=	Tidal channels
3. Laminite subfacies	=	Supratidal levees
a. planar laminites	=	levee crest
b. mudcracked laminites	=	levee backslope
c. wavy fenestral laminites	=	high algal marsh
4. Thin-bedded micrite subfacies	=	Inland freshwater algal marsh

Mitchell noted that the subfacies of the St. Paul tidal-flat facies are not arranged in a clear-cut succession of repetitive cycles, and he attributes this to accumulation in a complex mosaic of contiguous channel-levee-marsh-pond subenvironments behind a shoreline beach-ridge system in the manner envisioned by Hardie and Ginsburg (1977) for the Andros Island tidal-flat system. However, there is a discernible stratigraphic pattern in that bioturbated micrite subfacies dominate the lower part of the tidal-flat facies section and are progressively replaced upward by thin-bedded and laminite subfacies which become more abundant toward the contact with the overlying coastal freshwater lake facies (figure 65). In addition, it is possible to recognize within this complex succession of meter-scale subfacies individual A-B and A-B-C shallowing upward sequences that record local progradation or vertical accretion such as pond ⧫ levee, pond ⧫ marsh ⧫ levee, marsh ⧫ levee (figure 65).

The coastal freshwater lake facies is characterized by a distinctive stromatolite subfacies which is cyclically interbedded with laminite subfacies and thin-bedded micrite subfacies (figure 65). The stromatolite subfacies is unusual in that it forms meter-scale beds composed entirely of LLH-C (laterally linked hemispheres-concentric) stromatolites (Logan and others 1964). The cryptalgal lamination is made of clotted micrite and micritic peloids and there is an abundance of vertically oriented filament molds. Conspicuously absent are marine macrofossils or burrows of any kind. In composition, fabric, and morphology, these stromatolitic beds are strikingly similar to modern freshwater stromatolites of the coastal freshwater lakes landward of the tidal flats and algal marsh of Andros Island (Monty 1972; Monty and Hardie 1976). For this reason, plus the exclusive association with supratidal subfacies (laminites and thin-bedded micrites), Mitchell (1981, 1985; Demicco and Mitchell 1982) interpreted this 10 - 70 m thick stromatolitic section of the St. Paul carbonates as a coastal freshwater lake deposit separated from the sea by a belt of rainy, low energy tidal flats. At the peak of the St. Paul mega-regression, then, these coastal freshwater lakes and marshes prograded over the tidal flats (figure 65) and in turn were covered by tidal flats as the sea returned in the final drowning of the huge, long-lived Cambro-Ordovician carbonate platform of the Appalachians.

Overall, the St. Paul Group presents some notable aspects of carbonate tidal-flat deposition. Worth stressing are the following:

(1) The dominance of lime mud, the absence of current and wave-worked structures, the abundance of soft-bodied burrowers and the low diversity of fauna are all hallmarks of a low energy, low tide range tidal flat with restricted circulation.

(2) Algal tufa, the abundance of stromatolites and thin beds in the supratidal zone, and the absence of any traces of evaporites indicate a rainy climate.

(3) The complex arrangement of subfacies, both laterally and vertically, signifies that accretion was not by simple progradation of the tidal flats across a shelf-lagoon, but, instead, carbonate mud filled in a complex mosaic of shallow tidal-flat subenvironments separated from the open shelf-lagoon by some form of barrier bars or beach ridges (compare with Gebelein 1974).

(4) The Andros Island tidal-flat system (Shinn and others 1969; Hardie 1977; see Chapter by Shinn, this *Quarterly*) has proved valuable in explaining many specific features and even subfacies in the St. Paul Group and demonstrates that the comparative sedimentology method can be applied on a small scale. But the close comparison also demonstrates that carbonate tidal flats with the same processes and style of accumulation as those of the Holocene were in existence at least by the early Paleozoic. Even the scale of the St. Paul tidal-flat facies, which seems to have covered an area of less than 1000 km^2 on the huge Middle Ordovician platform (Mitchell 1981, 1985; Demicco and Mitchell 1982), is "Holocene-size" rather than the epicontinental-sea scale regarded to be charactertistic of early Paleozoic carbonate tidal flats (Ginsburg 1982). The occurrence of small-scale Andros Island-type tidal flats can be extended back to at least the Upper Cambrian. Howe (1968) described repetitions of meter-scale cycles composed of alternations of burrowed peloidal carbonate mud and laminites of Upper Cambrian age in Missouri (Bonneterre, Davis, Potosi and Eminence equivalents) that nucleated on islands of Precambrian basement rocks (Shinn 1983a, figure 50) and prograded over an area of no more than 5000 km^2.

The Wills Creek Shale (Upper Silurian), Central Appalachians. The Upper Silurian Wills Creek Shale and the overlying Tonoloway Limestone make up a 350-m-thick sequence of shallow-water carbonates (dominated by tidal-flat facies) that lie between the Salina evaporites of the Appalachian, Ohio and Michigan intracratonic basins to the west, and the Upper Silurian clastic wedge that was shed from the Taconic (Late Ordovician) orogenic belt to the east (see Alling and Briggs 1961; Tourek 1970; and Smosna and others 1977, for the paleogeography of the area during the Upper Silurian).

The Wills Creek Shale in the Pennsylvania-Maryland-West Virginia region is 140-200 m thick and covers an area of at least 5000 km^2. Despite its name, it is a limestone-dolomite succession, but it contains subordinate mudstones and quartz siltstones that are most abundant near the base and in eastern outcrops of the formation. The entire Wills Creek succession is composed of meter-scale tidal-flat sequences especially notable for their thick laminites with spectacular mudcracks and prism-cracks. These sequences provide an interesting contrast to the St. Paul Group just described. Both are lime-mud deposits (micrite and peloidal micrite predominate) with a very restricted marine fauna confined to thin-bedded, "low energy," subtidal subfacies, but their enviromental settings were very different.

Tourek (1970) described in detail the array of primary and early diagenetic features in both the Wills Creek and Tonoloway rocks that are diagnostic of a tidal-flat origin: laminites, thin beds, stromatolites, thrombolites, multi-filled mudcracks, prism-cracks, sheet-cracks, fenestrae, burrows, coquina lenses, flat-pebble conglomerates, wave ripples, convolute beds, and evaporite casts and molds. Subfacies characterized by particular assemblages of these features are organized into repetitive, well defined and asymmetrical shallowing-upward sequences (Tourek 1970; Reinhardt and Hardie 1976). Tourek (1970) recognized, in both the Wills Creek and Tonoloway, four cycle-types which are variations on the same basic theme. Cycles

range from 1-6 m thick and average 2.5 m. Cycle boundaries are sharp and commonly erosional, internal boundaries between subfacies are gradational, and all cycles are capped by a massive, disrupted dolomite mudstone subfacies. The following trends occur within these cycles: layer thickness decreases progressively upward from thin beds to laminites; mudcracks and disruption by evaporite mineral growth increases upward; and marine fossils and cryptalgal mounds are confined to the lower parts.

A modal cycle (typical of 80 percent of the cycles) (figure 66) is as follows:

(1) A basal subfacies composed of cm-scale thin beds of fossiliferous calcisiltite with argillaceous partings. Skeletal debris (ostracodes, brachiopods, echinoderms) may form small coquinoid lenses. Isolated stromatolites (stacked hemisphere and laterally linked hemispheres), oncolites, and small thrombolitic mounds are confined to this subfacies but are uncommon. Small tubular burrows are also uncommon and confined to this subfacies. Some wavy thin beds are ripple cross-laminated peloid grainstones (with variable quartz and skeletal grains). Small scours may be filled with intraclasts. Load casts and convolute bedding may occur where sandy beds overlie muddy interbeds. Transitional upward into (2).

(2) A mudcracked laminite subfacies composed of alternating calcisiltite and calcilutite laminae. Very thick (mm-scale) laminae occur at the base, but they thin progressively upward until laminae near the top average less than 0.2 mm thick. Prominent are polygonal mudcracks and deep prism-cracks that may penetrate up to 70 cm of the laminite unit. The mudcracks V-downwards and are commonly stacked one over the other.

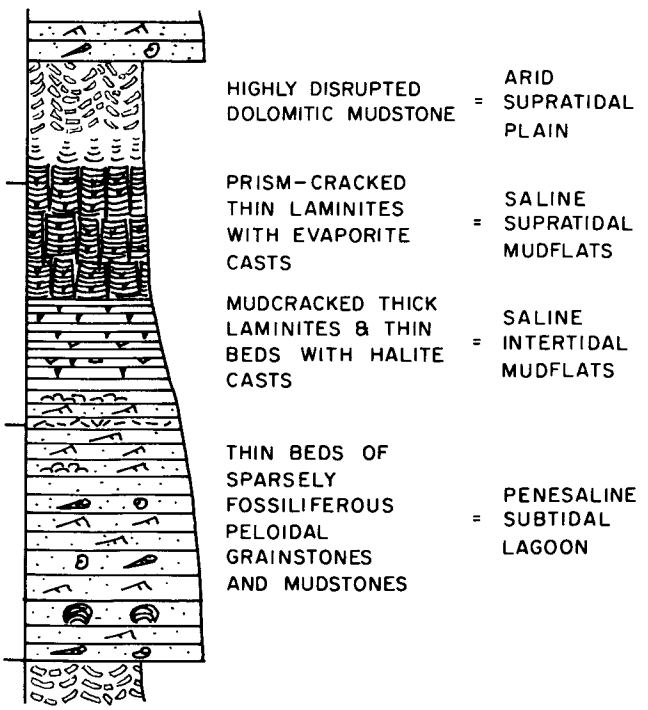

Figure 66.—A typical shallowing-upward peritidal sequence of the Upper Silurian Wills Creek Shale of the central Appalachians, Maryland.

They are filled with sediment from overlying layers, so that each mudcrack-fill reproduces the local microstratigraphy of the laminite. Horizontal sheet-cracks, also with sediment fills, propagate from the mudcracks and prism-cracks. Some wavy lamination may drape mudcrack edges and rare "jelly-roll" lamination is found. Characteristically, in the lower part of this subfacies, the basal bedding planes of the silty laminae are covered with casts of skeletal and hopper halite cubes. In cross-sectional view, these casts penetrate the underlying muddy lamina to produce a rectangular silhouette, commonly infilled with cross-laminated peloidal silt. Elongate to blocky fenestrae appear to represent desiccation vugs and evaporite molds. Transitional upward to (3).

(3) A cycle-cap subfacies consisting of massive, highly disrupted dolomitic mudstone. In polished slabs, traces of lamination can be recognized, as well as multiple polygonal cracks. Rounded quartz grains and scattered nodular vugs, lined or filled with calcite spar, are minor but distinctive components.

Tourek (1970) interpreted the massive cap of the cycle to be the result of repeated disruption by desiccation and the growth of ephemeral evaporite minerals in a sabkha separated from a shallow low-energy lagoon by a wide intertidal mudflat. He considered several options for the origin of the cycles but chose a progradation mechanism.

Tourek (1970) realized that the Persian Gulf sabkha with its gypsum-anhydrite evaporite cap would not serve as an accurate counterpart for the Wills Creek and Tonoloway cycles. We now recognize that a closer environmental analog exists. Castens-Seidell (1984), in a detailed study of the siliciclastic sabkha attached to the Colorado River delta, Gulf of California (Thompson 1968), described prism-cracked laminites overlain gradationally by a massive mud cap that is highly disrupted (see illustrations in Thompson 1968; and Weimer and others 1982, figures 26, 27). These laminites are accumulating on the seaward side of the sabkha on the high, dry supratidal mudflats that separate the 5 km wide intertidal mudflats from the evaporite depocenter on the landward side of the sabkha (figure 68; see also Castens-Seidell 1984; Castens-Seidell and Hardie 1984). The lamination is made of silt-clay couplets mechanically deposited by periodic storm surges that flood the sabkha. These laminites are not only repeatedly mudcracked along the same polygonal fractures to produce Wills Creek-type stacked prism-cracks, but like the Wills Creek laminites, they are replete with horizontal sheet-cracks and gypsum and halite euhedra. Algal mats grow on the surface during wet periods, but their only sedimentary record is in the form of "jelly rolls." The overall analogy with the Wills Creek-Tonoloway laminites is truly striking. What is more, where the distal supratidal flats are no longer active due to isolation by distance or by supratidal beach-ridge barriers, repeated mudcracking and growth and dissolution of halite efflorescent crusts has reduced the near-surface laminites to a massive, soil-like zone resembling the disrupted cap-rock of the Wills Creek cycles. Perhaps this mode of diagenesis in an arid setting is the inevitable result of extensive progradation of the shoreline that leaves the elevated distal parts of the supratidal area essentially abandoned. The evaporite depocenters on the sabkha are depressions on the landward side of the high supratidal flats where floodwaters become ponded and eventu-

ally evaporate. This style of arid tidal-flat deposition is covered in the Permian example described next.

III. Upper Paleozoic

Middle and Upper Devonian carbonate platforms existed on all continents and have been extensively studied as the first massive radiation of coral-stromatoporoid reefs (Wilson 1975). Carbonate tidal-flat deposits associated with these Devonian buildups were described, for example, by Wilson (1967) from the Williston basin, by Read (1973) from the Canning Basin (Australia), and by Laporte (1967, 1975) from the Helderberg Group in New York State.

The Carboniferous was the time of the Walsortian mounds in Europe and elsewhere, and in North America extensive carbonate platforms ran from the Southwest along the length of the West Coast (Dott and Batten 1971, figures 12.1 and 12.12). The late Carboniferous is notable for the astonishing Pennsylvanian coal-bearing cyclothems and their limestone components that dominated the North American craton. Much less attention has been given to Carboniferous tidal-flat carbonates, but Schenk (1967, 1969) described evaporitic tidal-flat carbonates from the Mississippian of Nova Scotia.

The Permian saw a continuation of carbonate platform development in the southwestern United States, particularly around basins such as the Delaware Basin of west Texas and New Mexico. Notable Permian tidal-flat carbonates from this region are those of the Clear Fork Formation (Lucia 1972; Handford 1981) and the San Andreas Formation (Meissner 1972; Shinn 1983a).

The Permian is well known as a period of extensive evaporite development. Two of the largest potash evaporite deposits in the world, the Zechstein of the North Sea area and the Salado of the Delaware Basin, are of Upper Permian age. It is appropriate to take our example of an evaporite-carbonate tidal-flat deposit from an Upper Permain equivalent of the Zechstein evaporite.

The Bellerophon Formation (Upper Permian), Northern Italy. The lower part of the Upper Permian Bellerophon Formation of the Dolomites region of northern Italy is a gypsum-dolomite cyclic succession up to 600 m thick that crops out over an area of about 16,000 km^2 (Bosellini and Hardie 1973). This gypsiferous deposit lies with transitional contact on continental red beds of the Middle Permian Gardena Sandstone and grades upward into shallow marine shelf-lagoon skeletal micrites of the upper Bellerophon Formation. Thus, this thick marginal marine evaporite-carbonate unit records the first stage of a major marine transgression. In the North Sea Basin the huge Zechstein evaporites also record the first incursion of the sea into post-Hercynian continental basins.

The spectacularly exposed Bellerophon gypsum-dolomite succession is remarkable for its organization into meter-scale cycles deposited in a marginal marine evaporite environment. Bosellini and Hardie (1973) measured in 141 m as many as 46 consecutive shallowing-upward sequences, each capped by layered nodular gypsum (figure 67).

The modal cycle (figure 67) consists of three members:

(1) The basal member is a thin bedded "earthy" dolomite with numerous tubular fenestrae and shaly partings (0.1 - 3 m). Fossils are uncommon, restricted to ostracodes, forams, green algae, bivalves and gastropods that become more abundant (but always minor) in each cycle toward the top of the evaporite succession as the upper Bellerophon marine facies is approached.

(2) A dark, sandy dolostone (up to 3 m) with scattered gypsum nodules is the middle member. Traces of flat lamination and cross-lamination are evident in places. Skeletal grains, mainly dasycladacean algal fragments, make up 30 percent of the rock. Oriented gastropod and bivalve shells (replaced by gypsum) delineate layering in places. The gypsum nodules (1 - 30 mm in diameter) become increasingly abundant upward in a single cyclic unit.

(3) The upper member of the modal cycle is a layered nodular gypsum unit (up to 2 m). Thin beds (up to 10 cm) of nodular and "chicken wire" gypsum (made of coalescing nodules) alternate with shaly-dolomitic partings and thin interbeds crowded with isolated gypsum nodules. Bedding is conspicuously undulatory, and in places, highly contorted into enterolithic folds.

Upper and lower boundaries of each cycle are sharp and easily defined in the field. Within each cycle the boundaries between the component subfacies most commonly are gradational in that there is a narrow zone of interbedding of lithologies.

One variation on this theme is the addition to some cycles of a cap unit (up to 1 m thick) of laminar gypsum in which the individual laminae are highly deformed and even isoclinally folded in the plane of lamination.

Bosellini and Hardie (1973) interpreted the cycles as the result of progradation of a sabkha evaporite subenvironment (subfacies 3) over a restricted penesaline lagoon (subfacies 1). An evaporitic, sandy intertidal-supratidal zone (subfacies 2) separated the sabkha from the lagoon. The evidence for a marine sabkha setting was based on the presence of marine fossils, a burrowed basal carbonate mud, and the close similarities of the nodular gypsum subfacies to the layered nodular anhydrite of the modern Persian Gulf sabkha (Kinsman 1966; Butler 1970).

In recent years it has been recognized that (1) nodular anhydrite is not an unequivocal criterion of a sabkha origin (Schreiber and others 1982; Hardie and others 1985), and (2) layered gypsum formed in shallow subaqueous lagoons (Arakel 1980; Warren 1982) may be altered to anhydrite to produce a layered nodular rock (Loucks and Longman 1982) very similar to the layered anhydrite of the standard sabkha model, the Holocene Persian Gulf sabkha. For these reasons the criteria for recognizing ancient sabkha deposits need to be re-evaluated. In this context the recent study by Castens-Seidell (1984) of the modern, active siliciclastic sabkha of the northwest Gulf of California has uncovered an important new element in sabkha deposition, the gypsum pan (Castens-Seidell and Hardie 1983, 1984). This sabkha gypsum pan evolves through the same cycle of stages as that outlined by Lowenstein and Hardie (1985) for salt pans. The features of this gypsum pan are discussed below and summarized in table 1.

The gypsum pan of the Gulf of California sabkha is a large

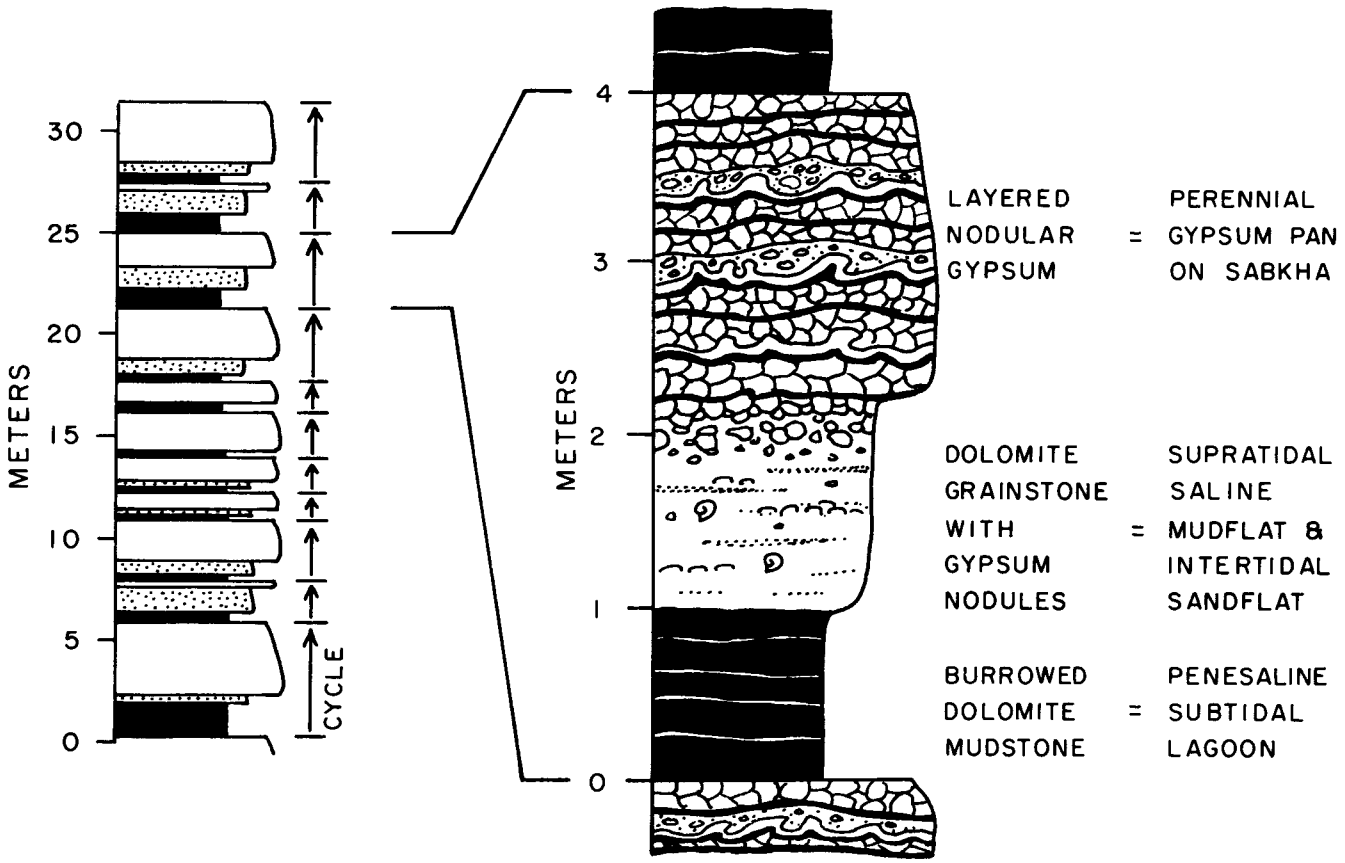

Figure 67.—Shallowing-upward sabkha sequences of the Upper Permian Bellerophon Formation of northern Italy (from Bosellini and Hardie 1973).

(100 km^2) very shallow (< 2m) depression on the sabkha and is bordered on the landward side by alluvial fans and on the seaward side by high, dry supratidal flats (figure 68). Floodwaters (both marine and meteoric) collect in this depression and evaporate to produce a temporary saline lake from which gypsum crystallizes. Each flood event generates a couplet of a mud layer overlain by a gypsum layer. The gypsum has all the attributes of subaqueous lagoon gypsum, that is, prismatic gypsum both as vertically grown "grass-like" bottom crusts and as crystal muds and sands. The bottom crusts nucleate on algal mats and buckle and fold as they grow (see Brantley and others 1984). If flood events are widely spaced in time (several years apart), the shallow gypsum lake dries out leaving a small "bullseye" halite pan in the lowest part (Shearman 1970; Lowenstein and Hardie 1985). During this desiccation stage, gypsum continues to grow in the gypsum sediments from groundwater brines beneath the dry pan surface. This diagenetic growth of gypsum leads to displacive cementation and subsequent polygonal cracking of the surface gypsum crusts. The polygonal cracks become the pathways for further gypsum growth, and diapir-like masses of gypsum crystals build up in the crack pathways and deform the polygon edges into folds and tepees. Renewed flooding may erode the tops of the polygonal pressure ridges and folds and redistribute the winnowed gypsum as a detrital layer. During the desiccation stage the subsurface brine extends into the muddy laminated sediments surrounding the gypsum pan, where intrasediment growth of gypsum, as discoidal crystals and rosette clusters, disrupts and destroys layering. This produces a saline mudflat (Hardie and others 1978) envelope around the gypsum pan (figure 68). In both the gypsum pan and the saline mudflat, dehydration of gypsum to anhydrite is generating nodular fabrics. These take the form of isolated nodules in the saline mudflat and contorted layers of nodules in the gypsum pan. Butler (1970) and Shinn (1983a, also see chapter by Shinn, this *Quarterly*) illustrated such features from the Abu Dhabi sabkha. The layered nature of the Persian Gulf nodular anhydrite suggests a gypsum pan origin rather than the *de novo* intrasediment growth mechanism generally accepted (for example, Kinsman 1966). The Persian Gulf sabkhas appear to be "dead" in that all the gypsum has been dehydrated to nodular anhydrite and the pan(s) filled in with eolian sand that now blankets the sabkhas.

Several important aspects of evaporite deposition on sabkhas emerge from the Gulf of California study (Castens-Seidell 1984; Castens-Seidell and Hardie, in preparation):

(1) Layered gypsum develops in ephemeral saline pans on the sabkha. A climatic pattern of infrequent flooding of the sabkha promotes a strong overprint of early diagenesis in the form of polygonal pressure ridges and tepees, diapir-like masses, and dissolution and erosional truncation of such ridges, tepees,

Table 1.—*The gypsum pan cycle, the sabkha, Salina Omotepec, Baja California*

(see Castens-Seidell 1984)

I. THE GYPSUM PAN CYCLE

The gypsum pan cycles through a flood stage (brackish lake) ⧫ evaporative concentration stage (saline lake) ⧫ desiccation stage (dry gypsum pan) ⧫ flood stage (start of next cycle). Compare Lowenstein and Hardie (1985).

II. FLOOD STAGE

(1) Dissolution of soluble salts in surface saline crusts (particularly halite efflorescent crusts).
(2) Reworking of gypsum crystals into detrital lags. Particularly susceptible to erosional truncation are the exposed crests of gypsum "folds", tepees (polygonal pressure ridges), and other antiform structures of the underlying layered gypsiferous sediments.
(3) Deposition of a lamina or thin bed of mud out of the brackish lake waters.
(4) Algal mat growth on settled-out mud layer.

III. EVAPORATIVE CONCENTRATION STAGE

(1) Evaporative concentration of the waters of the temporary lake leads eventually to precipitation of aragonite, Mg-calcite and gypsum, which settle as a rain of tiny needles, plates, and other euhedra to make a thin "drape" of chemical mud on the contorted algal mat surface.
(2) As the saline lake shrinks, bottom growth of gypsum produces a firm to hard crust of vertically oriented blade-shaped and swallow-tail twin crystals. This bottom-grown crystalline layer mimics the contortions of the algal mat-chemical mud substrate. Continued outward growth then exaggerates the contortions to produce an "enterolithically folded" layer of crystalline gypsum.
(3) Shrinking of the evaporating lake exposes the newly deposited mud layer at the lake periphery, and leads to mud-cracking and intrasediment growth of discoidal gypsum in the vadose zone, which thoroughly disrupts the sediment layering. This is the origin of the saline mudflat that surrounds the gypsum pan (figure 68).

IV. DESICCATION STAGE

(1) Complete drying out of the gypsum pan leads to intrasediment growth of diagenetic gypsum from the shallow subsurface brines beneath the pan. This growth occurs as syntaxial overgrowths on primary gypsum crystals, syntaxial rehealing of partially dissolved gypsum grains, and as cements in intergranular pores, desiccation cracks, and other voids in the bedded gypsum.
(2) Displacive growth of gypsum cement fractures the gypsum crusts into polygons (meters to decameters across), the edges of which buckle up into pressure ridges (tepees, cm to dm high).
(3) The polygon cracks act as conduits for upward movement of subsurface brine resulting in the massive displacive precipitation of a gypsum crystal mush in the form of wedge-shaped "diapirs" beneath the pressure ridges extending down to the brine table. This "intrusive" growth of gypsum uptilts the polygon edges and further buckles and deforms the interbedded soft mud and gypsum layers in the ridge zone.
(4) Intrasediment growth of discoidal gypsum crystals and rosettes continues in the mud beneath the saline mudflat.
(5) Dehydration of gypsum to bassanite and anhydrite occurs to a limited extent to produce putty-like nodules and layered nodular anhydrite. Anhydritization seems to be much slower than sedimentation and perhaps only goes to completion after abandonment of the gypsum pan as the sabkha progrades seaward and the pan infills with windblown sediment (as appears to have happened in the Abu Dhabi sabkhas).
(6) During the last stages of drying out of the gypsum pan the saline lake shrinks to a small shallow brine pool from which halite precipitates. This halite pan (Shearman 1970; Lowenstein and Hardie 1985) within the gypsum pan is quite transitory because of massive re-solution of the very soluble halite with each flooding event. Major floods may totally remove all trace of salt pan deposition by carrying the dissolved NaCl back to the sea, leaving the less soluble gypsum behind. By this differential dissolution mechanism, coastal sabkhas become preferential sites for gypsum-anhydrite accumulation, which explains the halite-free layered gypsum-anhydrite caps to tidal-flat cycles so common in the geologic record.
(7) Evaporative pumping of subsurface brines during the desiccation stage results in the entire gypsum pan and surrounding saline mudflat becoming encrusted with a puffy halite efflorescence. This porous efflorescent crust quickly re-dissolves on the next flooding, leaving its record only in the disruption ("haloturbation"?) of the near-surface sediments.

V. THE END-PRODUCT OF GYPSUM PAN DEPOSITION

The characteristic signature of gypsum pan deposition is the alternation, on a lamination to thin-bed scale, of mud (or sand) layers and contorted gypsum layers. The gypsum layer contortions take the form of enterolithic folds, overthrust folds (pressure ridges or tepees), disharmonic folds, and diapir-like mounds. Erosional truncation of fold and ridge crests results in discontinuously scalloped layering. Gypsum layers are both detrital lags and crystalline crusts with vertical growth fabrics. Dehydration of gypsum produces bedded, nodular anhydrite that inherits all the above features (see, for example, illustrations of sabkha anhydrite in Butler 1970 and Shinn 1983a).

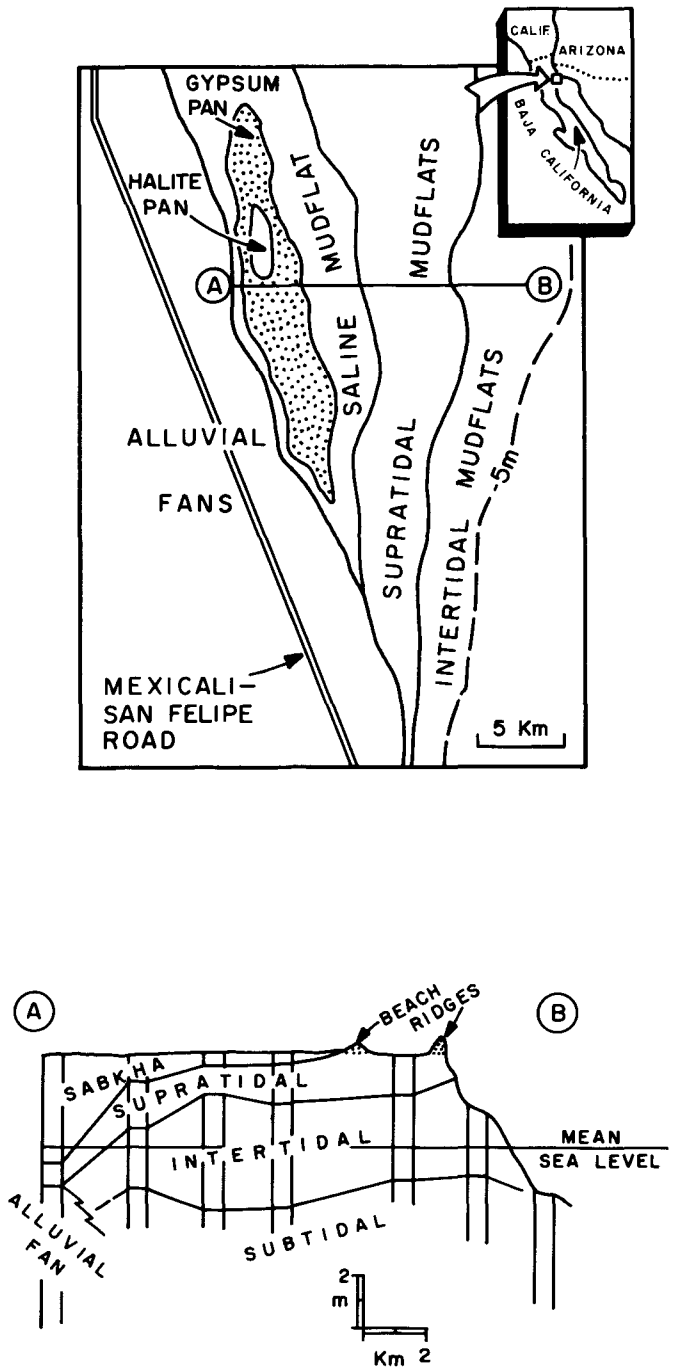

Figure 68.—The modern siliciclastic sabkha of the northwest Gulf of California, Baja California, Mexico. Map shows areal distribution of the major subenvironments of the sabkha. Lower panel is a cross section across depositional strike showing the stratigraphic mosaic of subfacies of Holocene age (from Castens-Seidell 1984; see also Thompson 1968). The position of mean sea level shown is that of the present day.

folds and "diapirs." In contrast, frequent flooding leads to a record dominated by primary subaqueous features such as successive, laterally continuous layers of contorted (enterolithic) gypsum, muddy partings that may be organic-rich, and a lack of polygonal disruption and erosional truncation. The Bellerophon layered gypsum belongs in this latter category.

(2) The supratidal sediments surrounding (and beneath) the gypsum pans are hosts to intrasediment growth of gypsum as isolated single discoidal (hemipyramidal) crystals or aggregates (rosettes) of such crystals.

(3) Supratidal sediments far from the gypsum pan-saline mudflat areas and isolated from ongoing sedimentation develop a disrupted soil-like surface zone, as described in the section of the Wills Creek Shale.

(4) The origin of the anhydrite is by dehydration of gypsum, as evidenced by partially dehydrated gypsum crystals in the sabkha sediments. This dehydration lags considerably behind deposition and the anhydrite inherits and mimics all the primary layering and diagenetic features of the parent gypsum, such as enterolithic folds, diapirs, tepees, etc. The nodular fabric results from the loss of wall shape as single gypsum crystals are replaced by a loose mass of easily deformed anhydrite laths.

(5) The halite pan on the sabkha is ephemeral and not an effective subenvironment in which to accumulate significant salt deposits. This latter follows from the fact that with each major flooding the soluble halite is dissolved and flushed off the sabkha, leaving behind the much less soluble gypsum to preferentially accumulate on the sabkha. The salt pan of the Gulf of California sabkha (Salina Omotepec) studied by Shearman (1970) has completely disappeared, and only the huge gypsum pan in which it was located has survived. Salt deposits require a closed system if they are to accumulate to any thickness (compare with Handford's 1981 interpretation of the 30 m or so thick halite of the Permian Clear Fork Formation as a sabkha salt pan deposit).

(6) The problem of distinguishing layered gypsum-anhydrite sabkha deposits from similar rocks deposited in a marginal marine lagoon setting cannot be easily resolved on the basis of the features of the evaporites themselves. It is necessary to look at the associated rocks, and their stratigraphic relationships with the evaporites, to discriminate between the two. Differences should be apparent at the subfacies-sequence scale, as suggested in figure 69 (from Castens-Seidell and Hardie, in preparation).

IV. Mesozoic

Carbonate buildups of Mesozoic age have long been of both scientific and economic importance. Outstanding examples are the Triassic buildups of the Dolomites (northern Italy) and the northern Alps, the Jurassic of Europe and the Middle East, and the Jurassic-Cretaceous of the Gulf of Mexico region (Wilson 1975). Examples of tidal-flat deposits from these Mesozoic buildups were described, for example, by Fischer (1964, 1975), Bosellini (1967), Wood and Wolfe (1969), Assereto and Kendall (1971), Bosellini and Rossi (1974), and Bradford (1984).

The Triassic of Austria and northern Italy offers some unusual examples of carbonate tidal-flat deposits. The work of Fischer

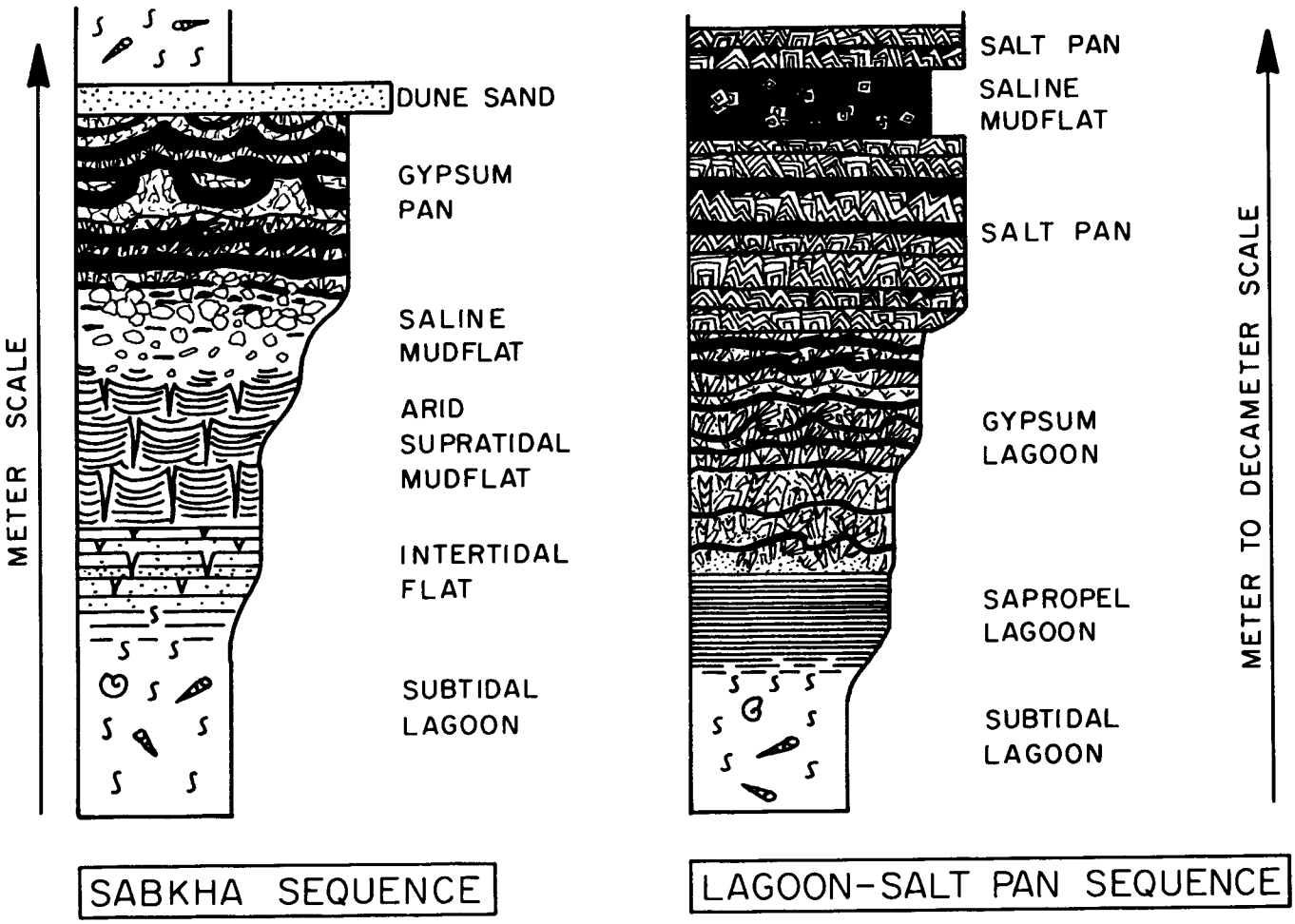

Figure 69.—Hypothetical vertical sections comparing a sabkha cycle to a lagoon-salt pan cycle. Based in part on the modern sabkha of the northwest Gulf of California (see figure 68 and text) and on the Upper Permian Salado Formation salt pan cycles (Lowenstein 1983). From Castens-Seidell and Hardie (in preparation).

(1964) on the Lofer cyclothems in the Dachstein Formation (Norian-Rhaetian) of Austria remains a classic study of cyclic tidal-flat carbonates. Fischer's paper should be read by all students of carbonates as a model of observation and description. His results deserve inclusion in this review, but the reader would be better served by referring to the original text and its shorter companion (Fischer 1975). The Triassic buildups of northern Italy carry a different type of cyclic carbonate than the Lofer, and are different from any of the examples discussed so far. They are shallowing-upward sequences in which the sequence cap is the result of intense diagenesis on subaerial exposure before the deposition of the succeeding sequence.

Triassic Platform Carbonates, Northern Italy. The Middle Triassic carbonate buildups of the Dolomites region of northern Italy are magnificently exposed banks and platforms in which complete platform-to-basin transitions are preserved. Bosellini (1984) documented the internal and external geometric relationships of the buildups and elegantly demonstrated how these buildups record interplay among platform progradation, basin aggradation, and sea-level changes. Offlap, toplap, erosional truncation, and horizontal, climbing and descending progradation are all recognized in vertical outcrops on the scale present in seismic stratigraphic profiles. The platform carbonates of these kilometer-thick buildups are made up of a repetitive succession of flat-lying, meter-scale shallowing-upward sequences, each with a diagenetic cap. A particularly illuminating example is the Ladinian platform sequence in the small but well-exposed Latemar buildup (Bosellini and Rossi 1974; Gaetani and others 1981; Bosellini 1984). This sequence, known as the Latemar Limestone, is 400 m thick and is composed of about 400 limestone-dolomite couplets ("cycles")

ranging in thickness from 0.1 to 5 m, with an average of about 1 m (figure 70). The following description of these Latemar cycles is taken directly from Hardie, Bosellini, and Goldhammer (1986, in review). The thicker, lower member of a couplet is a thin- to medium-bedded limestone consisting of packstones and grainstones containing micritized skeletal grains (gastropods, crinoids, dasycladacean algae, foraminifera), peloids, oncoids and grapestone lumps. Large irregular fenestrae (shelter pores beneath lumps; see figure 9 and Shinn 1983b) and tubular fenestrae (burrows) are lined with isopachous fibrous calcite cements (early marine), reflecting a high pre-cement porosity (no compaction). The upper member of a couplet is a thin dolomitic cap (5-35 cm thick) that in thin section is seen simply to be the underlying limestone lithology in which microcrystalline dolomite has infilled framework pores and preferentially replaced micritized grains and micrite coatings on allochems. Small fenestral pores contain typical meniscus cements, whereas large pores are draped with pendant cements. These microdolomite and cement features are very similar to those of vadose dolomite-aragonite crusts of modern carbonate tidal flats (as in the Bahamas, Shinn and others 1965; Hardie 1977). Additionally, pisoids and perched internal sediment are present in the dolomitic caps. Each limestone-dolomite couplet is interpreted to be subtidal, early cemented lime sand that

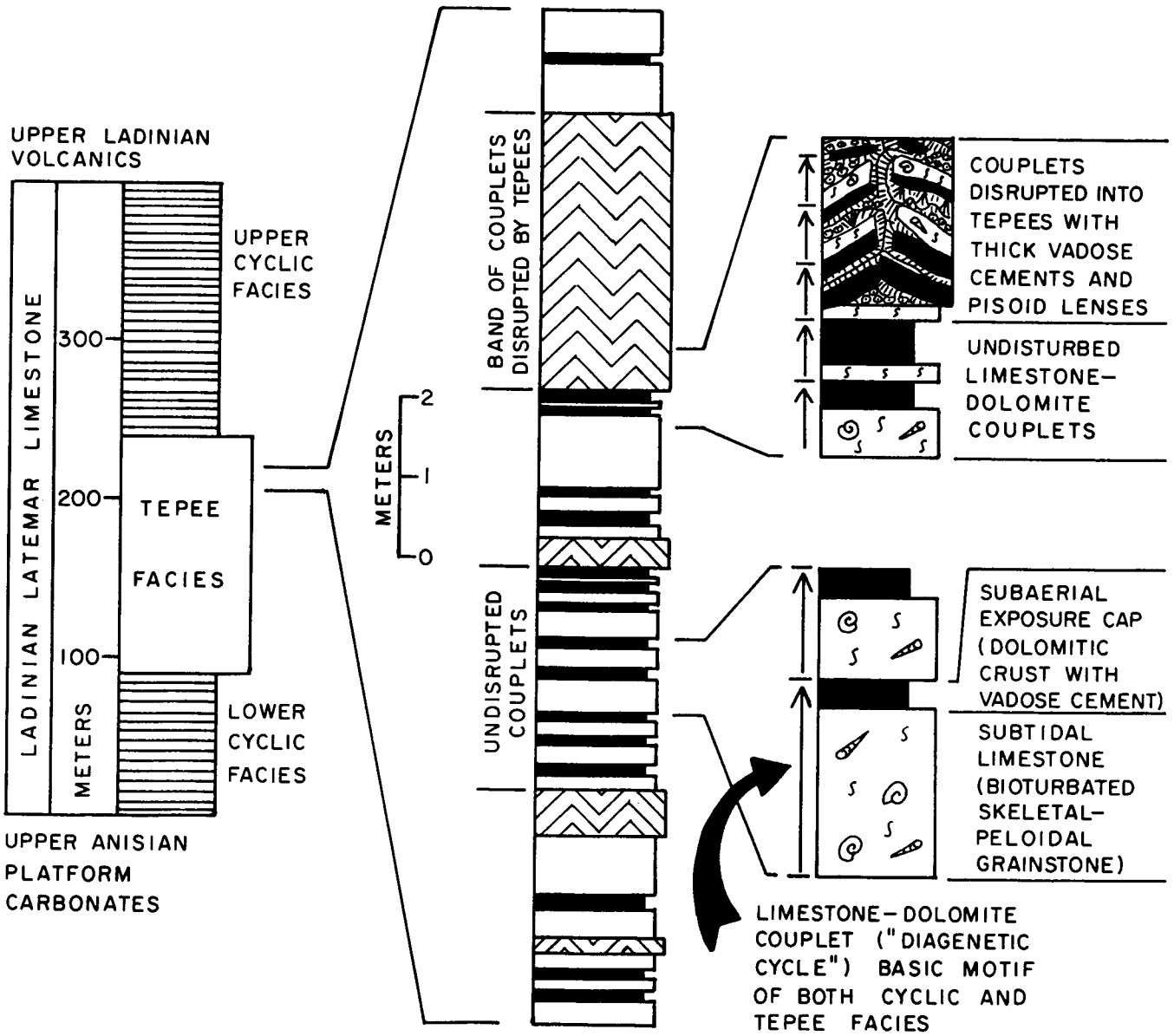

Figure 70.—"Diagenetic" cycles of the Middle Triassic Latemar Limestone of the Dolomites, northern Italy (from Hardie and others 1986).

suffered minor vadose diagenesis (dolomite crust formation) on subaerial exposure. Of major significance is the absence of well developed peritidal deposits between the subtidal limestones and their very thin diagenetic caps. Hence, these are not normal shallowing-upward depositional cycles but rather are "diagenetic cycles."

In the middle of this evenly bedded sequence is a 150-m section characterized by thick (1-13 m) tepee zones (Bosellini and Rossi 1974, figure 22; Assereto and Kendall 1977, figure 3c) that extensively disrupt whole packages of the "diagenetic cycles" (figure 70). These tepee zones consist of brecciated and uparched slabs of "mother rock" (the limestone-dolomite couplets) that are separated by cm-scale sheetcracks and shelter-pores filled with a variety of calcite cements, laminated internal sediments and pisoids. The tepee ridges, with relief up to 3 m, display truncated tops, and overlying beds onlap the tepee flanks, indicating the syndepositional origin of the tepees. Tepee cements include festooned "cellular" paleoflowstone crusts, large radially arranged ray crystals ("raggioni"), small hemispheres of radial fibrous crystals, and radiaxial fibrous isopachous crusts ("coconut meat" cement) that were described so well by Assereto and Folk (1980) from the late Ladinian Calcare Rosso to the east of the Dolomites in Lombardy, Italy. The laminated internal sediments are calcite microspar mosaics (vadose silt) that contain weathered, oxidized mafic mineral grains (probably windblown volcanogenic material) that impart a red color to the sediments (so-called "terra rossa"). Pisoids occur within diagenetically altered mother rock and within tepee shelter pores admixed with cements and internal sediments, and in places have a fitted fabric typical of *in situ* growth. These diagenetic components may occupy as much as 75 percent of the volume of the tepee zones.

Each tepee zone is interpreted as the product of massive expansive cementation in a vadose zone several meters deep under semiarid or arid conditions, formed when the Latemar platform was exposed for a substantial period. These tepee zones are superimposed on the repeating pattern of smaller scale "diagenetic cycles," incorporating several pre-existing cycles, and so must be responses to a pulse of subaerial exposure different from that of the limestone-dolomite couplets. The cm-scale dolomitic diagenetic caps of the meter-scale limestone-dolomite couplets could easily form slightly above sea level in periods measured in centuries, to judge by modern supratidal analogs. On the other hand, to produce the thick sheetcrack cements and pisoid lenses of the tepee zones would seem to require many thousands of years (compare the Holocene tepees of Shark Bay, Western Australia, where cements have apparently grown at 2-4 mm/1000 years; Handford and others 1984). Any explanation of the cause of the repeated exposure of the Ladinian Latemar platform must involve two separate pulses, a basic small-scale pulse to account for the "diagenetic cycles," and a larger amplitude, more irregular and longer period pulse to account for the superimposed tepee zones.

Carbonate platforms constructed of stacks of meter-scale diagenetic cycles with prominent brecciated, pisolitic tepee caps occur throughout the Triassic record of northern Italy. Examples are the Ladinian Calcare Rosso in Lombardy (Assereto and Kendall 1971, 1977; Assereto and Folk 1980), and the Carnian Dürrenstein formation and Norian Dolomia Principale in the Dolomites (Bosellini and Hardie 1986; Hardie, Bosellini, and Goldhammer 1986). Similar, tepee-capped cycles are well known from the Permian Carlsbad Group of the Guadalupes, New Mexico (Dunham 1969).

The Triassic diagenetic cycles of the Dolomites are of special importance because they provide unequivocal evidence that the repeated exposure recorded by the diagenetic caps must be the result of sea-level oscillations rather than gradual abandonment of supratidal flats by progradation. This conclusion follows from the conspicuous absence of peritidal deposits between the subtidal sediments and the vadose diagenetic cap, as is particularly well demonstrated by the Ladinian Latemar cycles described above. Repeated subaerial exposure of subtidal sediments without the accumulation of intertidal and supratidal deposits calls for rapid falls in relative sea level due to glacio-eustatic oscillations or pulses of tectonic uplift (see full discussion in the following section on stratigraphic models).

Another significant aspect of diagenetic cycles is that the characteristics of the alteration cap reflect the prevailing climate. In the Triassic of the Dolomites the massive, expansive cementation that produced the sheet-crack brecciation and tepees must reflect extensive flow-through of seawater (or groundwater) in the vadose zone under semiarid or arid climatic conditions. In contrast, in a wet climate, prolonged subaerial exposure should result in the development of a karstic soil cap, as for example, occurred when the Great Bahama Bank was periodically exposed by the sizable glacio-eustatic sea-level drops during the Plio-Pleistocene ice age. Beach and Ginsburg (1978) report 18 minor karstic surfaces spaced only a few meters apart in the Plio-Pleistocene platform carbonates beneath the Great Bahama Bank. Significantly, no intertidal-supratidal deposits developed between the subtidal sediments and the karstic caps, so these Bahamian Plio-Pleistocene diagenetic cycles are exemplary wet-climate analogs of the Italian Triassic diagenetic cycles.

One final matter that needs to be confronted here is the absence from many tidal-flat cycles in the geological record of evidence of extensive disruptive vadose cementation or karstification at their upper boundaries. As supratidal flats grow by vertical accretion and progradation (see next section), large areas must be left exposed to subaerial diagenesis (see Ginsburg 1982), yet many supratidal laminite caps in ancient tidal-flat sequences show no massive vadose alteration (for example, see figures 64 and 65). Is the presence of a diagenetic cap a function of the length of time the supratidal flats are exposed? Comparison of the average duration of cycles with diagenetic caps (as in Ladinian Latemar Limestone) or without diagenetic caps (Cambrian Conococheague Limestone) does not support this explanation (see table 2). Another possibility is that the position of mean sea level with respect to the supratidal flats is important. If sea level does not fall during progradation, then (1) major storms could continue to slowly add sediment to even the remotest parts of the supratidal plain (much as happens today on the huge Rann of Kutch in western India and southeastern Pakistan), a process that would discourage the focussing of subaerial diagenesis at a single exposure surface; and (2) the seawater table would be very close to the tidal-flat surface. This

latter situation in an arid climate would promote sabkha evaporite formation instead of expansive carbonate cementation, and in a wet climate would not allow the development of a freshwater lens thick enough to produce a karstic soil cap. However, in a semiarid climate, this scenario may not rule out the growth of a pisolitic tepee cap. If, on the other hand, the tidal flats are abandoned by a fall in sea level, then not only will supratidal sedimentation be shut off completely but the resulting drop in the seawater table could allow extensive freshwater or brackish water diagenetic alteration of the exposed tidal-flat sediments.

In conclusion, the Ladinian-type "diagenetic cycles" are an important end member in our spectrum of shallowing-upward carbonate sequences because they record a direct connection between platform accretion, syndepositional diagenesis and sea-level oscillations. However, much more work is needed before we fully understand these singular deposits.

Summary: Types of Tidal-Flat Deposits

Tidal-flat deposits in the geologic record may be "typed" in a simplified way by reference to a set of hypothetical end members. These end members can be constructed assuming that the major factors influencing the style of deposition are (1) the climate, which shapes the supratidal record, and (2) the "energy" of the tidal-flat system, mainly the intensity of the daily wave and tidal current activity, which affects the subtidal and intertidal records. This is, of course, a highly simplistic approach in view of our recognition that no two modern or ancient tidal-flat deposits are quite the same, but it can be helpful in identifying general types. Such a scheme is shown in figure 71 (compare James 1984, and Wilson 1975, page 309).

REFERENCES

Ahr, W.M., 1971, Paleoenvironment, algal structures and fossil algae in the upper Cambrian of central Texas: Journal of Sedimentary Petrology, volume 41, pages 205-216.

Aitken, J.D., 1966, Middle Cambrian to Middle Ordovician cyclic sedimentation, Southern Rocky Mountains of Alberta: Bulletin of Canadian Petroleum Geology, volume 14, pages 405-411.

Aitken, J.D., 1967, Classification and environmental significance of cryptalgal limestones and dolomites with illustrations from the Cambrian and Ordovician of southwestern Alberta: Journal of Sedimentary Petrology, volume 37, pages 1163-1178.

Alling, H.L., and Briggs, L.I., 1961, Stratigraphy of Upper Silurian Cayugan evaporites: American Association of Petroleum Geologists Bulletin, volume 45, pages 515-547.

Arakel, A.V., 1980, Genesis and diagenesis of Holocene evaporitic sediments in Hutt and Leeman lagoons, Western Australia: Journal of Sedimentary Petrology, volume 50, pages 1305-1326.

Assereto, R., and Folk, R.L., 1980, Diagenetic fabrics of aragonite, calcite, and dolomite in an ancient peritidal-spelean environment: Triassic Calcare Rosso, Lombardia, Italy: Journal of Sedimentary Petrology, volume 50, pages 371-394.

Assereto, R., and Kendall, C.G. St.C., 1971, Megapolygons in Ladinian limestones of Triassic of southern Alps: evidence of deformation by penecontemporaneous desiccation and cementation: Journal of Sedimentary Petrology, volume 41, pages 715-723.

Assereto, R., and Kendall, C.G. St.C., 1977, Nature, origin and classification of peritidal tepee structures and related breccias: Sedimentology, volume 24, pages 153-210.

Ball, M.M., 1967, Carbonate sand bodies of Florida and the Bahamas: Journal of Sedimentary Petrology, volume 37, pages 556-591.

Beach, D.K., and Ginsburg, R.N., 1978, Facies succession of Pliocene-Pleistocene carbonates, northwestern Great Bahama Bank: American Association of Petroleum Geologists Bulletin, volume 64, pages 1634-1642.

Black, M., 1933, The algal sediments of Andros Island, Bahamas: Philosophical Transactions of the Royal Society, London, series B, volume 222, pages 165-192.

Bosellini, A., 1967, La tematica deposizionale della Dolomia Principale (Dolomiti e Prealpi Venete): Bollettino della Società Geologica Italiana, volume 86, pages 133-169.

Bosellini, A., 1984, Progradation geometries of carbonate platforms: examples from the Triassic of the Dolomites, northern Italy: Sedimentology, volume 31, pages 1-24.

Bosellini, A., and Hardie, L.A., 1973, Depositional theme of a marginal marine evaporite: Sedimentology, volume 20, pages 5-27.

Bosellini, A., and Hardie, L.A., 1986, Facies e cicli della Dolomia Principale della Alpi Venete: Bollettino della Società Geologica Italiana (in press).

Bosellini, A., and Rossi, D., 1974, Triassic carbonate buildups of the Dolomites, northern Italy: Society of Economic Paleontologists and Mineralogists, Special Publication 18, pages 209-233.

Bradford, C.A., 1984, Transgressive-regressive carbonate facies of the Smackover Formation, Escambia County, Alabama: Society of Economic Paleontologists and Mineralogists, Gulf Coast Section, 3rd Annual Research Conference Proceedings, pages 27-39.

Brantley, S.L., Crerar, D.A., Moller, N.E., and Weare, J.H., 1984, Geochemistry of a modern marine evaporite: Bocana de Virilà, Peru: Journal of Sedimentary Petrology, volume 54, pages 447-462.

Braun, M., and Friedman, G.M., 1969, Carbonate lithofacies and environments of the Tribes Hill Formation (Lower Ordovician) of the Mohawk Valley, New York: Journal of Sedimentary Petrology, volume 39, pages 113-135.

Butler, G.P., 1970, Holocene gypsum and anhydrite of the Abu Dhabi sabkha, Trucial Coast: an alternative explanation of origin: Third Symposium on Salt: Northern Ohio Geological Society, Cleveland, Ohio, pages 120-152.

Castens-Seidell, B., 1984, The anatomy of a modern marine siliciclastic sabkha in a rift valley setting: northwest Gulf of California tidal flats, Baja California, Mexico: Ph.D. dissertation, The Johns Hopkins University, Baltimore, Maryland, 386 pages.

Castens-Seidell, B., and Hardie, L.A. ,1983, Gypsum-anhydrite deposition in sabkhas: new observations from the Holocene tidal flats of the northwest Gulf of California, Baja California: Geological Society of America, Abstracts with Programs, Indianapolis, Indiana.

Castens-Seidell, B., and Hardie, L.A. 1984, Anatomy of a modern marine sabkha in a rift valley setting, northwest Gulf of California, Baja California, Mexico: American Association of Petroleum Geologists Bulletin, volume 68, page 460.

Castens-Seidell, B., and Hardie, L.A., (in preparation), The gypsum pan: a critical element in sabkha evaporite deposition.

Cecile, M.P., and Campbell, F.H.A., 1978, Regressive stromatolite reefs and associated facies, middle Goulburn Group (Lower Proterozoic) in Kilohigok Basin, Northwest Territories: an example of environmental control in stromatolite forms: Bulletin of Canadian Petroleum Geology, volume 26, pages 237-267.

Colton, G.W., 1970, The Appalachian Basin—its depositional sequences and their geologic relationships, *in* Weaver, K.N., Fisher, G.W., Pettijohn, F.J., and Reed, J.C., editors, Studies in Appala-

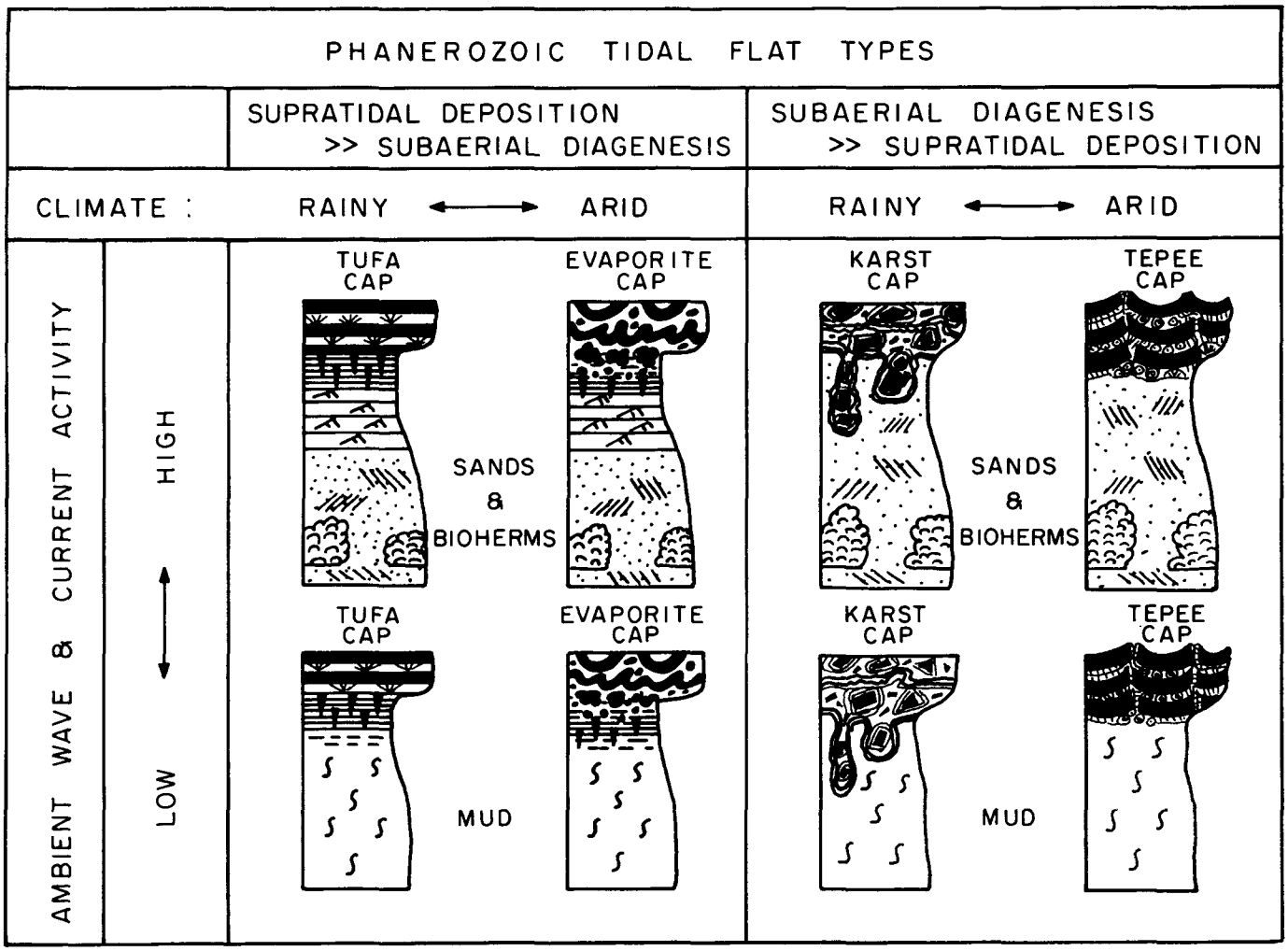

Figure 71.—Highly simplified scheme showing end-member types of tidal flat shallowing-upward sequences occurring in the Phanerozoic.

chian geology, Central and Southern: Wiley Interscience, New York, pages 5-48.

Demicco, R.V., 1981, Comparative sedimentology of an ancient carbonate platform: the Conococheague Limestone of the central Appalachians: Ph.D. dissertation, The Johns Hopkins University, Baltimore, Maryland, 333 pages.

Demicco, R.V., 1983, Wavy and lenticular-bedded carbonate ribbon rocks of the Upper Cambrian Conococheague Limestone, Central Appalachians: Journal of Sedimentary Petrology, volume 53, pages 1121-1132.

Demicco, R.V., 1985, Platform and off-platform carbonates of the Upper Cambrian of western Maryland, U.S.A.: Sedimentology, volume 32, pages 1-22.

Demicco, R.V., and Hardie, L.A., 1981, Patterns of platform and off-platform carbonate sedimentation in the upper Cambrian of the central Appalachians and their implications for sea level history: 2nd International Symposium on the Cambrian System: U.S. Geological Survey Open-File Report 81-743, pages 67-70.

Demicco, R.V., Hardie, L.A., and Haley, J.S., 1982, Algal mounds of upper Cambrian carbonates of Appalachians, western Maryland: American Association of Petroleum Geologists Bulletin, volume 66, page 563.

Demicco, R.V., and Mitchell, R.W., 1982, Facies of the Great American Bank in the central Appalachians, *in* Lyttle, P.T., editor, Central Appalachian geology, field trip guidebook: American Geological Institute, Falls Church, Virginia, pages 171-266.

Donaldson, J.A., 1966, Marion Lake map-area, Quebec-Newfoundland: Geological Survey of Canada Memoir, number 338, 85 pages.

Donaldson, J.A. 1976, Paleoecology of Conophyton and associated stromatolites in the Precambrian Dismal Lakes and Rae Groups, Canada, *in* Walter, M.R., editor, Stromatolites: Elsevier, New York, pages 523-534.

Dott, R.H., and Batten, R.L., 1971, Evolution of the earth: McGraw-Hill, New York, 649 pages.

Dravis, J.J., 1983, Hardened subtidal stromatolites, Bahamas: Science, volume 219, pages 385-386.

Dunham, R.J., 1969, Vadose pisolite in the Capitan Reef (Permian), New Mexico and Texas: Society of Economic Paleontologists and Mineralogists, Special Publication 14, pages 182-191.

Eriksson, K.A., and Truswell, J.F., 1974, Tidal flat associations from a Lower Proterozoic carbonate sequence in South Africa: Sedimentology, volume 21, pages 293-309.

Fischer, A.G., 1964, the Lofer cyclothems of the Alpine Triassic: Geological Survey of Kansas Bulletin, volume 169, pages 107-149.

Fischer, A.G. 1975, Tidal deposits, Dachstein Limestone of the North-Alpine Triassic, *in* Ginsburg, R.N., editor, Tidal deposits: Springer-Verlag, New York, pages 235-242.

Gaetani, M., Fois, E., Jadoul, F., and Nicora, A., 1981, Nature and evolution of Middle Triassic carbonate buildups in the Dolomites (Italy): Marine Geology, volume 44, pages 25-57.

Garrett, P., 1970, Phanerozoic stromatolites: noncompetitive ecological restriction by grazing and burrowing animals: Science, volume 169, pages 171-173.,

Gebelein, C.D., 1974, Modern Bahamian platform environments: Field trip guidebook, Geological Society of America Annual Meetings, Miami Beach, 106 pages.

Ginsburg, R.N., 1955, Recent stromatolitic sediments from south Florida (abstracts): Journal of Paleontology, volume 19, page 723.

Ginsburg, R.N. 1975, editor, Tidal deposits: Springer-Verlag, New York, 428 pages.

Ginsburg, R.N., 1982, Actualistic depositional models for the Great American Bank (Cambro-Ordovician): International Association of Sedimentologists, 11th International Congress on Sedimentology, Abstracts, Hamilton, Ontario, Canada, page 114.

Grotzinger, J.P., 1985, Evolution of early Proterozoic passive-margin carbonate platform, Rocknest Formation, Wopmay Orogen, Northwest Territories, Canada: Unpublished Ph.D. dissertation, Virginia Polytechnic Institute and State University, Blacksburg, Virginia, 225 pages.

Grover, G., and Read, J.F., 1978, Fenestral and associated vadose diagenetic fabrics of tidal flat carbonates, Middle Ordovician New Market Limestone, southwestern Virginia: Journal of Sedimentary Petrology, volume 48, pages 453-473.

Halley, R.B., 1975, Peritidal lithologies of Cambrian carbonate islands, Carrara Formation, southern Great Basin, *in* Ginsburg, R.N., editor, Tidal deposits: Springer-Verlag, New York, pages 279-288.

Handford, C.R., 1981, Coastal sabkha and salt pan deposition of the lower Clear Fork Formation (Permian), Texas: Journal of Sedimentary Petrology, volume 51, pages 761-778.

Handford, C.R., Kendall, A.C., Prezbindowski, D.R., Dunham, J.B, and Logan, B.W., 1984, Salina-margin tepees, pisolites, and aragonite cements, Lake MacLeod, Western Australia: their significance in interpreting ancient analogs: Geology, volume 12, pages 523-527.

Hardie, L.A., 1977, editor, Sedimentation on the modern carbonate tidal flats of northwest Andros Island, Bahamas: Johns Hopkins Press, Baltimore, 202 pages.

Hardie, L.A., Bosellini, A., and Goldhammer, R.K. 1986, Repeated subaerial exposure of subtidal carbonate platforms, Triassic, northern Italy: evidence for high frequency sea level oscillations on a 10^4 year scale: Paleoceanography (in review).

Hardie, L.A., and Ginsburg, R.N., 1977, Layering: the origin and environmental significance of lamination and thin bedding, *in* Hardie, L.A., editor, Sedimentation on the modern carbonate tidal flats of northwest Andros Island, Bahamas: Johns Hopkins Press, Baltimore, pages 50-123.

Hardie, L.A., Lowenstein, T.K., and Spencer, R.J., 1985, The problem of distinguishing between primary and secondary features in evaporites: Sixth Symposium on Salt: Northern Ohio Geological Society, Cleveland, Ohio, pages 11-39.

Hardie, L.A., Smoot, J.P., and Eugster, H.P., 1978, Saline lakes and their deposits: a sedimentological approach: International Association of Sedimentologists, Special Publication 2, pages 7-42.

Harris, P.M., 1979, Facies anatomy and diagenesis of a Bahamian ooid shoal: Comparative Sedimentology Laboratory, University of Miami, Miami, Florida, 163 pages.

Hoffman, P., 1973, Evolution of an early Proterozoic continental margin in the Coronation Geosyncline and associated aulacogens of the northwestern Canadian Shield: Philosophical Transactions of the Royal Society, London, Series A, volume 273, pages 547-581.

Hoffman, P., 1974, Shallow and deep-water stromatolites in lower Proterozoic platform-to-basin facies change, Great Slave Lake, Canada: American Association of Petroleum Geologists Bulletin, volume 58, pages 856-867.

Hoffman, P., 1975, Shoaling-upward shale-to-dolomite cycles in the Rocknest Formation (Lower Proterozoic), Northwest Territories, Canada, *in* Ginsburg, R.N., editor, Tidal deposits: Springer-Verlag, New York, pages 257-265.

Hoffman, P., 1976, Environmental diversity of Middle Precambrian stromatolites, *in* Walter, M.R., editor, Stromatolites: Elsevier, New York, pages 599-612.

Hofmann, H.J., 1973, Stromatolites: characteristics and utility: Earth-Science Review, volume 9, pages 339-373.

Howe, W. B., 1968, Planar stromatolites and burrowed carbonate mud facies in Cambrian strata of the St. Francois Mountain area: Missouri Geological Survey and Water Resources, Report of Investigations, 42, 113 pages.

James, N.P., 1984, Shallowing-upward sequences in carbonates, *in* Walker, R.G., editor, Facies models: Geoscience Canada, Reprint Series 1, pages 213-228.

James, N.P., and Choquette, P., 1984, Diagenesis 6: Limestone—the sea floor diagenetic environment: Geoscience Canada, volume 10, pages 162-179.

James, N.P., and Kobluk, D.R., 1978, Lower Cambrian patch reefs and associated sediments, southern Labrador, Canada: Sedimentology, volume 25, pages 1-32.

Kinsman, D.J.J., 1966, Gypsum and anhydrite of Recent age Trucial Coast, Persian Gulf: Second Symposium on Salt, volume 1, Northern Ohio Geological Society, Cleveland, Ohio, pages 302-326.

Kinsman, D.J.J., and Park, R.K., 1976, Algal belt and coastal sabkha evolution, Trucial Coast, Persian Gulf, *in* Walter, M.R., editor, Stromatolites: Elsevier, New York, pages 421-434.

Klein G. deV., 1971, A sedimentary model for determining paleotidal range: Bulletin of Geological Society of America, volume 82, page 2585-2592.

Laporte, L.F., 1967, Carbonate deposition near mean sea level and resulting facies mosaic: Manlius Formation (Lower Devonian) of New York State: American Association of Petroleum Geologists Bulletin, volume 51, page 73-101.

Laporte, L.F., 1975, Carbonate tidal-flat deposits of the early Devonian Manlius Formation of New York State, Ginsburg, R.N., editor, Tidal deposits: Springer-Verlag, New York, pages 243-250.

Logan, B.W., Hoffman, P., and Gebelein, C.D., 1974, Algal mats, cryptalgal fabrics and structures, Hamelin Pool, Western Australia: American Association of Petroleum Geologists Memoir 22, pages 140-194.

Logan, B.W., Rezak, R., and Ginsburg, R.N., 1964, Classification and environmental significance of algal stromatolites: Journal of Geology, volume 72, pages 68-83.

Loucks, R.G., and Longman, M.W., 1982, Lower Cretaceous Ferry Lake Anhydrite, Fairway Field, East Texas: products of shallow-

subtidal deposition: Society of Economic Paleontologists and Mineralogists Core Workshop, number 3, pages 130-173.

Lowe, D.R., 1980, Stromatolites 3,400-Myr old from the Archaean of Western Australia: Nature, volume 284, pages 441-443.

Lowenstein, T.K., 1983, Deposits and alteration of an ancient potash evaporite: the Permian Salado Formation of New Mexico and West Texas: unpublished Ph.D. dissertation, The Johns Hopkins University, Baltimore, Maryland, 411 pages.

Lowenstein, T.K., and Hardie, L.A., 1985, Criteria for the recognition of salt-pan evaporites: Sedimentology, volume 32, pages 627-644.

Lucia, F.J., 1972, Recognition of evaporite-carbonate shoreline sedimentation: Society of Economic Paleontologists and Mineralogists, Special Publication 16, pages 160-191.

Markello, J.R., Tillman, C.G., and Read, J.F., 1979, Lithofacies and biostratigraphy of Cambrian and Ordovician platform and basin facies, carbonates and clastics, southwestern Virginia: Geological Society of America Southeastern Section Field Trip, number 2, pages 43-85.

Matter, A., 1967, Tidal flat deposits in the Ordovician of Western Maryland: Journal of Sedimentary Petrology, volume 37, pages 601-609.

Meissner, F.F., 1972, Cyclic sedimentation in Middle Permian strata of the Permian Basin, West Texas and New Mexico, *in* Elam, J.C., and Chuber, S., editors, Cyclic Sedimentation in the Permian Basin: Texas Geological Society, Midland, Texas, pages 203-232.

Miall, A.D., 1978, editor, Fluvial sedimentology: Canadian Society of Petroleum Geologists, Memoir 5, 859 pages.

Mitchell, R.W., 1981, The comparative sedimentology of the Bahamian-type shelf carbonates of the Middle Ordovician St. Paul Group of the central Appalachians: Ph.D. dissertation, The Johns Hopkins University, Baltimore, Maryland, 495 pages.

Mitchell, R.W., 1985, Comparative sedimentology of shelf carbonates of the Middle Ordovician St. Paul Group, central Appalachians: Sedimentary Geology, volume 43, pages 1-41.

Monty, C.L.V., 1972, Recent algal stromatolite deposits, Andros Island, Bahamas: Geologische Rundschau, volume 62, pages 742-783.

Monty, C.L.V., and Hardie, L.A., 1976, The geological significance of the freshwater blue-green algal calcareous marsh, *in* Walter, M.R., editor, Stromatolites: Elsevier, New York, pages 447-478.

Mukherji, K.K., 1969, Supratidal carbonate rocks in the Black River (Middle Ordovician) Group of southwestern Ontario, Canada: Journal of Sedimentary Petrology, volume 39, pages 1530-1545.

Pfeil, R.W., and Read, J.F., 1980, Cambrian carbonate platform margin facies, Shady Dolomite, southwestern Virginia, U.S.A.: Journal of Sedimentary Petrology, volume 50, pages 91-116.

Pratt, B.R., and James, N.P. 1982, Cryptalgal metazoan bioherms of early Ordovician age in St. George Group, western Newfoundland: Sedimentology, volume 29, pages 543-569.

Raaben, M.E., 1969, Columnar stromatolites and late Precambrian stratigraphy: American Journal of Science, volume 267, pages 1-18.

Read, J.F., 1973, Carbonate cycles, Pillara Formation (Devonian), Canning Basin, Western Australia: Bulletin of Canadian Petroleum Geology, volume 21, pages 38-51.

Read, J.F., 1980, Carbonate ramp-to-basin evolution, Middle Ordovician, Virginia Appalachians: American Association of Petroleum Geologists Bulletin, volume 64, pages 1575-1612.

Reinhardt, J., 1974, Stratigraphy, sedimentology and Cambro-Ordovician paleogeography of the Frederick Valley, Maryland: Maryland Geological Survey, Report of Investigations, number 23, 74 pages.

Reinhardt, J., 1977, Cambrian off-shelf sedimentation, central Appalachians: Society of Economic Paleontologists and Mineralogists, Special Publication 25, pages 83-112.

Reinhardt, J., and Hardie, L.A., 1976, Selected examples of carbonate sedimentation, Lower Paleozoic of Maryland: Maryland Geological Survey Guidebook, number 5, Baltimore, Maryland, 53 pages.

Roehl, P.O., 1967, Stony Mountain (Ordovician) and Interlake (Silurian) facies analogs of Recent, low-energy marine and subaerial carbonates, Bahamas: American Association of Petroleum Geologists Bulletin, volume 51, pages 1979-2032.

Root, S.I., 1964, Cyclicity of the Conococheague Formation: Pennsylvania Academy of Science Proceedings, volume 38, pages 157-160.

Root, S.I., 1968, Geology and mineral resources of southeastern Franklin County, Pennsylvania: Pennsylvania Geological Survey, 4th Series Atlas 119 edition, 118 pages.

Sarin, D.D., 1962, Cyclic sedimentation of primary dolomite and limestone: Journal of Sedimentary Petrology, volume 32, pages 451-471.

Schenk, P.E., 1967, The Macumber Formation of the Maritime Province, Canada—a Mississippian analogue to Recent strand-line carbonates of the Persian Gulf: Journal of Sedimentary Petrology, volume 37, pages 365-376.

Schenk, P.E., 1969, Carbonate-sulfate-redbed facies and cyclic sedimentation of the Windsorian Stage (Middle Carboniferous), Maritime Province: Canadian Journal of Earth Science, volume 6, pages 1037-1066.

Schreiber, B.C., Roth, M.S., and Helman, M.L., 1982, Recognition of primary facies characteristics of evaporites and the differentiation of these forms from diagenetic overprints: Society of Economic Paleontologists and Mineralogists Core Workshop, number 3, pages 1-32.

Shearman, D.J., 1970, Recent halite rock, Baja California, Mexico: Transactions of Institute of Mining and Metallurgy, volume 79B, pages 155-162.

Shinn, E.A., 1983a, Tidal flat environment: American Association of Petroleum Geologists Memoir 33, pages 173-210.

Shinn, E.A., 1983b, Birdseyes, fenestrae, shrinkage pores, and loferites: a re-evaluation: Journal of Sedimentary Petrology, volume 53, pages 619-628.

Shinn, E.A., Ginsburg, R.N., and Lloyd, R.M., 1965, Recent supratidal dolomite from Andros Island, Bahamas: Society of Economic Paleontologists and Mineralogists, Special Publication 13, pages 112-123.

Shinn, E.A., Lloyd, R.M., and Ginsburg, R.N., 1969, Anatomy of a modern carbonate tidal flat, Andros Island, Bahamas Journal of Sedimentary Petrology, volume 39, pages 1202-1228.

Smoot, J.P., 1983, Depositional subenvironments in an arid closed basin: the Wilkins Peak Member of the Green River Formation (Eocene), Wyoming, U.S.A.: Sedimentology, volume 30, pages 801-828.

Smosna, R.A., Patchen, D.G., Warshauer, S.M., and Perry, W.J., 1977, Relationships between depositional environments, Tonoloway Limestone, and distribution of evaporites in the Salina Formation, West Virginia: American Association of Petroleum Geologists, Studies in Geology, volume 5, pages 125-144.

Smosna, R.A., and Warshauer, S.M., 1981, Rank exposure index on a Silurian carbonate tidal flat: Sedimentology, volume 28, pages 723-731.

Thompson, R.W., 1968, Tidal flat sedimentation on the Colorado River delta, northwestern Gulf of California: Geological Society of America Memoir 107, 133 pages.

Tourek, T.J., 1970, The depositional environments and sediment accumulation models for the Upper Silurian Wills Creek Shale and

Tonoloway Limestone, Central Appalachians: Ph.D. dissertation, The Johns Hopkins University, Baltimore, Maryland, 282 pages.

Walker, K.R., 1972, Community ecology of the Middle Ordovician Black River Group of New York State: Geological Society of America Bulletin, volume 83, pages 2499-2524.

Walker, K.R., and Ferrigno, K.F., 1973, Major Middle Ordovician reef tract in east Tennessee: American Journal of Science, volume 273-A, pages 294-325.

Walker, R.G., 1984, Facies models: Geoscience Canada Reprint Series 1, pages 1-9.

Walter, M.R., Buick, R. and Dunlop, J.S.R., 1980, Stromatolites 3,400-3,500 Myr old from the North Pole area, Western Australia: Nature, volume 284, pages 443-445.

Warren, J.K., 1982, The hydrological setting, occurrence and significance of gypsum in late Quaternary salt lakes in South Australia: Sedimentology, volume 29, pages 609-637.

Weimer, R.J., Howard, J.D., and Lindsay, D.R., 1982, Tidal flats: American Association of Petroleum Geologists Memoir 31, pages 191-245.

Wilson, J.L., 1967, Carbonate-evaporite cycles in lower Duperow Formation of Williston Basin: Bulletin of Canadian Petroleum Geology, volume 15, pages 230-312.

Wilson, J.L., 1975, Carbonate facies in geologic history: Springer-Verlag, New York, 469 pages.

Wood, G.V., and Wolfe, M.J., 1969, Sabkha cycles in the Arab-Darb Formation of the Trucial Coast of Arabia: Sedimentology, volume 12, pages 165-191.

Young, R.B., 1935, A comparison of certain stromatolitic rocks in the dolomite series of South Africa with marine algal sediments in the Bahamas: Transactions of the Geological Society of South Africa, volume 37, pages 153-162.

STRATIGRAPHIC MODELS FOR CARBONATE TIDAL-FLAT DEPOSITION

Lawrence A. Hardie

Tidal-flat deposits and their associated shelf-lagoon deposits typically occur as a vertical succession of shallowing-upward sequences (Wilson 1975; James 1984) that in rugged mountainous exposures such as the Canadian Rockies or the Southern Alps appear as spectacular layer-cake stacks of meter-scale strata. In this section we consider how this particular kind of stratigraphic geometry comes about. In essence, the study of the facies stratigraphy of platform carbonates that carry tidal-flat deposits boils down to a study of the nature and causes of the cyclical repetition of platform subfacies and facies (for a succinct discussion of carbonate platform cycles and their causes, see Wilson 1975, pages 49-55).

Progradation and the Tidal-Flat Wedge

Modern carbonate tidal flats, such as those of the Bahamas and the Persian Gulf, have grown in volume and area during the last few thousand years as the rate of Holocene sea-level rise has slowed. The mechanism of growth is progradation, that is, carbonate sediment from the offshore "carbonate factory" was added progressively to the tidal flats by storm deposition (Hardie and Ginsburg 1977) so that the shoreline has advanced seaward faster than sea level has risen (figure 72). The Persian Gulf tidal flats have prograded during the latest Holocene at a rate of 0.5-2 km/1000 years (Kinsman 1969; Patterson and Kinsman 1977), while in the same period the southwest Andros Island tidal flats have advanced at about 5-20 km/1000 years (see figure 23; note that in the northwest where the Andros shoreline at present is retreating, the net rate of Holocene progradation is 1.5-3.5 km/1000 years, but it must have been at least twice this before the recent retreat—see chapter by Shinn, this *Quarterly*). For comparison, Holocene siliciclastic shorelines have prograded at rates of from 1.5-4.5 km/1000 years and deltas at 2-22 km/1000 years (Evans 1979).

Tidal flats must nucleate on an established shoreline. If they are to prograde to produce extensive sheets of tidal-flat strata, such as we find in the geologic record, this shoreline must be the feather edge of a wide, shallow, shelf-lagoon. Shallow water is necessary to provide the conditions for optimum carbonate production, which occurs in clear, warm tropical waters less than 10 m deep (Schlager 1981, figure 2). Shallow water also promotes progradation in that only relatively small volumes of sediment are needed to build the tidal-flat sheet up to sea level and to keep sediment accretion rate ahead of sea-level rise. Under these conditions tidal flats will grow laterally into the gently shelving subtidal lagoon to produce a flat wedge of tidal-flat sediments that gradually thickens seaward (figure 72).

Carbonate tidal flats may nucleate on a continental mainland where a carbonate shelf meets the craton (figure 73). Stratigraphically, the deposits of such tidal flats would interfinger landward with continental siliciclastic deposits and wedge out seaward into shelf-lagoon carbonate deposits. The Persian Gulf sabkhas (Purser 1973; see chapter by Shinn, this *Quarterly*) are modern examples of this process, and the Cambrian of Missouri (Howe 1968; Shinn 1983) is an ancient counterpart. Carbonate platform margins may also be the sites of tidal-flat nucleation in the lee of fringing islands (figure 73). These islands may have been inherited from previous sea-level highstands, as, for example, Andros Island, which is a Pleistocene ridge behind which the modern tidal flats accreted. Or islands may be produced by accretion above sea level of sand bars, as at Joulter's Cays, Bahamas, where new tidal flats are beginning

0163-9153/86/8101-0059 $00.20/0

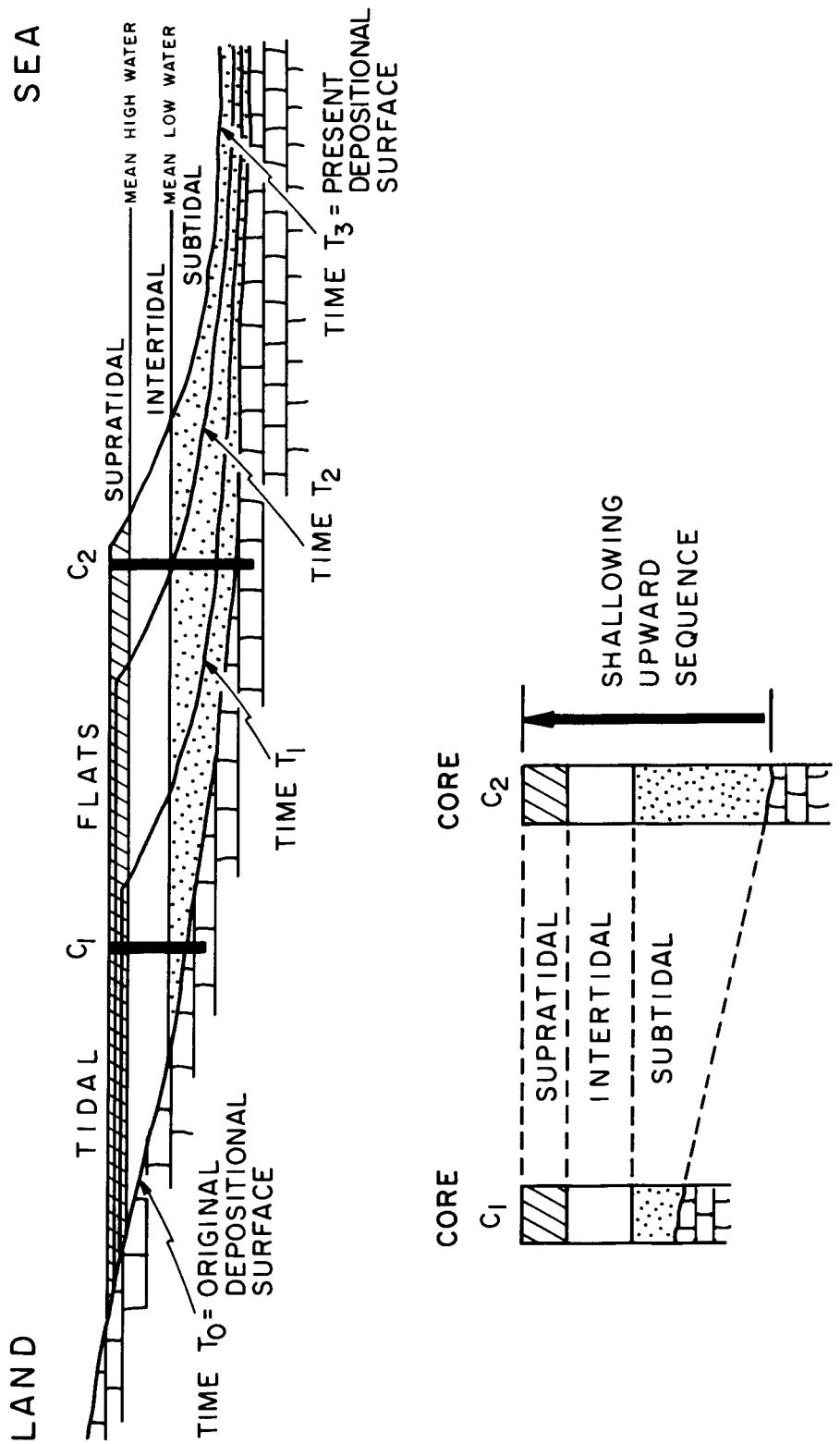

Figure 72.—Generation of a shallowing-upward sequence by progradation of tidal flats.

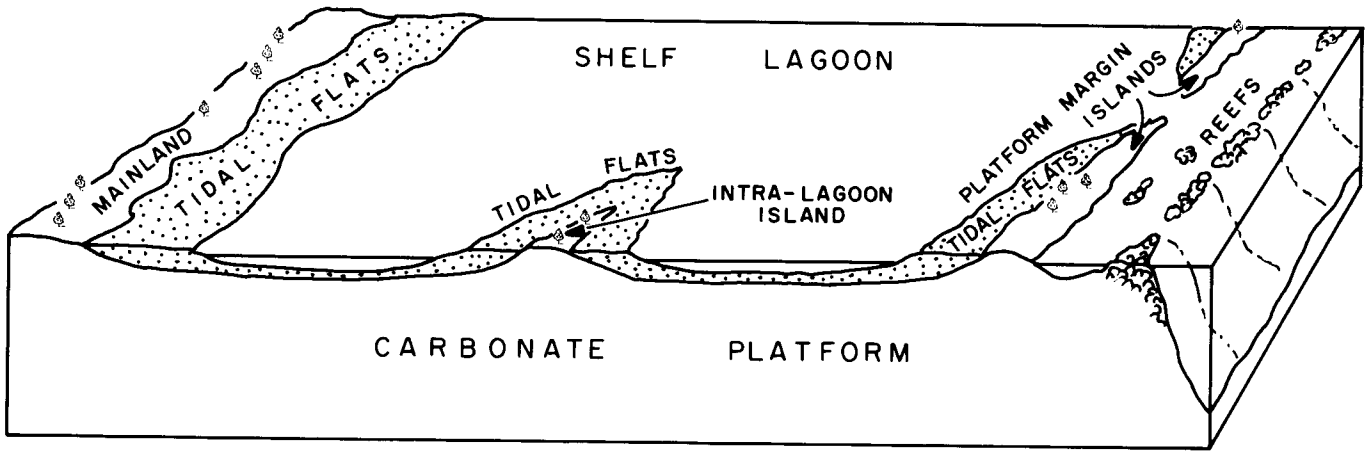

Figure 73.—Typical nucleation sites for tidal flats on carbonate platforms.

to grow behind low islands made of recently cemented Holocene ooid sand shoals (Harris 1979). Stratigraphically, such tidal-flat facies would be found separating platform margin shoal and reef facies from shelf-lagoon facies, as, for example, is the case for the Triassic Lofer tidal-flat facies of the northern Alps, Austria, (Zankl 1971; see Wilson 1975, figure VIII-20). If such a carbonate platform is attached to the craton, then tidal flats may also develop on the craton side of the shelf, but such tidal flats might be siliciclastic, as on the Great Barrier Reef shelf or the Belize shelf (Ginsburg and James 1974). It is also possible that islands scattered across the shelf-lagoon could be nucleation sites for isolated tidal-flat systems (figure 73) (for example, the island-tidal flats of modern Florida Bay, Enos and Perkins 1979), leaving a stratigraphic record of isolated lenses of tidal-flat facies embedded in the shelf-lagoon facies (James 1984).

Vertical Succession of Subfacies: The Basic Shallowing-Upward Model

Progradation of tidal flats over the shallow shelf-lagoon should generate a vertical succession of subfacies as predicted by Walther's Law (Middleton 1973). In its general form this succession is a shallowing-upward sequence (Wilson 1975, pages 281-309; James 1984) of subtidal subfacies overlain by intertidal subfacies overlain by supratidal subfacies. It is exactly this shallowing-upward succession of subfacies that is the common repetitive theme of ancient carbonate deposits interpreted to be of tidal-flat origin, as outlined earlier (figures 64 and 65, etc.). Significantly, modern prograding carbonate tidal-flat systems reveal this shoaling succession in cores and trenches (figure 74). They thus provide a powerful support to the idea that progradation is one of the fundamental factors controlling the facies stratigraphy of platform carbonates throughout the geologic record. R.N. Ginsburg in his carbonate facies seminars at the University of Miami uses the Florida Bay island-tidal flat stratigraphy (Enos and Perkins 1979) to illustrate his lag-trap-cap concept of shallowing-upward sequences (figure 75). The "lag" is the basal unit and represents the residual sandy sediment of the subtidal offshore "carbonate factory" from which the finer sediment fractions have been winnowed (this is not the transgressive lag of some workers, for example, James 1984). The "trap" unit is the bulk of the muddy sediment transported to the tidal flats and trapped onshore in the network of shallow subtidal and intertidal subenvironments. The "cap" is the storm-deposited supratidal unit that normally preserves mechanical and algal laminations, mudcracks, intraclast gravels, fenestral pores, etc. This is the "laminite cap" of Hardie and Ginsburg (1977).

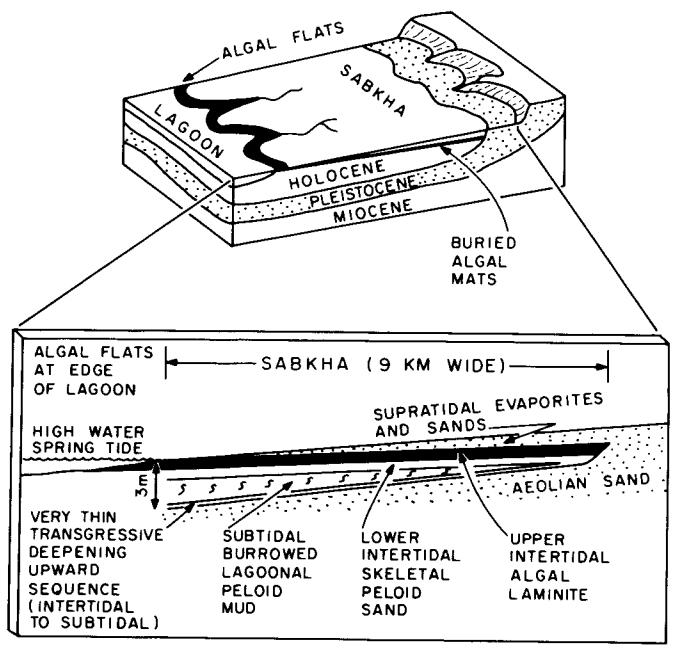

Figure 74.—The Holocene deposits of the Abu Dhabi (Persian Gulf) arid tidal flats as an example of active accumulation of a shallowing-upward tidal-flat sequence by progradation (after Patterson and Kinsman 1977). Compare with figure 72.

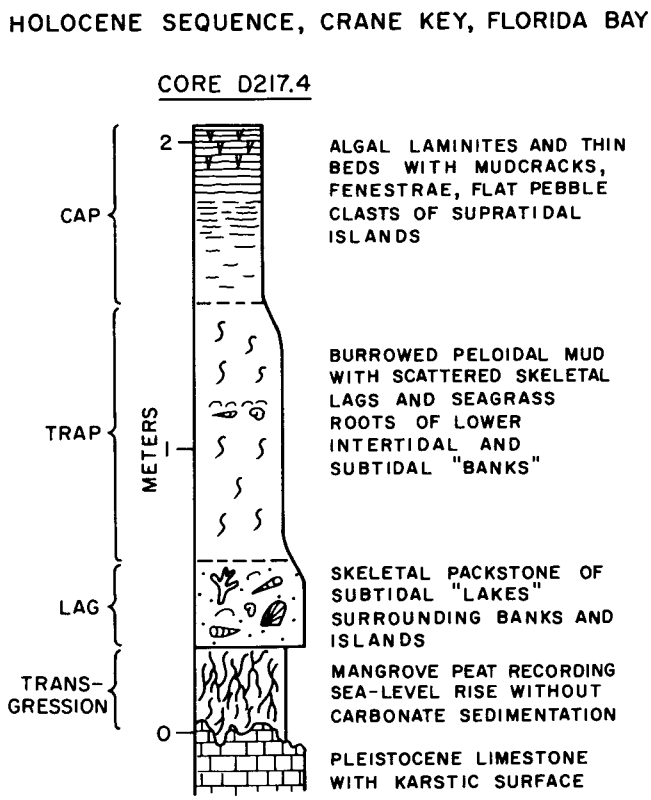

Figure 75.—A Holocene shallowing-upward sequence from Florida Bay, Florida (data of Enos and Perkins 1979) showing R.N. Ginsburg's lag-trap-cap concept of tidal-flat accumulation (R.N. Ginsburg, personal communication).

This shallowing-upward sequence has often been referred to as a "regressive sequence," meaning that it results from a seaward migration of the shoreline, and is so distinguished from a "transgressive sequence," which results from drowning as the shoreline advances landward due to a relative sea-level rise. However, it is important to recognize that progradation can occur with rising sea level so long as accumulation rate exceeds the rate of sea-level rise. This situation applies to many modern carbonate and siliciclastic depositional systems. Only a careful reconstruction of the 3-dimensional geometry of the platform subfacies and facies could reveal whether accretion occurred under conditions of rising, falling or stationary sea level (see below).

Critical to the interpretation of the origin of the shallowing-upward tidal-flat sequence is the nature of the boundaries between subfacies. In a classic Walther's Law succession, the boundaries between subtidal, intertidal and supratidal should be transitional because the tidal zones are in reality gradational, one into the other (figure 3). The lower and upper boundaries of a single tidal-flat sequence, on the other hand, are likely to be sharp because they are disconformities that record exposure followed by drowning. These characteristics of sharp upper and lower boundaries, but transitional internal boundaries, to asymmetric shallowing-upward sequences are well illustrated in the Upper Cambrian and Upper Silurian examples described above (figure 64 and 66). To explain the sharp upper and lower boundaries without invoking an "instantaneous" drowning event, Ginsburg (many unpublished lectures and personal communication) suggested that when relative sea-level rise initiates a new cycle of deposition, there is a "lag time" before sediment production restarts, which leads automatically to a sharp sequence boundary. Ginsburg contends that the platform "carbonate factory" cannot go into full production and delivery of sediment until the rising sea is deep enough to allow efficient circulation (1-2 m?). As a consequence the sediment surface does not track sea-level rise but lags behind no matter how fast or slow the rate of sea-level rise. However, once the water is deep enough, then sediment production easily catches up and tidal-flat growth begins once again. In this way an asymmetric shallowing-upward sequence is produced with a sharp non-depositional (omission) lower boundary that brings subtidal sediments directly on supratidal sediments. Strong support for this idea comes from the Holocene sequence beneath Crane Key, Florida Bay (figure 75), where basal mangrove peat free from sediment testifies that carbonate production initially lagged behind sea-level rise (and peat production), but then caught up as the water deepened. In some sequences, internal boundaries may be sharp rather than transitional, and care must be taken to properly interpret their meaning. Such boundaries could simply be due to local erosion (such as channel migration), etc. But if they carry evidence of drastic and prolonged change in conditions, such as karstification, etc., then an entire reassessment of the genesis of the sequence must be made. An example of this is the well-known Triassic "Lofer cyclothem" of Fischer (1964), in which the boundary between the subtidal subfacies and the overlying intertidal subfacies is interpreted as a record of abrupt sea-level drop, a scenario radically different from progradation of the tidal-flat wedge in accordance with Walther's Law.

Lateral Accretion Patterns

Shoreline migration during progradation may be relatively continuous or it may be staggered. Continuous regression leads to a simple offlap relationship in which laterally traceable subfacies lie one on top of the other (figure 76). Staggered regression will result from the development of a series of offshore barrier bars behind which the tidal flats accrete laterally and vertically (figure 76). In this back-barrier accretion model, exemplified by the modern tidal-flat system of Andros Island, the lateral patterns of subfacies can be complex because of infilling of the mosaic of tidal ponds separated by channels and levees. In such a system the whole tidal-flat wedge progrades seaward with time in a series of major jumps of the shoreline followed by back-filling (figure 23; see Gebelein 1974; Hardie and Ginsburg 1977, pages 121-122). Such staggered offlap can be confused with island tidal-flat accretion (figure 73).

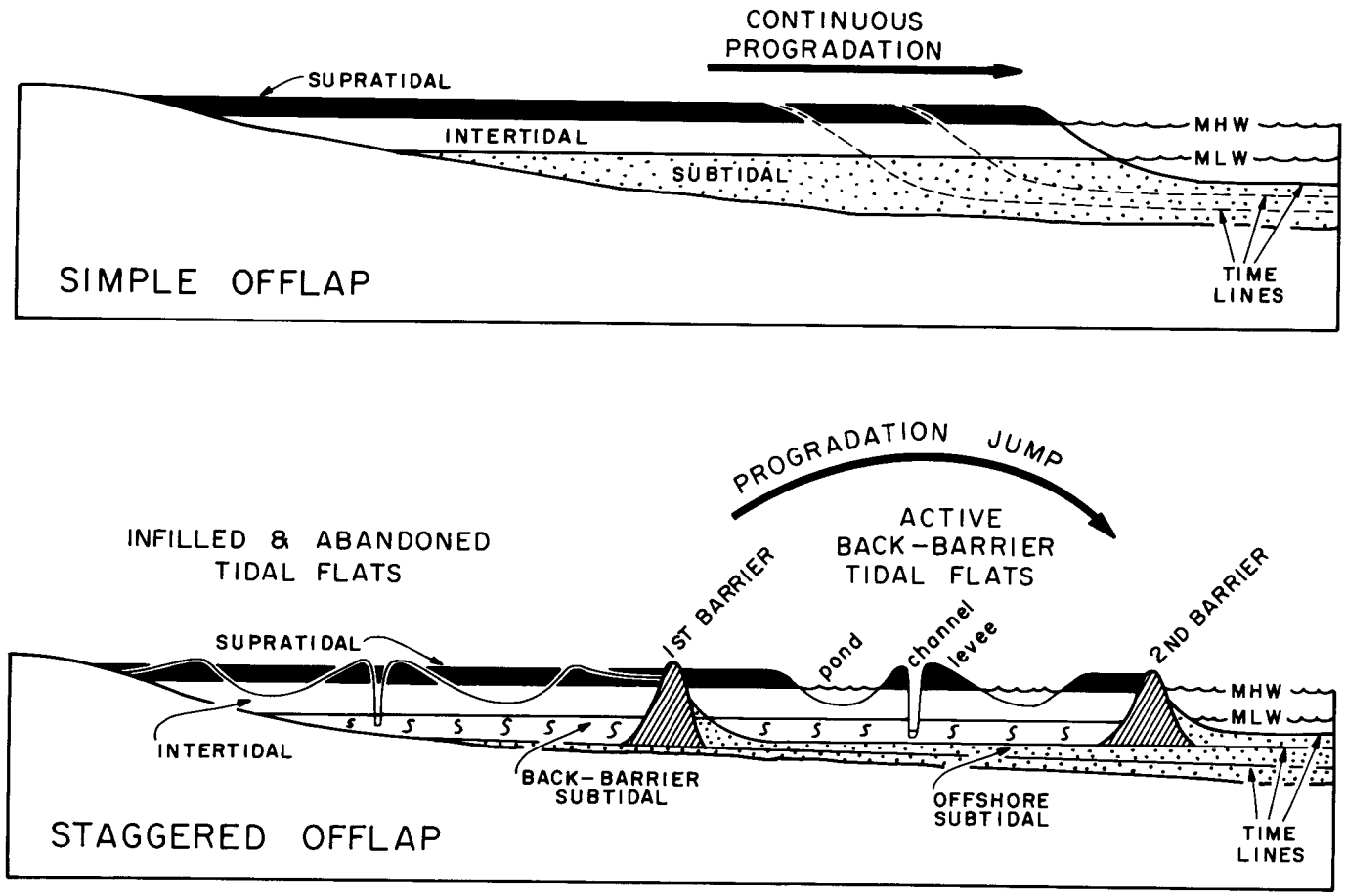

Figure 76.—Two styles of tidal flat lateral accretion patterns produced by progradation.

In considering lateral accretion patterns of tidal-flat deposits, relative sea-level changes during progradation must be taken into account. However, during periods of active progradation, sediment accumulation rate must have exceeded rate of sea-level changes, and sea-level changes must have been less than the depth of water on the platform, generally less than 10 m.

Progradation with relative sea-level rise will result in a progressive thickening of the tidal-flat wedge seaward and climbing contacts between subfacies (figure 77). This is a small-scale version of the climbing progradation of Bosellini (1984), and can be recognized by a comparison of different sections of a single tidal-flat wedge across the depositional strike. At the landward side the wedge will have a relatively thick supratidal subfacies component while at the seaward side the wedge will be characterized by a relatively thick subtidal subfacies component (figure 77). A Holocene example of this geometry is the prograding siliciclastic sabkha of the northwest Gulf of California (figure 68).

Progradation with a stationary sea level will result in a gradual thickening of the tidal-flat wedge due entirely to an increase in the thickness of the subtidal subfacies as it progressively infills the gently sloping offshore lagoon (figure 77). This pattern is a small-scale version of the toplap of Vail and others (1977, figure 6), and is found in the Lower Ordovician Stonehenge Limestone peritidal cycles in the central Appalachians (figure 78) and in the Lower Cretaceous Edwards Group, Texas (Mueller 1975, figure 8).

Progradation with a falling sea level most likely will result in a tidal-flat wedge with little change in thickness across depositional strike (figure 77). The subfacies boundaries will roughly trace the slope of the platform to give a pattern of descending progradation.

Cyclicity of Carbonate Tidal-Flat Deposits

Carbonate buildups composed of interbedded shelf-lagoon and tidal-flat facies may reach spectacular aggregate thicknesses measured in kilometers, such as the Cambro-Ordovician of the Appalachians (see preceding section). Thick sections of these buildups consist of stacks of meter-scale tidal-flat wedges superimposed one on the other (see, for example, figures 64,

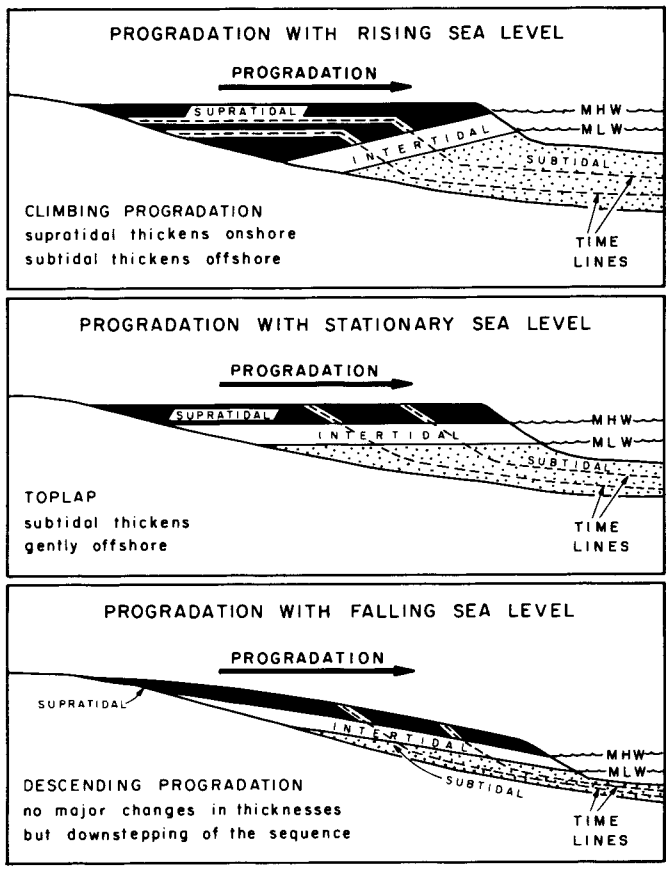

Figure 77.—Likely effects of relative sea-level changes on the across-strike geometry of tidal-flat wedges as they grow laterally by progradation.

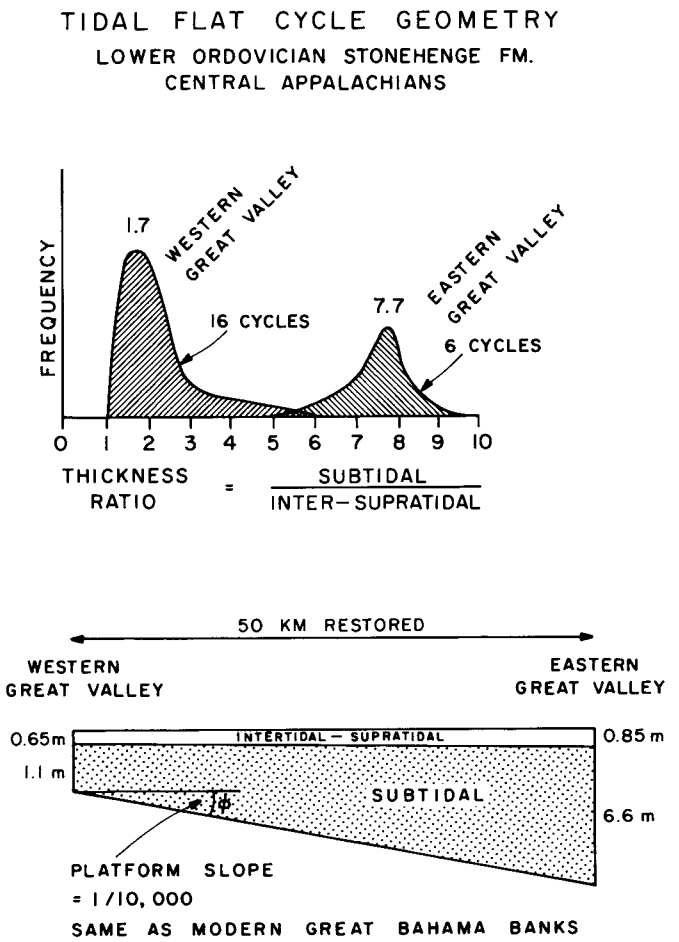

Figure 78.—Comparison of the thickness of intertidal + supratidal caps and their subtidal bases in carbonate tidal-flat cycles across depositional strike, Lower Ordovician Stonehenge Formation, western Maryland (unpublished measurements of Chau Nguyen, The Johns Hopkins University, Balitmore, Maryland). With easterly progradation of the tidal flats, the subtidal base of each cycle thickened, but without corresponding increase in the intertidal-supratidal cap, indicating that progradation occurred with a stationary sea level (see figure 77).

65, 67, and 69). The critical question becomes what is the cause of this striking repetition or cyclicity?

Of particular significance in this meter-scale cyclicity is that the individual tidal-flat "cycles" are most commonly, although not invariably, asymmetrical units separated by sharp, disconformable boundaries between the supratidal cap of one cycle and the subtidal base of the overlying one (figures 64, 65, 66, etc.). Such shallowing-upward sequences are actually "hemicycles" and their repetition produces an A-B-C, A-B-C, A-B-C, . . . vertical pattern that records alternating periods of progradation and drowning.

Factors that determine whether progradation or drowning will prevail at any one time are: (1) rate of sediment supply, (2) rate of subsidence or uplift, and (3) rate of eustatic sea-level rise or fall.

The "carbonate factory" at platform margins (reef and ooid shoals) is exceedingly efficient, so much so that only glacio-eustatic sea-level rise such as occurred in the Early Holocene (6-10 m/1000 years), or tectonic pulses (up to 4 m/1000 years), can outpace the upward "growth potential" of modern platform margins (1 m/1000 years, Schlager 1981). Mud and skeletal sand production in the interior shelf-lagoon may also be efficient but not nearly at the same rate as reef or ooid-shoal growth. The high depositional rates of about 1 m/1000 years reported for Holocene carbonate lagoons (for example, Wilson 1975, page 15) are misleading because they are maximum values for storm-built features (for example, islands in Florida Bay) and are not representative of the normal rates of production across modern lagoonal "carbonate factories." For example, in the Bight of Abaco, Little Bahama Bank, Holocene lagoonal lime sediment (70 percent sand, 30 percent mud) accumulated over the last 5,500 years at a net rate of 12 cm/1000 years (Neumann and Land 1975). At present-day growth rates calcareous algae (*Penicillus, Rhipocephalus, Halimeda)* are producing lime mud at a rate of between 5 and 11 cm/1000 years, more than enough to account for the mass of Holocene mud

in the lagoon today. In the Florida inner reef tract, Stockman and others (1967) determined an accumulation rate of 2.3 cm (± 50 percent) per 1000 years for mud from *Penicillus* alone, and if other sources (other green algae, invertebrates, chemical precipitation) are added then the actual accumulation rate of lagoonal sediment could be about that of the Bight of Abaco. If these Holocene rates are typical of Phanerozoic rates then shelf-lagoon sediment production can keep ahead of platform subsidence which is typically less than 10 cm/1000 years (Kay 1955; Wilson 1975, page 15; Schlager 1981). However, the competing rates of sedimentation and subsidence are close enough that relatively small increases in subsidence or decreases in production during platform evolution could turn the balance. This is critical for tidal-flat development, because progradation rate is directly linked to shelf-lagoon sediment production rate. This production rate will slow down, and limit tidal-flat growth, when the shelf-lagoon "carbonate factory" becomes (1) too small to provide the amounts of sediment needed for continued progradation, (2) too deep for optimal carbonate production (› 10 m, Schlager 1981), (3) too shallow for efficient circulation and sediment dispersal (‹ 1-2 m? see above) or (4) too salty, too fresh or too cold for biogenic or chemical production of carbonate.

Long-term platform subsidence due to the combined effects of thermal cooling and sediment loading (Watts and Ryan 1976; Pittman 1978) may reach 20-25 cm/1000 years, but overall net subsidence of Phanerozoic passive margins seems to be in the range of 1-10 cm/1000 years (Pittman 1978; Schlager 1981). Therefore, as a rule, long-term platform subsidence should be outpaced by carbonate sediment accumulation across the entire platform from margin to tidal flats. In contrast, short-term subsidence accompanying pulses of block or wrench faulting (up to 4 m/1000 years, Yeats 1978) could be drastic enough to cause temporary drowning that even reef growth on the platform margins cannot match. Pulses of uplift from the same tectonic causes are likely to lead to widespread exposure of the entire shelf-lagoon that will punctuate the platform stratigraphic record with a significant disconformity or, if tilting occurs, an unconformity.

Eustatic sea-level changes result from: (1) changes in volume of ocean water due to changes in the volume of continental ice-sheets (maximum change of 100-150 m at rates up to 10 m/1000 years, Donovan and Jones 1979; Schlager 1981), or to desiccation of isolated ocean basins (maximum change 15 m at rates of up to 10 m/1000 years, Donovan and Jones 1979); (2) changes in volume of the ocean basins due to changes in the volume of midocean ridges (maximum change of 300 m at rates of 1 cm/1000 years) or to changes in the volume of ocean sediment (rates of 1 cm/1000 years) (Donovan and Jones 1979). Clearly, of these two, only sea-level fluctuations due to changes in ocean water volume are fast enough to overcome carbonate sedimentation rates on platforms, which as noted above, may be as fast as 1 m/1000 years (Wilson 1975, page 15; Schlager 1981).

One final factor that must be considered is the time scale represented by a single tidal-flat cycle. It is not possible to determine the actual amount of time taken for the deposition of any one cycle, but a rough estimate of the average duration of a cycle can be obtained by dividing overall formation elapsed time (taken from radiometric ages) by the total number of cycles in the formation. Some average cycle durations calculated in this way are given in table 2. Although all these calcuations are rough estimates of average values (with large uncertainties), they do suggest that tidal flat and shelf-lagoon carbonate cycles range from tens of thousands to a few hundred thousand years, perhaps over the range 10,000 to 200,000 years. With such a time span only short term geological, oceanographical or climatological processes can have a significant influence on stratigraphic cyclicity, ruling out processes associated with sea-floor spreading, which are far too slow (Donovan and Jones 1979).

Considering all these factors, three basic models to explain meter-scale cyclicity in platform carbonate deposits emerge. They are: (1) internal self-regulating, or autocyclic, models, (2) global eustasy models based on variations in ocean-water volume, such as the Milankovitch climatic cycles that cause ice cap volume oscillations, and (3) tectonic models related to local pulses of block- or wrench-faulting.

THE AUTOCYCLIC MODEL OF R. N. GINSBURG

Ginsburg (1971) proposed an autocyclic model that elegantly explains superimposed A-B-C shallowing-upward sequences in platform carbonates (figure 79). The model calls on continuous, steady basinal subsidence coupled with carbonate sediment supply rates that are self-regulated by the extent of progradation. The crux of the model lies in the recognition that carbonate sediment production rate will fall behind subsidence rate as progradation drastically reduces the size of the shelf-lagoon "factory" (see above), and will not recover until the lagoon once again becomes deep enough (due to subsidence) to allow efficient carbonate production and sediment dispersal (perhaps 1-2 meters, see above). This factor introduces an automatic lag time in deposition so that subtidal sediments lie directly on supratidal sediments (figure 79).

Time scales for cycle generation predicted with this model are on the order of tens of thousands to a few hundred thousand years, depending on the size of the platform and the rates of subsidence and progradation. For example, at a subsidence rate of 5 cm/1000 years, a period of 20,000-40,000 years would be needed for a shelf-lagoon 1-2 m deep to develop in the absence of sedimentation. With onset of sediment production, tidal-flat progradation at rates of 1-5 km/1000 years (see earlier) would infill a platform 200 km wide (twice the width of the present Great Bahama Banks) in 40,000-200,000 years. However, progradation rate may be coupled directly with platform width in that wide platforms are likely to have a higher production area/shoreline ratio than narrow platforms. If this is so, then progradation on huge platforms that were several hundred kilometers wide, such as the Cambro-Ordovician of the Appalachians, could have been accomplished in much less than 200,000 years.

Overall, then, this autocyclic model not only accounts for the common A-B-C cyclic pattern of shoaling-upward se-

Table 2.—*Average durations of shallowing-upward cycles of some Phanerozoic platform carbonates.*

Age	Formation	Average Duration (years/cycle)		Source of Field Data
		Mean	Range of Uncertainty	
U. Cambrian (Dres. - Tremp.)	Conococheague Ls., Maryland	70,000 - 110,000	30,000 - 220,000	Demicco (1981)
L. Ordovician (Tremadocian)	Stonehenge Ls., Pennsylvania	145,000	35,000 - 260,000	C. Nguyen (unpubl. data)
L. Ordovician (Trem.-Arenigian)	Nittany Dolomite, Pennsylvania	100,000 - 130,000	20,000 - 300,000	R. Goldhammer (unpubl. data)
U. Silurian (Ludlovian)	Wills Creek Fm., Maryland	30,000	8,000 - 60,000	Tourek (1970)
U. Permian (Kazanian)	Bellerophon Fm., N. Italy	65,000	5,000 - 125,000	Bosellini & Hardie (1973)
M. Triassic (Ladinian)	Latemar Ls., N. Italy	10,000 - 17,500	0-62,000	R. Goldhammer (unpubl. data)
U. Triassic (Norian)	Dolomia Principale, N. Italy	24,000 - 40,000	0-92,000	Bosellini & Hardie (unpubl. data)
U. Triassic (Norian-Rhaetian)	Dachstein Ls., Austria	40,000 - 53,000	10,000 - 93,000	Fischer (1964)

Note: Age dates for these calculations were taken from Odin (1982) and Harland and others (1982); they carry large uncertainties which are reflected in the large range of values possible for cycles. Field data of C. Nguyen and R. Goldhammer are from Ph.D. theses in progress at The Johns Hopkins University, Baltimore, Maryland.

quences, but also has a built-in time scale of tens-of-thousands to a few hundred-thousand years that is consistent with the duration of cycles estimated for ancient platform carbonates (table 2).

One difficulty with the model as proposed is that it requires progradation to encroach on the platform margins to choke off the carbonate mud "factory." But a number of ancient platform carbonates seem to have maintained a wide shelf-lagoon between the tidal flats and the platform margin (see figure 85). In these circumstances, it may well be that as the shoreline progrades down the sloping platform into deeper water, it automatically slows because the increasing thickness of the tidal-flat wedge requires increasing supplies to maintain the same rate of advance (figure 80). At the same time the decreasing area of the lagoon will lead to a decrease in carbonate mud production. In this way tidal-flat progradation will come to a halt well before reaching the platform margin, while subtidal skeletal sandy sediment and patch reefs will continue to accrete in the deeper shelf-lagoon separating the tidal flats from the platform margin shoals and reefs (figure 85).

MILANKOVITCH CYCLES

The dating of uplifted successions of Pleistocene coral reefs in Barbados and New Guinea (Broecker and others 1968; Mesolella and others 1969; Bloom and others 1974) sparked the revival of the Milankovitch theory of climatic cycles by demonstrating that high sea level had occurred 82,000, 105,000, and 125,000 years ago, precisely coincident with peaks of high summer radiation at low latitudes predicted by Milankovitch theory. At the same time Broecker and von Donk (1970) showed that oxygen isotope ratios in deep-sea cores from the Caribbean oscillated with a 100,000-year pulse similar to the cycle of eccentricity of the earth's orbit about the sun (figure 81). The recognition that the variations in oxygen isotopes in the ocean were related to volume variations in the ice caps, together with the development of magnetic dating, led to a convincing demonstration that the Pleistocene deep-sea sedimentary record was indeed linked to global climatic cycles with a strong peak at 100,000 years (Shackleton and Opdyke 1973; Ruddiman and McIntyre 1976). Finally, the benchmark study of Hays and others (1976) showed that in deep sea cores there is a clear record that climatic changes over the last half-million years were linked, not only to the 100,000-year orbital eccentricity cycle, but also to the 41,000 year axial tilt (obliquity) cycle and the 23,000 and 19,000-year precession of the equinoxes cycles predicted by recent refinements of the Milankovitch theory (figures 81 and 82; Berger 1977a, 1977b; Imbrie and Imbrie 1980; Imbrie 1985).

The revival was in full swing (Imbrie and Imbrie 1979, have written a readable history of the revival), and culminated in an international symposium on "Milankovitch and Climate" in New York late in 1982 (Berger and others 1984). At this symposium several papers on Mesozoic cyclic sedimentation were presented that suggested that Milankovitch climatic periodicity may extend back beyond the Pleistocene ice ages.

In the present context the question becomes whether Milankovitch climatic cycles could have influenced deposition on tropical carbonate platforms. Twenty years ago Fischer (1964) suggested that the approximately 50,000-year Triassic Lofer

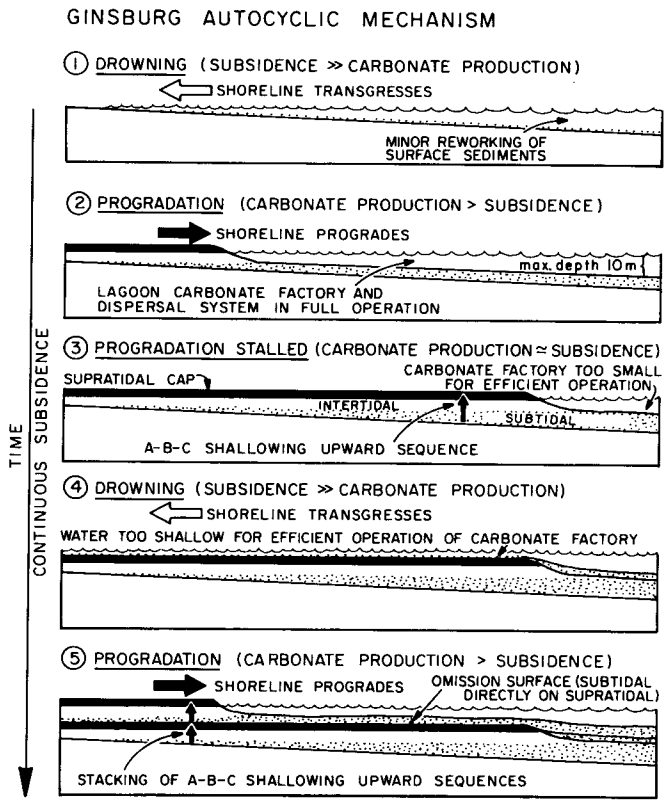

Figure 79.—Schematic representation of R.N. Ginsburg's autocyclic model for the generation of repetitive asymmetrical tidal-flat cycles (after an unpublished diagram of R.N. Ginsburg, personal communication; see also Demicco and Mitchell 1982, figure 77, and James 1984, figure 18).

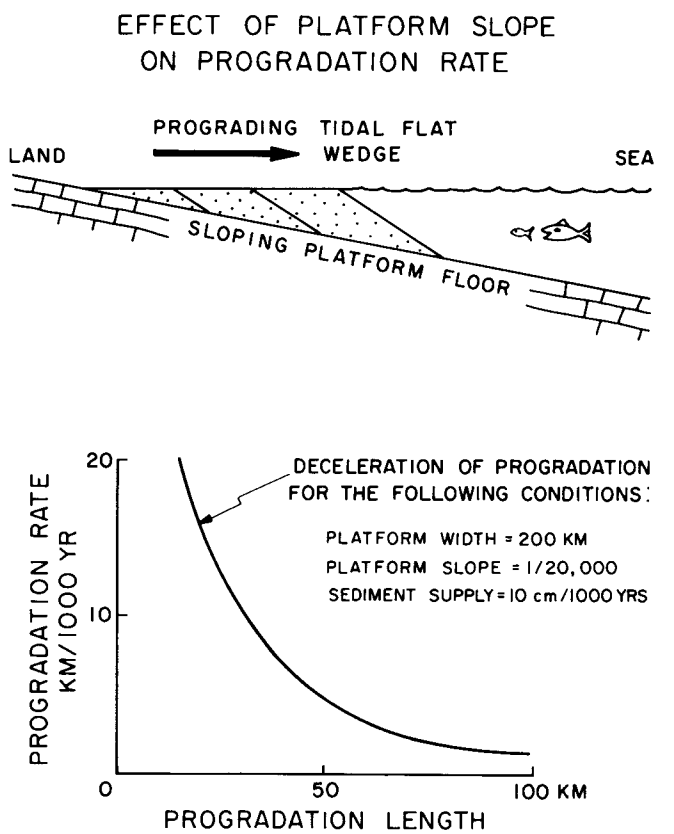

Figure 80.—Effect of platform slope on the rate of progradation of a tidal flat. Progradation rate decreases rapidly as the volume of sediments needed to build the sediment wedge up to sea level progressively increases.

tidal-flat cycles were dictated by eustatic sea-level changes of up to 15 m related to a small Upper Triassic ice cap that varied in volume with the 41,000 year obliquity rhythm. There are enough other cyclic platform carbonate deposits in which the average cycle duration falls within the Milankovitch band of 19,000 to 100,000 years (see table 2) to warrant serious consideration of a Milankovitch mechanism for platform carbonate cycles.

Milankovitch astronomical rhythms might influence platform carbonate sedimentation in three basic ways:

(1) Cause variations in continental ice cap volumes, which in turn would cause eustatic sea-level changes;

(2) Cause ocean temperatures to change sufficiently that ocean water volume would change;

(3) Cause climatic changes in the tropics so that shallow water carbonate production rates would change.

Shrinking and expanding of continental ice sheets is, of course, the basic mechanism long appealed to for eustatic sea-level changes. Under control of Milankovitch rhythms, eustatic sea-level oscillations could produce cycles with periods of 100,000, 41,000, and approximately 21,000 years. However, the known approximately 21,000-year oscillations of sea level during the Late Pleistocene have not produced sequences of deposition on the Florida and Bahama platforms. Instead, in Florida only the transgression of 125,000 years ago left a depositional record as the Miami Formation. In the Bahamas, Beach and Ginsburg (1978) found 15 exposure surfaces with terra rossa in 40 m of Late Pliocene-Recent platform carbonate deposits beneath the Great Bahama Bank. If we accept the Lower Pliocene-Upper Pliocene boundary at 3.2 m.y. ago, then the average time between exposure surfaces is 213,333 years, an order of magnitude greater than the 21,000 year sea-level oscillations recorded by the Late Pleistocene platform margin reefs of Barbados and New Guinea (figure 84; also see Aharon 1984, figure 2). It appears that these lower-order oscillations of the Late Pleistocene occurred during the latest 100,000-year cycle low stand so that sea level remained below the top of the platforms from about 120,000 years ago until the latest rise began 18,000-20,000 years ago (figures 83 and 84). This is likely to be a characteristic of large amplitude glacio-eustatic sea-level changes associated with major ice ages such as occurred in the Precambrian, the Permo-Carboniferous, and the Pleistocene. But to explain successions of tidal-flat cycles that do not exhibit massive subaerial diagenesis at the top of each cycle, changes of smaller amplitude are needed. The abundance of such cyclic successions throughout the geologic record also

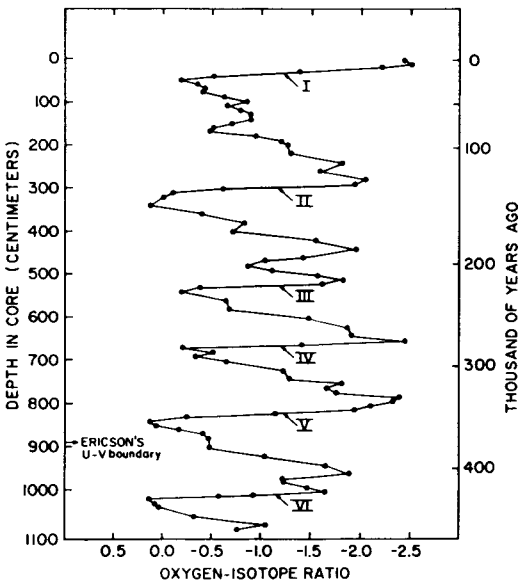

The 100,000-year pulse of climate. Climatic variations shown here are recorded by changes of the oxygen-isotope ratio in a deep-sea core from the Caribbean (V12-122). After determining the approximate time scale, W.S. Broecker and J. van Donk concluded that the major pulsebeat of climate was a 100,000-year cycle. Six intervals of rapid deglaciation are indicated by Roman numerals and referred to as *terminations*. (Adapted from W.S. Broecker and J. van Donk, 1970.)

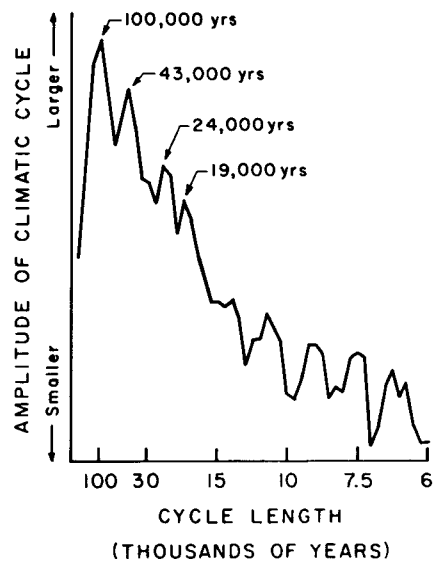

Spectrum of climatic variation over the past half-million years. This graph—showing the relative importance of different climatic cycles in the isotopic record of two Indian Ocean cores—confirmed many predictions of the Milankovitch theory. (Data from J.D. Hays et al., 1976.)

Figure 81.—Milankovitch rhythms preserved in the oxygen isotope record of Pleistocene to Holocene deep-sea sediments (reproduced from Imbrie and Imbrie 1979, figures 38 and 42, with permission).

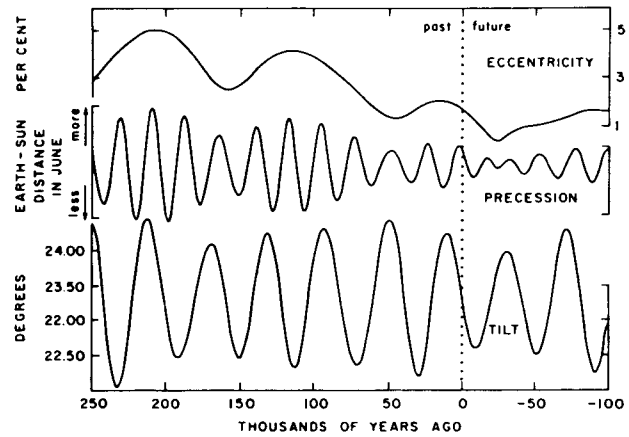

Changes in eccentricity, tilt, and precession. Planetary movements give rise to variations in the gravitational field, which in turn cause changes in the geometry of the earth's orbit. These changes can be calculated for past and future times. (Data from A. Berger.)

Figure 82.—The basic Milankovitch astronomical rhythms over the last few thousand years (from Imbrie and Imbrie 1979, figure 41, with permission).

demands that the mechanism be disconnected from the few unusual periods of massive continental glaciation. Waxing and waning of small ice caps during nonglacial times is what we are looking for, oscillations in volume that would cause small sea-level changes measured in meters or a couple of tens of meters at most. But a difficulty immediately arises. Glacio-eustatic sea-level changes, even relatively small ones such as the 15-m oscillations called on by Fischer (1964), require that continents be at the poles because it is the amount of land-ice that controls the volume of ocean water. This presents a major drawback to the Milankovitch glacio-eustatic cycle model for those geologic periods when there were no polar continents. From the paleocontinental maps of Smith and others (1981) (see also Morel and Irving 1978; Scotese and others 1979; Ziegler and others 1979; McElhinny and Valencio 1981), it appears that for the Phanerozoic the polar regions were completely devoid of continents only in the Cambrian. The poles were not covered by continents in the Early Ordovician or Late Jurassic through Mid-Cretaceous, although the Laurussian and Siberian continental masses were within 20° of the North Pole. For the remainder of the Phanerozoic, a continental mass overlay one pole or the other. From Late Ordovician to the Permian, Gondwanaland covered the South Pole. From the Triassic to the Mid-Jurassic the Laurussian-Siberian continents surrounded the North Pole which was situated at the northeast corner of the Siberian mass. From Late Cretaceous to the present, the Antarctic continent has remained over the South Pole. Clearly, polar land ice sheets, however small, could have existed through almost all the Phanerozoic. One unsubstantiated possibility for those periods without polar continents is that during cold periods ice would accumulate at the poles as floating ice-shelves nucleated on sea-ice. Because the meltwater of this ice would have the density of salt-free water while the seawater on which the ice-shelf was floating would have a density of

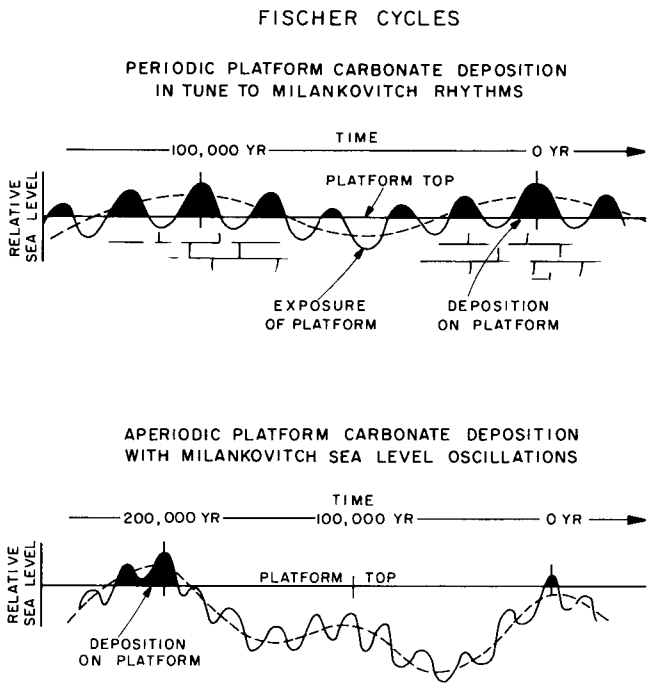

Figure 83.—Scenarios for deposition of carbonate cycles dictated by Milankovitch rhythms. These scenarios are simple extensions of Fischer's (1964) idea for the generation of carbonate tidal-flat deposits by Milankovitch glacio-eustasy. The top panel shows the rhythms of drowning and exposure of a carbonate platform due to glacio-eustasy produced by superimposition of 20,000-year and 100,000-year Milankovitch pulses. Small variations in the amplitude of the 100,000-year pulse should produce packaging of tidal-flat cycles into clusters of five based on progressive cycle thickness variations and degree of subaerial exposure (see text and Goldhammer and others 1986). With large variations in the amplitude of the 100,000-year pulse, as occurred in the Pleistocene (figure 84), deposition on carbonate platforms is likely to be erratic and apparently non-Milankovitchian, as depicted in the lower panel and as demonstrated by the core data of Beach and Ginsburg (1978) for the Plio-Pleistocene of the Great Bahama Bank.

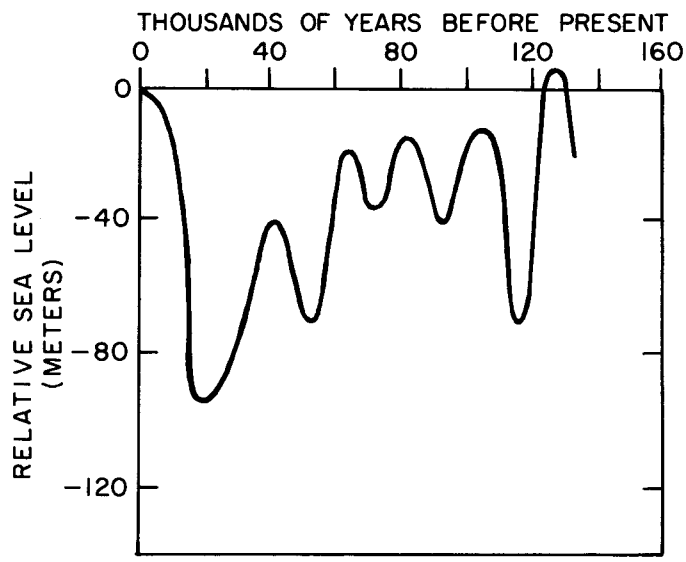

Figure 84.—Sea-level curve over the last 125,000 years based on coral reef dating in Barbados (see Broecker and others 1968; Mesolella and others 1969; Bloom and others 1974). Note the superimposition of 20,000-year cycles on an approximately 100,000-year cycle, and note also the marked asymmetry of the 100,000-year cycle.

about 1.03 g/ml, then an increase in ocean volume equivalent to 3 percent of the ice mass could occur upon melting of this floating ice. Rough calculations show that melting of a huge ice sheet the size of the present Antarctic sheet would be needed to raise sea level by 2 m. The same volume of ice on land would change sea level by 60-75 m (Donovan and Jones 1979).

In summary, during periods when polar continents existed, glacio-eustatic oscillations driven by Milankovitch rhythms could have influenced platform carbonate sedimentation patterns. If present-day astronomical cycles can be extrapolated back through geologic time, then, with this Milankovitch model and the evidence of Pleistocene sea-level rhythms, we should expect tropical carbonate tidal flat and shelf-lagoon carbonate cycles to occur in small clusters of cycles 100,000 years apart and each about 21,000 years in duration (figure 83). For periods when there were no polar continents, as during the Cambrian, other mechanisms than Milankovitch glacio-eustasy must be sought.

Donovan and Jones (1979) calculated that a 10° C change in overall temperature of the oceans would produce a sea-level change of 10 m, roughly 1 m/°C. Seawater temperature changes should vary with climatic changes dictated by Milankovitch rhythms and could produce meter-scale cyclic oscillations in sea level. However, the inertia of bottom ocean water against temperature changes probably rules out this mechanism for high-frequency cycles (10^4-10^5 years), but it may be an overlooked factor in much longer term (10^6 years) sea-level trends (compare the apparent large changes in ocean bottom temperatures from the Cretaceous to the present, as recorded by oxygen isotope trends, Shackleton and Kennett 1975; Savin 1982; etc.).

Green algae that produce carbonate mud are tropical marine plants that live in warm shallow waters and therefore it is very probable that their productivity would be reduced by lowering of the temperature of the shallow, slowly circulating platform waters during global climatic cooling cycles. Inorganic precipitation would also be reduced by lower water temperatures because of the increase in solubility of $CaCO_3$ polymorphs with decrease in temperature. Therefore, it is conceivable that the mud supply from the shelf-lagoon carbonate mud "factory" will slow down and speed up in concert with global climatic cycles. Drowning (low sediment supply during cool periods) and progradation (high sediment supply during warm periods) within the interior shelf-lagoon could thus be dictated by Milankovitch rhythms, while the platform margins would continue to be maintained by ongoing massive production of shelf-edge

sands and reefs. Because the 41,000 year obliquity cycles are prominent only at high latitudes, it follows that a Milankovitch mechanism for influencing tropical climate should result only in the 100,000-year and 21,000-year cycles. But rates of progradation will limit the lateral extent of tidal-flat cycles with a 21,000-year period to only a few tens of kilometers.

It is clear that Fischer's (1964) idea that carbonate platform facies stratigraphy may be dictated by Milankovitchian eustatic sea-level oscillations is a viable one, and its exploration is well under way after a two-decade lag time (Grotzinger 1985; Goodwin and Anderson 1985; Read and others 1986; Bosellini and Hardie 1986; Hardie and others 1986; Goldhammer and others 1986). But for shallowing-upward sequences with tidal-flat caps, the difficulty of establishing unambiguous criteria for distinguishing Fischer's Milankovitchian eustatic cycles from Ginsburg's autocycles still remains. Neither asymmetry of shallowing-upward cycles nor the 10^4-10^5-year average duration of such cycles (table 2) can unequivocally prove that a Milankovitchian dictator was in operation (compare with Goodwin and Anderson 1985), because these are also characteristics of Ginsburg's autocycles (see above). On the other hand, the "diagenetic cycles" typical of the Triassic of northern Italy (see preceding section) provide compelling evidence that sea-level oscillations were the primary cause of at least some platform cycles in the geological record, and firmly establish that high frequency (10^4 years) sea-level fluctuations can occur during periods not considered as glacial ages. The particular evidence offered by the Triassic (Ladinian to Norian) "diagenetic cycles" of northern Italy is the absence of peritidal deposits between the subtidal sediments and their vadose diagenetic caps (figure 70), an absence that immediately negates shoreline progradation as the cause of the subaerial exposure. These cycles, therefore, cannot be Ginsburg's autocycles, and must be the result of sea-level oscillations of either eustatic or tectonic origin, or some combination of the two (Hardie and others 1986). Continuous tectonic "yo-yoing" over millions of years (at least 30 m.y. for the Ladinian-Norian interval) seems improbable, so that eustasy remains the only viable mechanism. The obvious candidate as the cause of this high-frequency eustasy is the Milankovitch climatic cycle, because it is the only applicable phenomenon known at this time that has the appropriate time scale (10^4-10^5 years). But direct evidence of Milankovitch cycles in platform carbonate sequences (for example, time series analysis of the type carried out on Pleistocene deep-sea cores, Hays and others 1976) remains out of reach given the large uncertainties in age-dating of pre-Pleistocene rocks. Nonetheless, Goldhammer and others (1986) found some significant time-dependent repetitions that have Milankovitchian characteristics in the stack of about 400 Ladinian "diagenetic cycles" of the Latemar, northern Italy (see preceding section). Plots of cumulative cycle thickness versus stratigraphic position (see Fischer 1964, figure 38) show that individual cycles are bundled into asymmetrical clusters of 5, distinguishable by a thick basal cycle followed by a progressive upward decrease in thickness in the remaining 4 cycles of the cluster. Autocorrelation analysis confirms the validity of the 5-cycle cluster motif. The significance of this pattern is that it shares two of the major characteristics of the sea-level record during the Pleistocene. Sea level over the past several hundred thousand years shows: (1) a basic 20,000-year pulse superimposed on a broader 100,000-year pulse, producing a 5-part repeat pattern (figure 84), as predicted by Milankovitch theory; (2) the 100,000-year pulse is asymmetrical with an initial steep rise followed by a gentler decline (figure 84); this behavior records the fact that glaciers melt faster than they grow. Considering that the rough average duration of each Ladinian cycle is, within measurement error, close to the 20,000-year Milankovitch precessional rhythm (table 2), these Ladinian patterns provide powerful support for Milankovitch-driven eustasy during the Triassic. The Ladinian cycle patterns have been closely simulated by computer using Pleistocene Milankovitch rhythms and typical carbonate flatform subsidence and sedimentation rates (Goldhammer and others 1986), adding further support to the interpretation.

Without doubt the case for Milankovitch cycles in sequences such as the Triassic of northern Italy is a strong one, but it is still only a circumstantial case that needs more rigorous testing on other cyclic carbonates in the record. Such testing must take the form of analysis of measured sections for rhythms in cycle thickness, cycle types, organization of cycle components, etc., using relative time series techniques; and independent checks must be searched out, such as systematic changes in cycle geometries across strike (see figure 77), etc. Only the results of such rigorous tests will determine what, if any, role Milankovitchian eustasy has played in platform-carbonate facies stratigraphy.

TECTONIC CYCLES

Carbonate platforms typically occur at divergent margins that are segmented by block faulting, and so may experience pulses of subsidence and uplift during accretion. Observations on historically active faults show that movement is episodic and vertical displacements are meter-scale for individual pulses. Such pulses of vertical movement by faulting, if operating beneath growing carbonate platforms, could periodically overcome the "growth potential" of a carbonate platform and cause episodic drowning followed by long periods of relative still-stand of sea level during which progradation would generate tidal-flat wedges. Such "tectonic cycles" might vary somewhat in thickness and duration, because the tectonic pulses may not recur with the rhythm of astronomical cycles or the built-in regularity of autocycles. However, H.F. Reid's classic elastic rebound mechanism could conceivably result in a rhythmic pulse of faulting wherein slow build-up of strain energy to the critical point of rupture is followed by a quiescent period while strain energy rebuilds back to the critical rupture point again, and so on. One stratigraphic hallmark of such a tectonic dictator may be the local rapid rate of accumulation compared to regional subsidence rates related to sediment loading and ocean-crust cooling. Yeats (1978), for example, calculated rates of vertical subsidence related to wrench faulting in the Cenozoic Ventura basin, California, at up to 4 m/1000 years. But even where long-term regional subsidence is not abnormally fast, differential subsidence can play a major role in platform facies

stratigraphy. For example, platform cycles in the Norian Dolomia Principale of northern Italy (Bosellini 1967; Bosellini and Hardie 1986) vary from locality to locality. In the Belluno basin, where the Dolomia Principale is 1500 m thick (subsidence rates up to 25 cm/1000 years), thick packages dominated by subtidal subfacies are separated by a thick stack of tidal-flat cycles characterized by mudcracked wavy laminite cycle caps. In contrast, on the adjoining Trento fault block, where the Dolomia Principale is as thin as 250 m (subsidence rate <4 cm/1000 years), there are far fewer cycles and they are characterized by the most intensively disrupted diagenetic caps of any cycles in the Dolomia Principale, suggesting long periods of exposure between cycles. Differential subsidence was clearly related to differential down-dropping of adjoining fault blocks, which in turn led to differing records of platform cyclicity. Fault movement is typically spasmodic on a meter scale and such staggered subsidence could initiate depositional cycles with thicknesses determined by the size of each spasm of tectonic down-dropping, as Bosellini (1967, figure 26) postulated. Such platform depositional cycles could properly be considered "tectonic cycles." Other platform successions in the Triassic of northern Italy also appear to have been influenced by syndepositional fault movements. The Ladinian Latemar platform, described in the preceding section, is made up of a 400 m stack of small scale (about 1 m) "diagenetic cycles." In the middle of this cyclic succession is a 150 m section where thick (up to 13 m) tepee zones were superimposed at irregular intervals on the basic repeating pattern of small-scale diagenetic cycles (figure 70). These thick tepee zones must represent periods of extended subaerial exposure that punctuated the normal rhythm of small-scale sea-level oscillations responsible for the basic small-scale cycles (Hardie and others 1986). There are two possible explanations: (1) eustatic sea-level fluctuations dropped mean sea level well below the platform top resulting in long periods of subaerial exposure (figure 83), as, for example, occurred with the Bahama platforms during the Plio-Pleistocene; (2) irregular pulses of tectonic uplift exposed the platform until background subsidence once again drowned the platform and allowed carbonate sedimentation to resume. The second explanation is very likely in view of the fact that the Latemar platform lies in a left-lateral strike-slip fault system that was active in Triassic times (Doglioni 1984) as the Latemar buildup was accreting. Furthermore, the Latemar sits directly adjacent to a sinistral transpressive "flower" structure of high-angle reverse faults that cut down to basement. Thus the Latemar during its growth must have experienced pulses of uplift, and Hardie and others (1986) suggested that the Latemar tepee interval is the sedimentary record of these pulses of uplift when the transpressive tectonic system was active. Such pulses of uplift can be rapid enough to outstrip even reef growth; for example, Bachman (1978) estimated rates of up to 1 m/1000 years for uplift associated with strike-slip faulting along the edge of the Plio-Pleistocene basin of Owens Valley, California.

Local tectonics clearly can play a major role in shaping the facies stratigraphy of carbonate platforms, and nonuniform subsidence and even tectonic uplift needs to receive more attention in the analysis of carbonate platform stratigraphy.

MEGACYCLES

Groups of cyclical deposits that are in essence "cycles of cycles" have long been recognized (Duff and others 1967), although there is no agreement on the terminology. "Cyclothems" in the Pennsylvanian of the Midwest are grouped into "megacyclothems" and "hypercyclothems," and so on. Other hierarchies have been used, such as meso-, macro- and megacycles, or the seismic stratigraphy terms of paracycles, cycles and supercyles (Vail and others 1977). The main point is that several orders of cyclicity occur in stratigraphic successions, and carbonates are no exception, as, for example, the "grand cycles" of Aitken (1978) for the Cambrian of the Canadian Rockies.

An example from the Lower Ordovician of the central Appalachians is instructive. Figure 85 is a vertical section of the lower part of the Beekmantown Group that shows the facies distribution across the depositional strike of the carbonate platform. This facies mosaic was constructed by Chau Nguyen and Robert Goldhammer (Nguyen and others 1985) from vertical sections measured using the subfacies approach and correlated using macrofossil and conodont zones. It is clear from this diagram that the lateral distribution of facies along time lines is a classic progression across a craton-attached carbonate platform of tidal flats ⧫ inner muddy lagoon ⧫ outer sandy, patch reef lagoon ⧫ platform margin reefs and sand shoals. As would be predicted from modern platform depositional patterns, these Lower Ordovician time-lines cut across facies and formation boundaries (figure 85). But the pattern of boundaries between facies traces out well-defined tongues of onlapping and offlapping facies on a 10^2 meter scale. These tongues record "megacycles" of transgressions and regressions that are roughly spaced at about 3.5 m.y. intervals. Significantly, McKerrow (1979), using depth-related brachiopod communities, found worldwide sea-level oscillations in the Ordovician that average 3 m.y. in duration. He ascribed a glacio-eustatic origin to these oscillations on the basis of known Ordovician Gondwanaland tillites, but he also recognized that changes in seafloor spreading rates (Rona 1973; Pittman 1978) could be involved. Megacycles have also been recognized in other Cambro-Ordovician carbonate sequences in the central Appalachians (figures 64 and 65).

Facies-mosaic sections such as figure 85 can be expanded into a 3-dimensional mosaic to yield a complete graphical summary of the facies stratigraphy of any carbonate platform deposit. Within such mosaics especially useful information about sea-level history is revealed by the variations in geometry of tidal-flat facies in their special role as "sea-level gauges."

TIDAL-FLAT CYCLES AS TIME-STRATIGRAPHIC UNITS

Individual tidal-flat cycles have a particular stratigraphic importance beyond their significance as "sea-level gauges." The mechanism of progradation that produces laterally extensive tidal-flat cycles also puts constraints on time lines. As figures

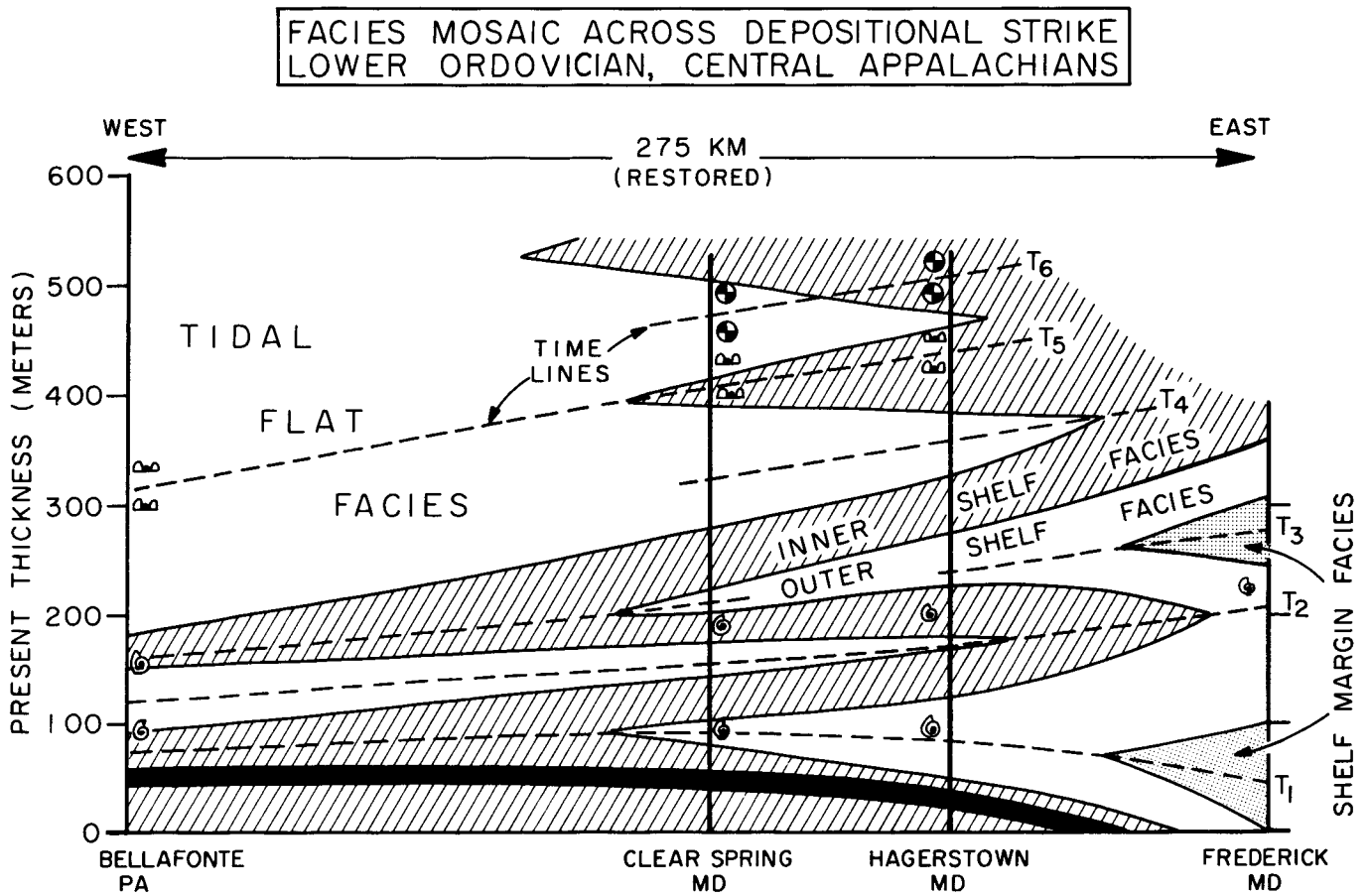

Figure 85.—Facies mosaic and time lines for the Lower Ordovician (Tremadoc-Arenig) platform carbonates of the central Appalachian, showing marked and systematic facies zonation across strike, as well as 3 megacycles of transgression and regression. Time lines based on facies intertonguing correlate extremely well with time zones based on macrofossils (time line T_6 is based on *Archeoscyphia*, T_5 is based on *Lecanospira compacta*, and the time zone between T_1 and T_3 is based on *Ophileta complanata*). This facies mosaic was constructed from unpublished field and laboratory data by Chau Nguyen and Robert Goldhammer, The Johns Hopkins University, Baltimore, Maryland (see also Nguyen and others 1985).

72, 76, and 77 show, time lines must be enclosed within the boundaries of a single tidal-flat cycle, so that such cycles are, for all practical purposes, time-stratigraphic units on a scale of tens of thousands to a few hundred thousand years, a level of internal stratigraphic refinement not matched by biostratigraphic control (see Wilson 1975, pages 53-55).

Tongues of tidal-flat facies can also be used to locate time lines using classic onlap-offlap arguments (Krumbein and Sloss 1963, pages 383-386). In such an intertonguing pattern, the apex of a tidal-flat facies tongue must represent a regression-transgression reversal point and so is a singular time node. Connecting equivalent nodes for shelf-lagoon facies allows the construction of time lines spaced on a 10^6 year scale, as shown in figure 85. Such time lines in figure 85 extend across the entire platform and clearly demonstrate that facies boundaries (and in this case also formational boundaries) are diachronous. Layer-cake stratigraphy, defined within the cyclical tidal-flat facies by the near-parallel bundles of time lines enclosed within cycle boundaries (figures 72, 76, and 77), should be correlatable across facies boundaries into synchronous shoaling-upward subtidal lagoon sequences that lack tidal-flat caps (compare with Goodwin and Anderson 1985).

EPILOGUE

The stratigraphic implications of the global eustasy concept of Vail and his co-workers (Vail and others 1977) revolutionized the way we look at sedimentary successions, and in combination with the rise of marine geology and the revival of Milankovitch theory, have stirred renewed interest in sedimentary cycles. The nature of cyclicity in platform carbonates, and its causes and influences, presents a new (or rather rediscovered) frontier in carbonate stratigraphy and sedimentology, one that is ripe for exploitation considering the fact that our rapid advances in the last two decades have solved the

problems of how to reconstruct paleoenvironments and paleogeography of ancient carbonate depositional systems.

Grabau, whose tour de force on global stratigraphic cycles (Grabau 1940) has gone unheralded, would be pleased with the rejoining of sedimentology and stratigraphy.

REFERENCES

Aharon, P., 1984, Implications of the coral-reef record from New Guinea concerning the astronomical theory of ice ages, pages 379-389, *in* Berger, A., and others, editors, Milankovitch and climate: Reidel Publishing Company, Boston.

Aitken, J.D., 1978, Revised models for depositional grand cycles, Cambrian of the southern Rocky Mountains, Canada: Bulletin of Canadian Petroleum Geology, volume 26, pages 515-542.

Bachman, S.B., 1978, Pliocene-Pleistocene breakup of the Sierra Nevada-White-Inyo Mountains block and formation of Owens Valley: Geology, volume 6, pages 461-463.

Beach, D.K., and Ginsburg, R.N., 1978, Facies succession of Pliocene-Pleistocene carbonates, northwestern Great Bahama Bank: American Association of Petroleum Geologists Bulletin, volume 64, pages 1634-1642.

Berger, A., 1977a, Support for the astronomical theory of climatic change: Nature, volume 269, pages 44-45.

Berger, A., 1977b, Long-term variation of the earth's orbital elements: Celestial Mechanics, volume 15, pages 53-74.

Berger, A., Imbrie, J., Hays, J., Kukla, G., and Saltzman, B., 1984, Milankovitch and climate: Part 1, pages 1-510; Part 2, pages 511-895, Reidel Publishing Company, Boston.

Bloom, A.L., Broecker, W.S., Chappell, J.M.A., Matthews, R.K., and Mesolella, K.J., 1974, Quaternary sea level fluctuations on a tectonic coast: Quaternary Research, volume 4, pages 185-205.

Bosellini, A., 1967, La tematica deposizionale della Dolomia Principale (Dolomiti e Prealpi Venete): Bollettino della società geologica italiana, volume 86, pages 133-169.

Bosellini, A., 1984, Progradation geometries of carbonate platforms: examples from the Triassic of the Dolomites, northern Italy: Sedimentology, volume 31, pages 1-24.

Bosellini, A., and Hardie, L.A., 1973, Depositional theme of a marginal marine evaporite: Sedimentology, volume 20, pages 5-27.

Bosellini, A., and Hardie, L.A., 1986, Facies e cicli della Dolomia Principale della Alpi Venete: Bollettino della società geologica italiana (in press).

Broecker, W.S., Thurber, D.L., Goddard, J., Ku, T., Matthews, R.K., and Mesolella, K.J., 1968, Milankovitch hypothesis supported by precise dating of coral reefs and deep-sea sediments: Science, volume 159, pages 1-4.

Broecker, W.S., and van Donk, J., 1970, Insolation changes, ice volumes, and O^{18} record of deep-sea cores: Reviews of Geophysics and Space Physics, volume 8, pages 169-197.

Demicco, R.V., 1981, Comparative sedimentology of an ancient carbonate platform: the Conococheague Limestone of the central Appalachians: Unpublished Ph.D. dissertation, The Johns Hopkins University, Baltimore, Maryland, 333 pages.

Doglioni, C., 1984, Triassic diapiric structures in the Central Dolomites: Eclogae Geologicae Helvetiae, volume 77, pages 261-285.

Donovan, D.T., and Jones, E.J.W., 1979, Causes of worldwide changes in sea level: Journal of Geological Society, London, volume 136, page 187-192.

Duff, P. McL.D., Hallam, A., and Walton, E.K., 1967, Cyclic sedimentation: Elsevier, New York, 280 pages.

Enos, P., and Perkins, R.D., 1979, Evolution of Florida Bay from island stratigraphy: Bulletin of Geological Society of America, volume 90, pages 59-83.

Evans, G., 1979, Quaternary transgressions and regressions: Journal of Geological Society, London, volume 136, pages 125-132.

Fischer, A.G., 1964, The Lofer cyclothems of the Alpine Triassic: Bulletin of Geological Survey of Kansas, volume 169, pages 107-149.

Gebelein, C.D., 1974, Modern Bahamian platform environments: Field trip guidebook, Geological Society of America Annual Meetings, Miami Beach, 106 pages.

Ginsburg, R.N., 1971, Landward movement of carbonate mud: new model for regressive cycles in carbonates (abstract): American Association of Petroleum Geologists Bulletin, volume 55, page 340.

Ginsburg, R.N., and James, N.P., 1974, Holocene carbonates of continental shelves, pages 137-155 *in* Burk, C.A., and Drake, C.L., editors, Geology of continental margins: Springer-Verlag, New York.

Goldhammer, R.K., Dunn, P.A., and Hardie, L.A., 1986, High frequency glacio-eustatic sea-level oscillations with Milankovitch characteristics recorded in Middle Triassic cyclic platform carbonates, northern Italy: American Journal of Science (in review).

Goodwin, P.W., and Anderson, E.J., 1985, Punctuated aggradational cycles: a general hypothesis of episodic stratigraphic accumulation: Journal of Geology, volume 93, pages 515-534.

Grabau, A.W., 1940, The rhythm of the ages: Reprinted 1978 by Robert E. Krieger Publishing Company, Huntington, New York, 561 pages.

Grotzinger, J.P., 1985, Evolution of early Proterozoic passive-margin carbonate platform, Rocknest Formation, Wopmay Orogen, Northwest Territories, Canada: Unpublished Ph.D. dissertation, Virginia Polytechnic Institute and State University, Blacksburg, Virginia, 225 pages.

Hardie, L.A., Bosellini, A., and Goldhammer, R.K., 1986, Repeated subaerial exposure of subtidal carbonate platforms, Triassic, northern Italy: evidence for high frequency sea level oscillations on a 10^4 year scale: Paleoceanography (in review).

Hardie, L.A., and Ginsburg, R.N., 1977, Layering: the origin and environmental significance of lamination and thin bedding, pages 50-123, *in* Hardie, L.A., editor, Sedimentation on the modern carbonate tidal flats of northwest Andros Island, Bahamas: Johns Hopkins Press, Baltimore.

Harland, W.B., Cox, A.V., Llewellyn, P.G., Picton, C.A.G., Smith, A.G., and Walters, R., 1982, A geological time scale: Cambridge University Press, Cambridge, 128 pages.

Harris, P.M., 1979, Facies anatomy and diagenesis of a Bahamian ooid shoal: Comparative Sedimentology Laboratory, University of Miami, Miami, 163 pages.

Hays, J.D., Imbrie, J., and Shackleton, N.J., 1976, Variation in the earth's orbit: pacemaker of the ice ages: Science, volume 194, pages 1121-1132.

Howe, W.B., 1968, Planar stromatolites and burrowed carbonate mud facies in Cambrian strata of the St. Francois Mountain area: Missouri Geological Survey and Water Resources, Report of Investigations 42, 113 pages.

Imbrie, J., 1985, A theoretical framework for the Pleistocene ice ages: Journal of Geological Society, London, volume 142, pages 417-432.

Imbrie, J., and Imbrie, J.Z., 1980, Modelling the climatic response to orbital variations: Science, volume 207, pages 943-953.

Imbrie, J. and Imbrie, K.P., 1979, Ice ages—solving the mystery: Enslow Publishing, Short Hills, New Jersey, 224 pages.

James, N.P., 1984, Shallowing-upward sequences in carbonates, pages

213-228, *in* Walker, R.G., editor, Facies models, Second Edition: Geoscience Canada Reprint Series 1.

Kay, M. 1955, Sediments and subsidence through time: Geological Society of America Special Paper 62, pages 665-684.

Kinsman, D.J.J., 1969, Modes of formation, sedimentary associations and diagnostic features of shallow-water and supratidal evaporites: American Association of Petroleum Geologists Bulletin, volume 53, pages 830-840.

Krumbein, W., and Sloss, L.L., 1963, Stratigraphy and sedimentation: Freeman, San Francisco, 660 pages.

McElhinney, M.W., and Valencio, D.A., 1981, editors, Paleoreconstruction of the continents: American Geophysical Union, Geodynamics Series, volume 2, Washington, D.C., 194 pages.

McKerrow, W.S., 1979, Ordovician and Silurian changes in sea level: Journal of Geological Society, London, volume 136, pages 137-145.

Mesolella, K.J., Matthews, R.K., Broecker, W.S., and Thurber, D.L., 1969, The astronomical theory of climatic change—Barbados data: Journal of Geology, volume 77, pages 250-274.

Mueller, H.W., 1975, Centrifugal progradation of carbonate banks: a model for deposition and early diagenesis, Ft. Terrett H Formation, Edwards Group, Lower Cretaceous, central Texas: Unpublished Ph.D. dissertation, University of Texas, Austin, Texas, 300 pages.

Middleton, G.V., 1973, Johannes Walther's Law of the correlation of facies: Bulletin of Geological Society of America, volume 84, pages 979-988.

Morel, P., and Irving, E., 1978, Tentative paleocontinental maps for the early Phanerozoic and Proterozoic: Journal of Geology, volume 86, pages 535-561.

Neumann, A.C., and Land, L.S., 1975, Lime mud deposition and calcareous algae in the Bight of Abaco, Bahamas: Journal of Sedimentary Petrology, volume 45, pages 763-786.

Nguyen, C., Goldhammer, R.K., and Hardie, L.A., 1985, Depositional facies mosaics and their time lines in the Lower Ordovician carbonates of the central Appalachians (abstract): American Association of Petroleum Geologists Bulletin, volume 69, pages 292.

Odin, G.S., editor, 1982, Numerical dating in stratigraphy, Part 1: Wiley-Interscience, New York, 630 pages.

Patterson, R.J., and Kinsman, D.J.J., 1977, Marine and continental groundwater sources in a Persian Gulf coastal sabkha: American Association of Petroleum Geologists, Studies in Geology, volume 4, pages 381-397.

Pittman, W.C., 1978, Relationship between eustasy and stratigraphic sequences of passive margins: Bulletin of Geological Society of America, volume 89, pages 1389-1403.

Purser, B.H., 1973, The Persian Gulf: Springer-Verlag, New York, 471 pages.

Read, J.F., Grotzinger, J.P., Bova, J.A., and Koerschner, W.F., 1986, Models for generation of carbonate cycles: Geology, volume 14, pages 107-110.

Rona, P.A., 1973, Relations between rates of sediment accumulation on continental shelves, sea-floor spreading, and eustasy inferred from the central north Atlantic: Bulletin of Geological Society of America, volume 84, pages 2851-2872.

Ruddiman, W.F., and McIntyre, A., 1976, Northeast Atlantic paleoclimatic changes over the past 600,000 years: Geological Society of America Memoir 145, pages 111-146.

Savin, S.M., 1982, Stable isotopes in climatic reconstructions: Climate in Earth History, Studies in Geophysics: National Academy Press, Washington, D.C., pages 164-171.

Schlager, W., 1981, The paradox of drowned reefs and carbonate platforms: Bulletin of Geological Society of America, volume 92, pages 197-211.

Scotese, C.R., Bambach, R.K., Barton, C., van der Voo, R., and Ziegler, A.M., 1979, Paleozoic base maps: Journal of Geology, volume 87, pages 217-277.

Shackleton, N.J., and Kennett, J.P., 1975, Late Cenozoic oxygen and carbonate isotopic changes at DSDP site 284: implications for glacial history of the northern hemisphere and Antarctica: Initial Report of Deep Sea Drilling Project, volume 19, pages 801-808.

Shackleton, N.J., and Opdyke, N.D., 1973, Oxygen isotope and paleomagnetic stratigraphy of equatorial Pacific core V28-238: oxygen isotope temperatures and ice volumes on a 10^5 and 10^6 year scale: Quaternary Research, volume 3, pages 39-55.

Shinn, E.A., 1983, Tidal flat environments: American Association of Petroleum Geologists Memoir 33, pages 173-210.

Smith, A.G., Hurley, A.M., and Briden, J.C., 1981, Phanerozoic paleocontinental world maps: Cambridge University Press, 102 pages.

Stockman, K.W., Ginsburg, R.N., and Shinn, E.A., 1967, The production of lime mud by algae in south Florida: Journal of Sedimentary Petrology, volume 37, pages 633-648.

Tourek, T.J., 1970, The depositional environments and sediment accumulation models for the Upper Silurian Wills Creek Shale and Tonoloway Limestone, central Appalachians: Unpublished Ph.D. dissertation, The Johns Hopkins University, Baltimore, Maryland, 282 pages.

Vail, P.R., and others, 1977, Seismic stratigraphy and global changes of sea level: American Association of Petroleum Geologists Memoir 26, pages 49-212.

Watts, A.B., and Ryan, W.B.F., 1976, Flexure of lithosphere and continental margin basins: Tectonophysics, volume 36, pages 25-44.

Wilson, J.L., 1975, Carbonate facies in geologic history: Springer-Verlag, New York, 471 pages.

Yeats, R.S., 1978, Neogene acceleration of subsidence rates in southern California: Geology, volume 6, pages 456-460.

Zankl, H., 1971, Upper Triassic carbonate facies in the northern limestone Alps, pages 147-185, *in* Müller, G., editor, Sedimentology of parts of central Europe: Guidebook, 8th International Sedimentological Congress, Heidelberg.

Ziegler, A.M., Scotese, W.S., McKerrow, W.S., Johnson, M.E., and Bambach, R.K., 1979, Paleogeography: Annual Review of Earth and Planetary Science, volume 7, pages 473-502.